

ABSTRACT

SONAWALA, CHAITANYA SAMIR. Thermo-Hydraulic and Economic Analysis for Improvement of a Process Cooling Network at a Chemicals Manufacturing Facility. (Under the direction of Dr. Stephen Terry and Dr. Alexei Saveliev).

Modern manufacturing facilities often utilize thermal and fluid processing equipment that is interconnected. The compatibility of installed process equipment is always subject to issues arising from changing operating conditions which can then possibly affect normal production capabilities. The focus of this thesis is to take an existing manufacturing facility where the quantity of the manufactured product is directly dependent on the performance of thermal and fluid equipment such as heat exchangers, cooling towers and centrifugal pumps, and analyze it to make it operate even better. A specific problem of erratic low product condensation was identified, defined and solutions to resolve the contributing factors were developed. Since there may be multiple contributing factors to such an operational issue, a root cause analysis of the problem was carried out, followed by on-site data collection and brainstorming for solutions. Economics drive the majority of decisions in facilities engineering and this thesis demonstrates how to check the feasibility of critical or expensive engineering investments by sizing equipment correctly. The results of this study involved estimation of the implementation costs for the recommended solutions and the annual operational costs for the same. Simple engineering economics calculations such as payback periods are calculated based on these costs and are used to provide insights that can help the decision-making process. The facility management has initiated the process of implementation on some of the findings of this study, whereas more expensive, long-term investments are being planned for the near future.

© Copyright 2019 by Chaitanya Samir Sonawala

All Rights Reserved.

Thermo-Hydraulic and Economic Analysis for Improvement of a Process Cooling Network at a
Chemical Manufacturing Facility

by
Chaitanya Samir Sonawala

A thesis submitted to the Graduate Faculty of
North Carolina State University
in partial fulfillment of the
requirements for the degree of
Master of Science

Mechanical Engineering

Raleigh, North Carolina
2019

APPROVED BY:

Dr. Stephen Terry
Committee Co-Chair

Dr. Alexei Saveliev
Committee Co-Chair

Dr. Brendan O'Connor

ProQuest Number:27529138

All rights reserved

INFORMATION TO ALL USERS

The quality of this reproduction is dependent upon the quality of the copy submitted.

In the unlikely event that the author did not send a complete manuscript and there are missing pages, these will be noted. Also, if material had to be removed, a note will indicate the deletion.



ProQuest 27529138

Published by ProQuest LLC (2019). Copyright of the Dissertation is held by the Author.

All rights reserved.

This work is protected against unauthorized copying under Title 17, United States Code
Microform Edition © ProQuest LLC.

ProQuest LLC.
789 East Eisenhower Parkway
P.O. Box 1346
Ann Arbor, MI 48106 – 1346

BIOGRAPHY

Chaitanya Samir Sonawala is the elder son of Dr. Samir B. Sonawala and Dr. Uma S. Sonawala from Mumbai, India. Born and brought up in a family of doctors, Chaitanya decided there were enough people in his family who could fix the living but not enough people to fix and sustain the inanimate objects critical to modern life and chose to correct this by becoming an engineer. Chaitanya pursued a Technical Diploma in Mechanical Engineering right out of secondary school and followed it up with a Bachelor's Degree in Mechanical Engineering at the University of Mumbai. Still academically unsatisfied with two engineering degrees, Chaitanya decided to pursue a graduate degree in engineering. After a long and arduous process of decision making involving too many "what-ifs" and "wait-buts", Chaitanya decided to come halfway around the world, to North Carolina State University in the wonderful city of Raleigh to pursue his ambition of becoming a world class mechanical engineer. After a taxing first year at graduate school, laced with unique challenges and experiences, Chaitanya finally found his calling in the field of energy conservation and thermal sciences and has been enjoying it ever since by being part of the Industrial Assessment Center at NC State. Upon graduation, Chaitanya is interested in exploring this field professionally by being part of an energy services company or a team of consulting engineers that deal with practical applications of thermal and fluid systems.

ACKNOWLEDGMENTS

As my long journey as an engineering student comes to an end, I would like to acknowledge the support of all the wonderful people who have had a part to play in this journey. Starting off with the two most important people in my life, my mom, Uma and my dad, Samir, thank you for being so ultra-inspirational and teaching me how to live and grow as a human being by raising me to be humble, patient and hard-working at all times. Next, I'd like to thank my little brother Harshit for always bringing a smile to my face and reciprocating with unending chortles after listening to my dumb jokes. I would also like to thank my grandma, Vishakha for her unwavering love and support, even when I am halfway across the world.

Next, I would like to thank my advisor, Dr. Stephen Terry, for being such a patient, kind and thoughtful mentor for me and fellow students. Dr. Terry, If I end up with even half of your professionalism and knowledge, I will consider myself to have been a successful engineer. I'd also like to sincerely thank Dr. Saveliev and Dr. O'Connor for being part of my master's thesis committee.

I'd like to thank all my friends at the Industrial Assessment Center: Alex, Harrison, Elizabeth, Zachary, Nicholas, Sanjyot, Kristine, Emily and Anvay. It was a pleasure sharing a workplace and many, many wonderful conversations with all of y'all!

Finally, I'd like to thank my buddies: Siddhant, Manthan, Ninad and Anushka for being such superb friends to share this journey with. I don't think I would have made it this far to the end without your camaraderie, love and support. You guys are the best!

Last but not the least, I'd like to thank all my friends, relatives, professors and numerous well-wishers across the world who go unmentioned here in interest of space. Thank you for believing in me, wherever you are.

TABLE OF CONTENTS

LIST OF TABLES	vi
LIST OF FIGURES	viii
CHAPTER 1: INTRODUCTION	1
1.1: The Big Picture	1
1.2 Heat Exchangers	3
1.2.1 Introduction to Heat Exchangers	3
1.2.2: Shell and Tube Heat Exchangers	6
1.3: Pumping Systems	16
1.3.1: Introduction to Industrial pumping systems.....	16
1.3.2: Components of a pumping network.....	18
1.3.3: Major and Minor Head losses	21
1.3.4: Pump Curves	22
CHAPTER 2: OVERVIEW OF COMPANY AND PROBLEM DEFINITION	25
2.1 Company Background	25
2.2 Process Description	27
2.3 Problem Overview	28
2.4 Initial thoughts	29
CHAPTER 3: LITERATURE REVIEW	35
3.1: Heat exchanger Fouling	35
3.2: Pressure Drop in Heat Exchangers	43
3.3: Multi-pump Pumping Systems.....	47
3.4: Cooling towers and Water side Economizers	50
CHAPTER 4: ANALYSIS AND PROBLEM SOLVING.....	59
4.1: Root Cause Analysis.....	59
4.2: Possible Solutions and Economic Analysis	65
4.2.1: Installing a bigger chiller with a water-side economizer	65
4.2.2: Reconfigure the pumping arrangement.....	83
4.2.3: Clean the Shell-sides of all Shell and Tube Heat Exchangers	114
CHAPTER 5: CONCLUSIONS	123
5.1: Summary of Recommendations	123
5.2: Current Measures and Future Work	125
5.3: Closing Remarks	129
REFERENCES	131

Appendix A: Summary of Friction Losses Calculation for Paths B-I	136
Appendix B: Summary of Heat Exchanger Dimensions and Shell Side Pressure Drops for Paths B-F	144
Appendix C: Summary of Heat Exchanger Shell side and tube side heat transfer coefficient calculations and additional revenue calculations	150

LIST OF TABLES

Table 1: List of Heat Exchangers at the facility	26
Table 2: Antoine Equation ranges and constants.....	67
Table 3: Enthalpy of Vaporization Calculation for Ethanol [37]	68
Table 4: Enthalpy of Vaporization Calculation for Ethanol Using PPSD12 Equation [40]	69
Table 5: Interpolation of Isobaric Specific Heat of Ethanol [37]	70
Table 6: Calculation of Ethanol Liquid Density via DIPPR105 State Equation [41].....	70
Table 7: Summary of Calculated Thermodynamic Properties in Vacuum	71
Table 8: Estimation of Heat Exchanger Yields	72
Table 9: Calculation of Total Heat Load on Cooling Tower Water	73
Table 10: Implementation Cost Estimation for 220 Ton Chiller Unit	76
Table 11: Operating Cost Estimation for 220 TR Chiller	77
Table 12: Calculation of Additional Annual Revenue after Implementation.....	78
Table 13: Water-side Economizer Operational Expenses	82
Table 14: Implementation Costs for Water-side Economizer	82
Table 15: Heat Balance at Desired Product Output	84
Table 16: Calculation of Path Flow Constants	87
Table 17: Calculation of Network Velocities	88
Table 18: Friction Constants for Valves and Fittings [15].....	90
Table 19: Friction Losses in Path A.....	92
Table 20: Summary of Network Friction Losses.....	93
Table 21: Dimensions of Heat Exchanger A	95
Table 22: Friction Factor for Heat Exchanger in cross-flow section.....	98
Table 23: Summary of Pressure drop calculation for Heat Exchanger in Path A	100
Table 24: Summary of Shell-side Pressure drops in each path	101
Table 25: Total Head loss at current operating point.....	102
Table 26: Possible new pumps from Manufacturer's catalog	106
Table 27: New Centrifugal Pump Purchase and Installation Costs	109
Table 28: Possible Options for Parallel Pumps	111
Table 29: Cost of Installing selected pumps in parallel	113
Table 30: Calculation of Simple Payback Period from Energy Savings on New Pump Arrangements.....	113
Table 31: Values of Constant 'C'	116
Table 32: Values of Constant 'n'	117
Table 33: Internal and External Heat Transfer Coefficients for Heat Exchanger C	118
Table 34: Heat transfer in Heat Exchanger C	119
Table 35: Calculation of Additional Profit from increased product output from Exchanger C ..	120
Table 36: Calculation of Payback period on cleaning all shell and tube heat exchangers.....	121
Table 37: Results with external fouling factors from various sources.....	121
Table 38: Summary of Analyzed Recommendations.....	123
Table 39: Pressure gauge readings in network before changes (psig)	126
Table 40: Pressure Readings before and after overhauling and cleaning pump (psig)	127
Table 41: Friction Losses in Path B	136
Table 42: Friction Losses in Path C	137
Table 43: Friction Losses in Path D.....	138

Table 44: Friction Losses in Path E	139
Table 45: Friction Losses in Path F	140
Table 46: Friction Losses in Path G.....	141
Table 47: Friction Losses in Path H.....	142
Table 48: Friction Losses in Path I	143
Table 49: Summary of Heat Exchanger Dimensions.....	144
Table 50: Summary of Pressure drop calculation for Heat Exchanger in Path B.....	145
Table 51: Summary of Pressure drop calculation for Heat Exchanger in Path C.....	146
Table 52: Summary of Pressure drop calculation for Heat Exchanger in Path D	147
Table 53: Summary of Pressure drop calculation for Heat Exchanger in Path E.....	148
Table 54: Summary of Pressure drop calculation for Heat Exchanger in Path F	149
Table 55: Summary of External and Internal Heat transfer coefficients.....	150
Table 56: Calculation of change in heat transfer after cleaning	151
Table 57: Calculation of Additional Annual Revenue from generated product	152

LIST OF FIGURES

Figure 1: Disassembled Shell and Tube Heat Exchanger [2]	3
Figure 2: Classification of Heat Exchangers Based on Operating Principle [4]	6
Figure 3: TEMA-type designations for Shell and Tube Heat Exchangers [6]	9
Figure 4: Cutaway drawings of: (a) 1-2 Fixed Tube-sheet B-E-M Shell and Tube Heat Exchanger, (b) 1-2 Internal Floating head A-E-S Shell and Tube Heat Exchanger, (c) 1-2 U-Tube C-F-U Shell and Tube Heat Exchanger [5]	10
Figure 5: Tube layouts [7]	12
Figure 6: Twisted Tube Configuration [4]	12
Figure 7: Baffle arrangements in a Shell and Tube Heat Exchanger:	14
Figure 8: Heat transfer surfaces, thermal resistances and the temperature profile around the tubes [10]	14
Figure 9: Components of a Typical Pumping System [12]	18
Figure 10: Classification of Pumps [5]	19
Figure 11: Components of a Centrifugal pump [13]	20
Figure 12: A typical Pump performance curve with a sample System Curve. [16]	23
Figure 13: Factory Plant Layout	26
Figure 14: Generic Product Flow	27
Figure 15: Cooling Tower and Heat Exchangers Loop at facility	31
Figure 16: Two Pipe System arrangements	32
Figure 17: Shell side fouling in a petrochemical heat exchanger	34
Figure 18: Average contact angles of water with common processing surfaces [23]	39
Figure 19: Idealized fouling curves: A) Linear, B) Falling Rate, C) Asymptotic [25]	41
Figure 20: Cleaning Map by Fryer and Asteriadou [25]	42
Figure 21: Complex Flow paths taken by the shell side fluid around a segmented baffle [27] ...	44
Figure 22: Pump and System Curves for multiple pumps [28]	49
Figure 23: Cooling Towers: (a) Open Circuit/"Wet" Tower (b) Closed circuit/"Dry" tower [30]	51
Figure 24: Range and Approach temperature in cooling tower operation [31]	52
Figure 25: Annual Free-Cooling hours possible with Ambient Wet bulb lower than 50°F [33] ..	54
Figure 26: Waterside Economizer Arrangements	55
Figure 27: Trane CenTraVac Centrifugal Chiller with condenser above evaporator [36]	57
Figure 28: Current Piping network	61
Figure 29: Root Cause Analysis	65
Figure 30: Proposed process cooling arrangement with chiller	75
Figure 31: Proposed Water-side Economizer Arrangement	80
Figure 32: Paths in Heat Exchanger Network	85
Figure 33: Moody Chart	90
Figure 34: Sections of Shell and Tube Heat exchangers in the Bell-Delaware Method (a) internal crossflow sections, (b) window sections, (c) entry/exit sections [46]	94
Figure 35: Dimensions within Shell and Tube Heat Exchangers [7]	95
Figure 36: Diametral Shell-to-tube clearance for various heat exchanger configurations [7]	96
Figure 37: Variation in the Shell side pressure drop with velocity	102
Figure 38: Pump Curve for Current Pump "E-1510-3E"	103
Figure 39: Obtained Pump and System Curve	104

Figure 40: Performance curves for Bell & Gossett in-line pumps from the e-1510 pump manual	105
Figure 41: Pump curve after using selected Pump model “e-1510-4BD”	109
Figure 42: Pump Curve for Pumps in Parallel with 2 units of the current pump	110
Figure 43: Pump Curves for 2 units of the selected “E1510-3BD” Pumps in Parallel.....	112

CHAPTER 1: INTRODUCTION

1.1: The Big Picture

In any modern manufacturing facility, there are a number of interconnected processes and systems that work simultaneously in conjunction with each other to develop a final product. This interconnectivity of intermediate processes often involves use of some form of thermal and fluid power equipment such as boilers, chillers, air compressors, pumps and heat exchangers. Since this equipment is critical to process functionality within most facilities, the overall operating effectiveness of the processing facility is directly dependent on the suitability and the operating efficiencies of these individual components.

It is estimated that the industrial sector in the United States consumes about 21,000 trillion BTU of energy annually which is about 31% of the total annual energy consumption of the United States [1]. Thus, looking at the interconnectivity of process equipment from an energy conservation perspective, one can conclude that the energy consumption and thus, the costs of operating a manufacturing facility both depend on the individual operating efficiencies of these thermal and fluid power components. With this outlook in today's energy conscious environment, there is a need for having such thermal and fluid power equipment in manufacturing facilities perform at the maximum operating efficiency possible. This can be achieved by either reducing the load, reducing distribution losses or by increasing the efficiency of the prime movers associated with the process. Keeping this end goal in mind, this thesis is an exercise in analyzing an actual existing industrial process with two interconnected mechanical systems. The challenge is in figuring out the engineering methodology to make such a process operate more efficiently by either suitably modifying existing equipment or by analyzing the feasibility of installing new mechanical equipment that reduces operational expenses and the energy footprint of the process. The goal of

this thesis is to make sure the facility in focus can achieve its production goals in the most energy and cost-efficient manner possible.

Economics and engineering often go hand in hand when making short-term or long-term decisions that impact a manufacturing facility. Most engineering decisions made by plant management are based on the engineer's answer to the inevitable question of "How soon will I get my money back?". A good way to look at the time value of any investment is to look at the simple payback period, which can give a finite (or sometimes near-infinite!) time period in which the total cash flow towards or from an investment becomes zero. Simple payback periods are often used in energy efficiency projects to compare equipment costs and to gain insights on the long-term value of projects. The only downside of using simple payback periods, is that the calculations do not account for changes in the value of money over time due to inflation and uncertainty. Such in-depth calculations can be conducted by using more sophisticated analysis methods like the Net Present Value or Internal Rate of Return methods.

This thesis is laid out as follows: Chapter 1 looks at heat exchangers and pumping networks, which are the focus of the analysis conducted later in this thesis. Chapter 2 introduces the facility being examined, the various steps in the manufacturing process that the company currently employs to develop its products and describes the present problems and areas of possible improvement at this facility. Chapter 3 is a review of existing relevant literature and possible practical solutions to the problems described in chapter 2. This is followed by Chapter 4, where the extent of the afore mentioned problems is looked at and the engineering feasibility of solutions to the specific causes are analyzed by assessing the economics of the solution via simple payback analysis. Finally, Chapter 5 summarizes the various solutions and provides closing remarks to the facility.

1.2 Heat Exchangers

1.2.1 Introduction to Heat Exchangers

Heat Exchangers are a vital part of most modern processing facilities that deal with some form of fluid medium on the way to processing a final product. Heat exchangers are typically closed-chamber pressure vessels that allow efficient exchange of thermal energy across two fluids at different thermo-physical conditions. The versatility of carrying out heat transfer efficiently, with or without mixing of fluids, makes heat exchangers a very useful tool in most industrial applications. Heat exchangers are widely used in a range of process-based applications in chemical processing and food processing facilities, but also across all modes of transport, homes and commercial spaces in the form of cooling towers and evaporator units for refrigeration and air-conditioning purposes, which illustrates the extent of the usage of heat exchangers across the world. Since heat exchangers are a vital part of most processing industries directly as part of the process or indirectly as part of the HVAC related equipment, the analysis and optimization of these components is a great way to improve the efficiency of the process and reduce its energy consumption.

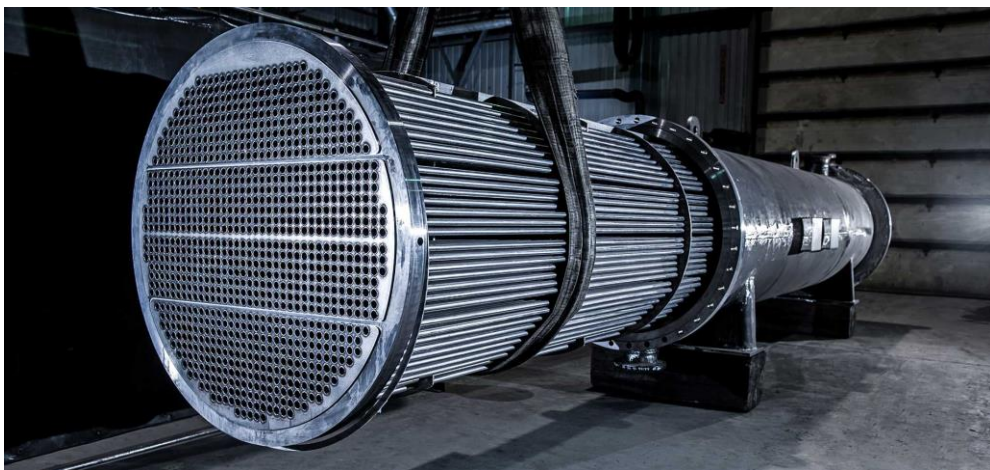


Figure 1: Disassembled Shell and Tube Heat Exchanger [2]

The underlying principles behind heat exchanger operation are very straightforward. Heat exchangers utilize the Zeroth Law of thermodynamics by bringing the two fluid streams, which are at different temperatures, into direct or indirect contact, during which, an attempt to reach thermal equilibrium is made. This attempt to achieve thermal equilibrium by using a heat exchanger is orchestrated to achieve either a temperature rise of one of the fluid streams, a temperature decrease of one of the fluid streams, or to have both these processes occur simultaneously. As per the First Law of thermodynamics, the total energy transfer must always be balanced and the heat gain and the heat loss of the respective fluid streams are always equal, if losses to the operating environment are neglected. In certain processes, heat exchangers can also be used to effect a change in phase of either of the fluids involved by exchanging the necessary latent heat.

Since the exact nature of the process application dictates the magnitude of heat transfer required, the process of heat exchanger design and selection is highly dependent on several factors such as purchasing and operating costs, process parameters, operating environment and the criticality of the process application [3]. For example, a heat exchanger that is used for a pharmaceutical cooling application, where precise temperature and fluid flow control is critical to the process, would be very different from the heat exchanger used in a waste heat recovery application, where more emphasis would be placed on the efficiency of the heat exchanger to maximize the desired heat recovery effect with minimum operating costs.

The simplicity of the operating principle of heat exchangers is contrasted by the complexity of accurately analyzing and predicting the thermal and hydraulic performance of a heat exchanger in actual practice. Due to the inherently complex flow paths and various dimensional constraints in the flow patterns of the fluids involved, there are several unique design parameters that the heat

exchanger behavior and efficiency is sensitive to. Some of these parameters include the variation of area of the fluid carrying components along the fluid flow path, the baffle arrangements and the significant pressure and velocity variations across the heat exchanger. Conventionally, heat exchangers that would be used in a practical application would be overdesigned for the typical heat duty that would be warranted in the application. However, over the years, there have been several advancements in using computing software for prediction and simulation of the fluid flows within a heat exchanger in practice to a considerable prediction accuracy. Such computing software often employ an iterative process of thermo-hydraulic analysis combined with some form of computational fluid dynamics to obtain critical parameter values such as the overall heat transfer coefficient value and the pressure drop across the tubes. Using such software tools in the design process has pushed the boundaries of equipment design by enhancing the design and manufacturing process for modern heat exchangers.

Heat exchangers can be classified based on their basic heat exchange flow pattern (parallel flow, counter flow or cross flow) or as per their configuration. Due to the simplicity of the operating principle, heat exchangers can be designed to accomplish their heat transfer goals in many different configurations as shown in Figure 2.

Regenerative heat exchangers deal with intermittent heat transfer and utilize thermal storage to accomplish the heat transfer, whereas recuperative heat exchangers deal with continuous heat transfer between two fluid streams via an intermediate medium of fluid separation.

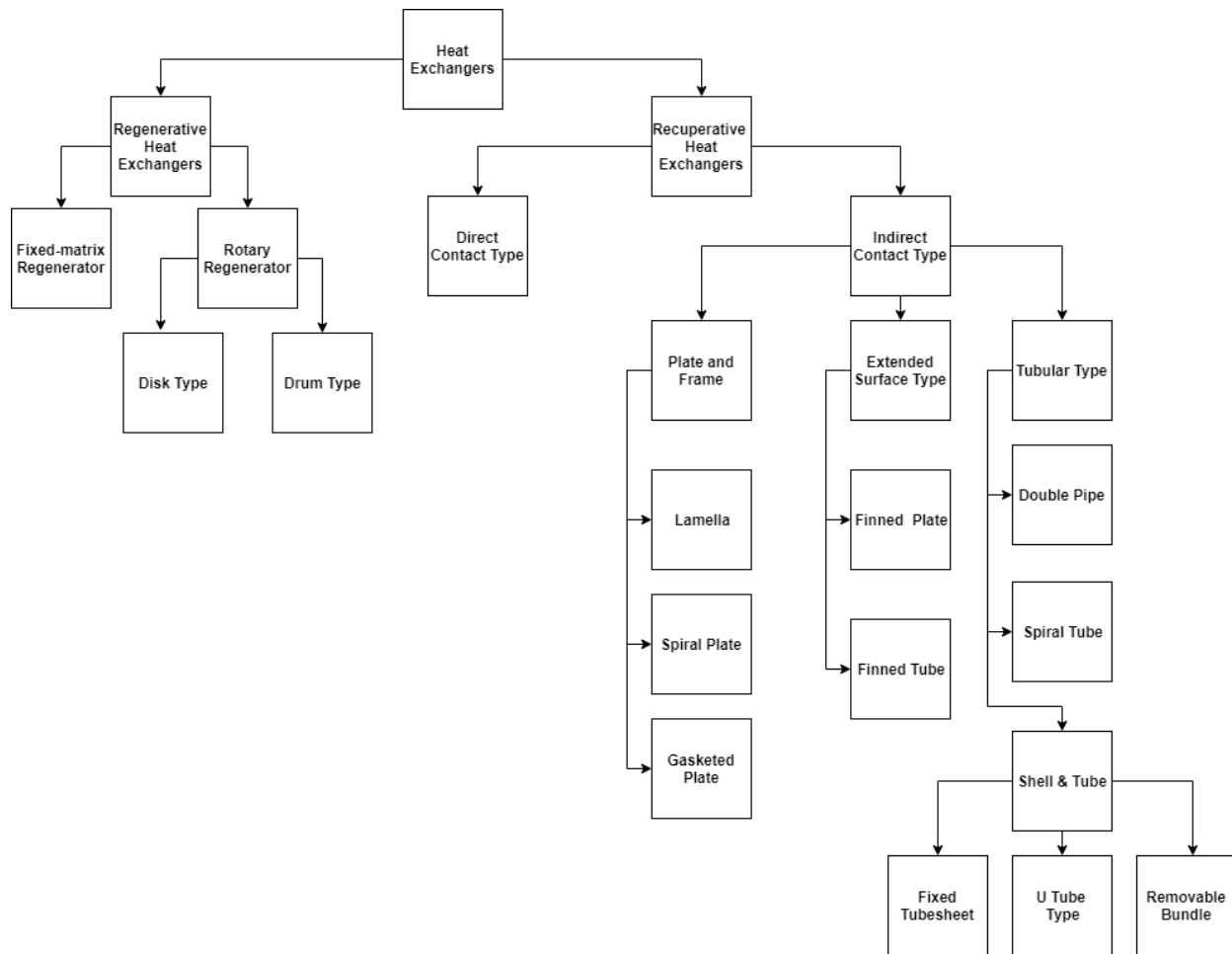


Figure 2: Classification of Heat Exchangers Based on Operating Principle [4]

1.2.2: Shell and Tube Heat Exchangers

A very common configuration of a heat exchanger used in the industry is the shell and tube configuration. This recuperative type heat exchanger configuration involves using multiple fluid carrying tubes, contained within a larger vessel called the shell, which has the second fluid flowing through it. The tubes are held in the form of systematically arranged tube-bundles within a tube-sheet or within supports at either end of the shell. The fluids do not mix, and the heat transfer occurs via thermal interaction between the fluid films at the extreme inner and outer surfaces of the tube. The shell and tube heat exchanger arrangement is commonly used because of its ease of

design, maintenance and ruggedness to sustain long-term usage. A typical shell and tube heat exchanger also typically costs less than the other possible configurations for a given heat transfer duty.

The shell side of a heat exchanger is a pressure vessel fabricated to sustain the necessary pressure it may see during operation. Shells are sized with relation to the tube bundle that they are designed to hold and generally have a corrosion allowance and a clearance from the tube surface factored into the wall thickness, and ultimately the shell diameter. There are three common and distinct types of shell and tube heat exchanger configurations on the basis of construction: A fixed tube-sheet type heat exchanger, a floating head type heat exchanger and a U-tube type heat exchanger [5].

A shell and tube heat exchanger typically contains one or multiple tube-sheets, which are heavy metallic plates that hold the tubes in place. The tubes are inserted into holes drilled into the tube-sheet, inserted with a metallic ferrule to form a leak-proof seal and then secured in place using tie rods, spacers and by welding the tube ends to the tube-sheet. As seen in Figure 4(a), the tube-sheet along with a longitudinal partition may also be configured to accommodate multiple tube passes. The tube bundle may or may not be removable depending on the design of the head of the exchanger and the number of tube-sheets. A fixed tube-sheet type heat exchanger generally uses a tube-sheet on either side of the heat exchanger shell, which reduces the complexity and the cost of construction, but increases the difficulty in cleaning the heat exchanger [5].

An alternative configuration is the floating head heat exchanger shown in Figure 4(b) that uses a stationary tube-sheet on one end of the exchanger and a floating tube-sheet on the other end that is free to move. Using this configuration allows two major advantages: movement due to thermal expansion is accommodated and it allows better cleaning of both the inside and the outside

of the tubes without necessitating complete overhaul and reassembly. However, this benefit comes at a greater expense, since these heat exchangers are complicated to design and expensive to purchase [5]. A U-tube heat exchanger as illustrated in Figure 4(c) uses long, continuous tubing which is bent into a U-shape to reduce the size of the shell by eliminating the head on one side of the heat exchanger. Again, the reduced cost of having U-tubes is offset by the increase in difficulty of cleaning the heat exchanger, since cleaning the U-bends would require flexible cleaning equipment to be used with overhauling being necessary. Due to these problems, the U-tube and fixed tube-sheet heat exchangers are used in operational conditions where low frequencies of cleaning and overhauling are acceptable and the cost of owning or fabricating a heat exchanger is the major selection or design criteria.

The standards for the design, installation and operation of a shell and tube heat exchanger are based on a document by the Tubular Exchanger Manufacturers Association [6], which is a trade group of heat exchanger manufacturers. Heat exchangers with a “TEMA Plate” attached, indicates a product manufactured by following these technical standards, and hence, a product with an assured level of manufacturing and design quality.

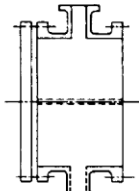
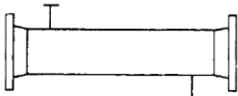
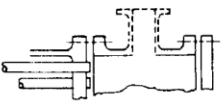
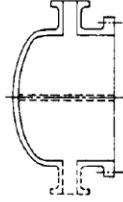
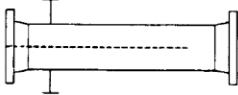
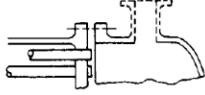
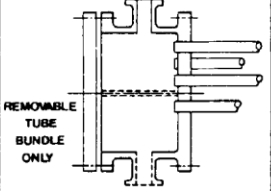
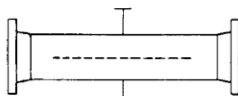
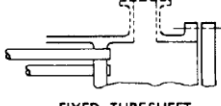
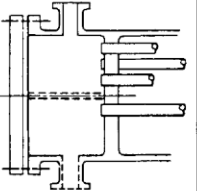
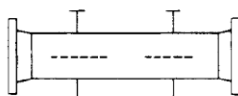
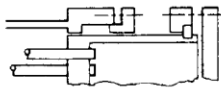
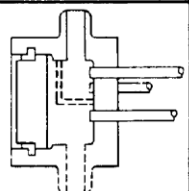

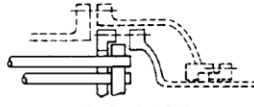
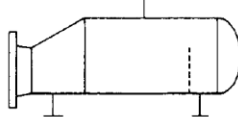
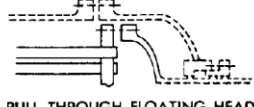
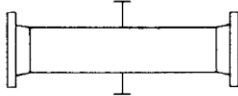
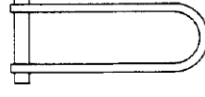

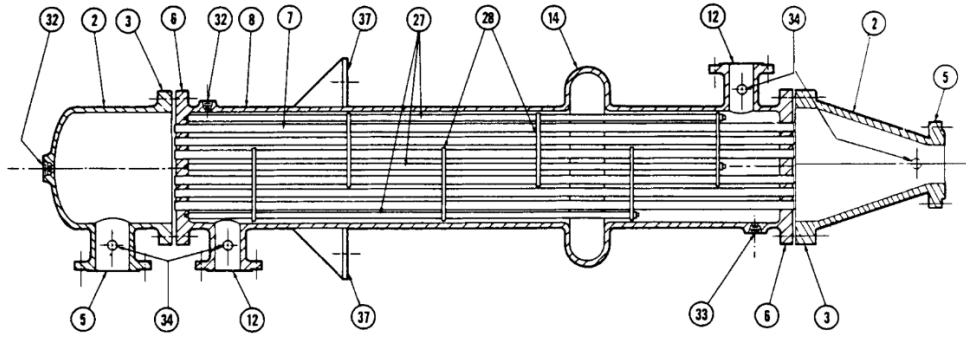
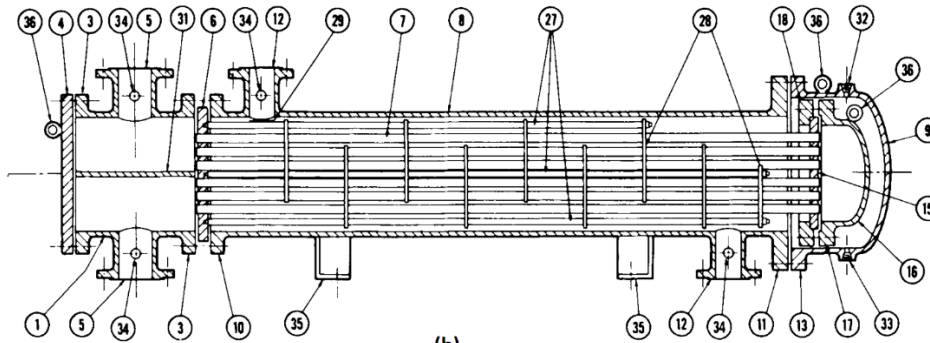
	FRONT END STATIONARY HEAD TYPES		SHELL TYPES		REAR END HEAD TYPES
A	 CHANNEL AND REMOVABLE COVER	E	 ONE PASS SHELL	L	 FIXED TUBESHEET LIKE "A" STATIONARY HEAD
B	 BONNET (INTEGRAL COVER)	F	 TWO PASS SHELL WITH LONGITUDINAL BAFFLE	M	 FIXED TUBESHEET LIKE "B" STATIONARY HEAD
C	 REMOVABLE TUBE BUNDLE ONLY CHANNEL INTEGRAL WITH TUBE- SHEET AND REMOVABLE COVER	G	 SPLIT FLOW	N	 FIXED TUBESHEET LIKE "N" STATIONARY HEAD
N	 CHANNEL INTEGRAL WITH TUBE- SHEET AND REMOVABLE COVER	H	 DOUBLE SPLIT FLOW	P	 OUTSIDE PACKED FLOATING HEAD
D	 SPECIAL HIGH PRESSURE CLOSURE	J	 DIVIDED FLOW	S	 FLOATING HEAD WITH BACKING DEVICE
		K	 KETTLE TYPE REBOILER	T	 PULL THROUGH FLOATING HEAD
		X	 CROSS FLOW	U	 U-TUBE BUNDLE
				W	 EXTERNALLY SEALED FLOATING TUBESHEET

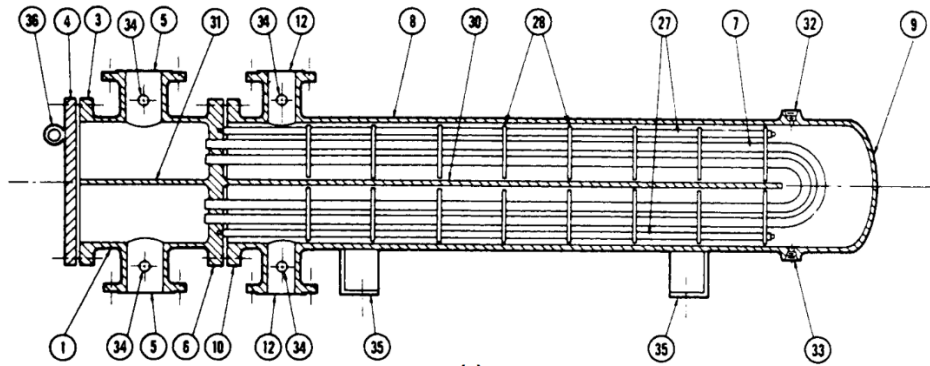
Figure 3: TEMA-type designations for Shell and Tube Heat Exchangers [6]



(a)



(b)



(c)

- | | |
|---|--|
| 1. Stationary Head—Channel | 20. Slip-on Backing Flange |
| 2. Stationary Head—Bonnet | 21. Floating Head Cover—External |
| 3. Stationary Head Flange—Channel or Bonnet | 22. Floating Tubesheet Skirt |
| 4. Channel Cover | 23. Packing Box Flange |
| 5. Stationary Head Nozzle | 24. Packing |
| 6. Stationary Tubesheet | 25. Packing Gland |
| 7. Tubes | 26. Lantern Ring |
| 8. Shell | 27. Tie Rods and Spacers |
| 9. Shell Cover | 28. Transverse Baffles or Support Plates |
| 10. Shell Flange—Stationary Head End | 29. Impingement Plate |
| 11. Shell Flange—Rear Head End | 30. Longitudinal Baffle |
| 12. Shell Nozzle | 31. Pass Partition |
| 13. Shell Cover Flange | 32. Vent Connection |
| 14. Expansion Joint | 33. Drain Connection |
| 15. Floating Tubesheet | 34. Instrument Connection |
| 16. Floating Head Cover | 35. Support Saddle |
| 17. Floating Head Flange | 36. Lifting Lug |
| 18. Floating Head Backing Device | 37. Support Bracket |
| 19. Split Shear Ring | 38. Weir |
| | 39. Liquid Level Connection |

Figure 4: Cutaway drawings of: (a) 1-2 Fixed Tube-sheet B-E-M Shell and Tube Heat Exchanger, (b) 1-2 Internal Floating head A-E-S Shell and Tube Heat Exchanger, (c) 1-2 U-Tube C-F-U Shell and Tube Heat Exchanger [5]

The convention for naming heat exchangers is based on the number of passes, so a 2 shell pass and 4 tube pass heat exchanger with a floating head is referred to as a '2-4 floating head heat exchanger'. Heat exchangers are almost always designed with even numbers of tube passes (except 1 pass) to avoid any mechanical problems in the construction of the heat exchanger [7]. TEMA standards also have a naming convention for the construction of the shell depending on the type of heads and the pressure vessel characteristics as shown in Figure 4.

The tube construction used in a shell and tube heat exchanger greatly influences the size and effectiveness of the heat exchanger. The tubes are designed with an intent to have a turbulent flow of the fluid within them which would allow better thermal mixing and hence, better heat transfer. The tubes are made capable of sustaining the high pressures of the fluid on either side of the tube surface and include a corrosion allowance, proportional to the corrosiveness of the fluids it is expected to encounter. Typically, the fluid on the tube side is the more corrosive or the dirtier fluid while the fluid on the shell side is a fluid with either higher viscosity or the fluid that experiences the change in phase. The reason for this is that the inside of the tubes can be cleaned much more easily and frequently than the shell side for most configurations.

The tube cross-section area is determined to optimize the velocity of the tube-side fluid and to prevent fouling due to stagnation of fluid flow within any spot inside the exchanger. The tube length within the heat exchanger is a very critical parameter as it directly influences the pressure drop that the fluid will experience going through the heat exchanger. A longer tube will increase the tube-side pressure drop as the friction increases, but reduce the shell diameter and the number of tubes that may be needed. Optimizing a heat exchanger for maximum thermal interaction and cost, primarily involves tinkering with these variables to achieve a suitable middle ground between these two effects. [5]

Tubes are generally made up of highly conductive metals like steel, copper or bronze to maximize the heat transfer via conduction between the shell and tube-side fluids. The tubes may generally have a smooth outer surface (and possibly an outer protective sheath) to prevent accumulation of sediments and other deposits which may reduce the heat transfer. In certain operational cases, particularly when dealing with viscous fluids, the tubes may have external fins attached, to increase the external surface area and the heat transfer. [7] The tubes in a heat exchanger are laid out in close proximity to each other to increase the heat transfer with the shell side fluid flow. The tubes are generally laid out in either a square or a triangular layout with a consistent distance between two adjacent tubes, also called the pitch, in the horizontal and vertical directions. The pitch of the tubes decides the shell diameter. A twisted tube configuration is an alternative to circular tubing and allows better rigidity, reduces flow induced vibration and is easier to clean on the inside and outside via hydro-jets.

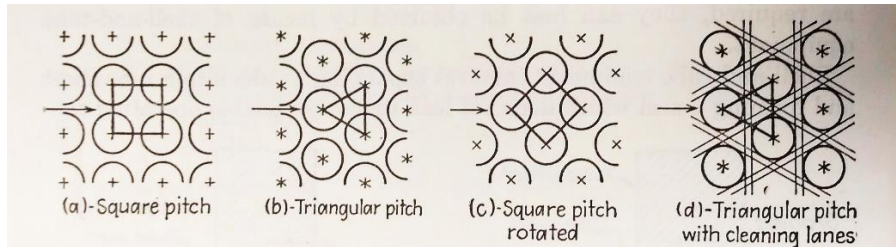


Figure 5: Tube layouts [7]

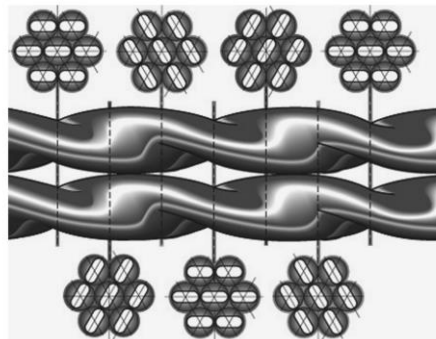


Figure 6: Twisted Tube Configuration [4]

Another constructional element in a heat exchanger is a baffle. Baffles are primarily used to increase the mixing of the shell side fluid, which is accomplished by introducing changes in the flow path and the associated cross-sectional flow area. Baffles act as barriers in the flow path and allow increase in the velocity as the flow progresses. The change in velocity causes a change in the inertial forces and directly affects the heat transfer coefficient on the outer side of the tubes. [5] [7] Baffles are also strategically positioned to support the tubes and to minimize the vibration induced in the exchanger due to the sudden change in flow direction and flow area. Baffles are classified based on their shape and their arrangement inside the shell. The baffles can be in a segmented arrangement or in a disk-doughnut type arrangement.

A segmented arrangement is simply a partition in the shell cross-sectional area that covers some portion of the flow area to induce mixing via a change in direction. The segmented baffle “cut” is expressed as a percentage of the shell area it shields and is typically about 45%-50% and constructed such that the baffle supports all the individual tubes in the bundle. A disk and doughnut baffle arrangement comprises of a circumferential partition baffle in the shell area, alternating with a central partition on the tube area. The disk and doughnut type of baffling has been practically proven to have a 15% higher heat transfer coefficient than the segmented type of baffling. [8] This lower value of the heat transfer coefficient in segmented baffles is understood to be an indication of the kinetic energy dissipation of the shell-side fluid within the eddy motion caused in the flow pockets, which form due to the flow around the segmented baffles. The spacing within the baffles influences the pressure drop on the shell side of the exchanger as it affects the quantity and the velocity of the shell-side fluid meeting the tubes at any given time. Accordingly, baffles spaced further away would allow for a higher heat transfer coefficient than baffles spaced closer to each other. The baffle spacing is generally not more than one-fifth the inside shell diameter. [5]

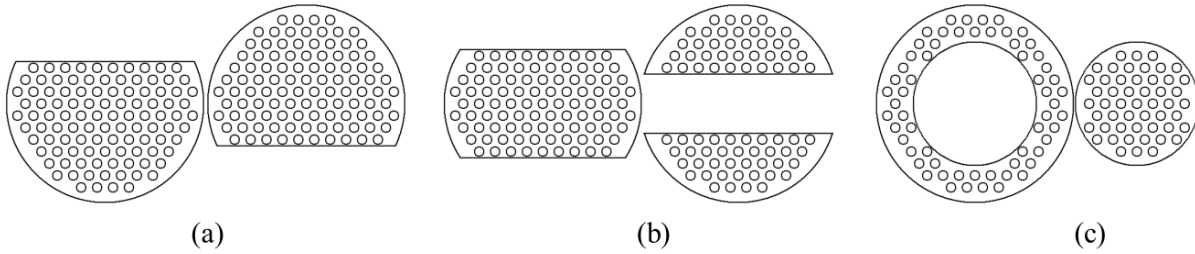


Figure 7: Baffle arrangements in a Shell and Tube Heat Exchanger:
a) Single-segmental, b) Double-segmental, c) Disk-and-Doughnut [9]

The mechanism of heat transfer in a shell and tube heat exchanger can be broken up into three distinct constituent phenomena:

- Convection heat transfer between the inner tube surface and the tube-side fluid film on it.
- Conduction heat transfer across the tube material.
- Convection heat transfer between the outer tube surface and the shell-side fluid film on it.

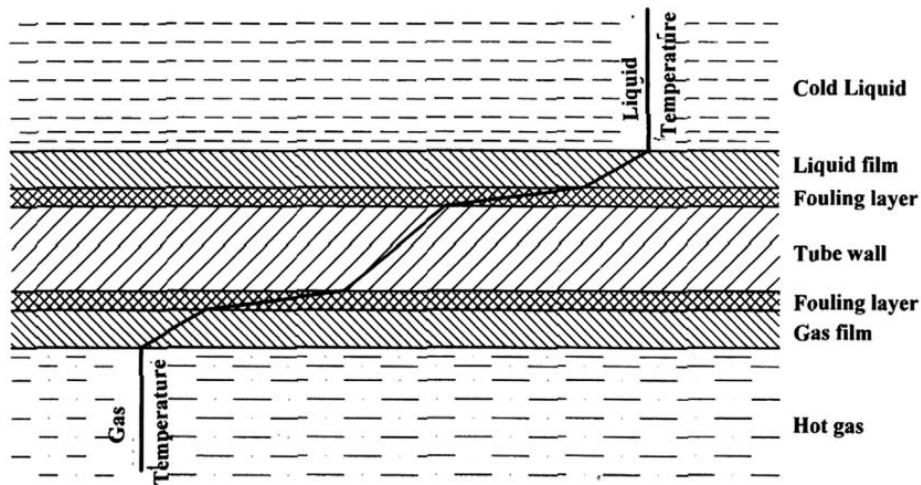


Figure 8: Heat transfer surfaces, thermal resistances and the temperature profile around the tubes [10]

Even though shell and tube heat exchangers are not the most efficient form of heat exchangers, their versatility and design flexibility is why almost 50% of all industrial process-based heat exchanger systems are shell and tube type exchangers [11]. Some other distinct

advantages to using a shell and tube heat exchanger over other forms of heat exchangers are as listed below:

- Due to the general construction of the shell and tube heat exchangers, the orientation of installation is not an issue and they can be mounted horizontally or vertically without any major detrimental effects.
- Due to the flexibility and overall robustness, a shell and tube heat exchanger is generally the least expensive option when considering a new heat exchanger installation. Especially for exchanger systems used in large chiller systems and power plants with a high-power generation capacity, all other heat exchanger alternatives would be very expensive to install.
- There is a lot of flexibility regarding the constructional materials used in shell and tube heat exchangers except when used with corrosive liquids.
- To enhance the heat transfer, fins can be used on the outer surface of the tubes.
- Periodic cleaning and repair can generally be accommodated if the heat exchanger has some room around it.
- Tube leakages can be easily identified, located and fixed in-house without use of special equipment.

The major disadvantages associated with shell and tube heat exchangers are listed below:

- The size can be a problem when a compact exchanger is needed since shell and tube heat exchangers are bulky and require some additional space all around the place of installation to allow maintenance.
- Shell and tube heat exchangers are typically designed with a fixed capacity for heat transfer called the maximum heat duty and hence, any more heat transfer capacity can only be accommodated by installing a new exchanger.

- A shell and tube heat exchanger system generates a lot of vibration due to the high pressure fluids flowing inside. This effect may be reduced by using additional baffles and impingement plates which provide a means of damping for the vibration.

1.3: Pumping Systems

1.3.1: Introduction to Industrial pumping systems

Fluid transport is frequently one of the major operations in a lot of industrial facilities that deal with processing fluids. An industrial pumping system refers to the assembly of various interconnected components within a fluid transport system used to move a fluid, in-process or otherwise, from one point in the facility to the other. The extent of fluid transport networks in a facility is generally proportional to the size and complexity of the facility. Very often, the flow paths of the pipes and ducts can grow with additions over time to become very complex, making the initial method of tracking very important. Fluids commonly dealt with in processing industries include air, water, steam, organic solvents, petrochemicals, oils and food-grade fluid compounds. Each fluid can have a range of operating parameters and quality conditions across the entire process which needs to be considered when designing and initially installing the pumping system.

Since the fluid pumping system can be extensive and complex, driving the fluid through the various flow paths can turn out to be a major portion of the energy usage in processing facilities. Thus, optimizing the system for minimal energy usage by taking the required steps during the design phase or via continuous improvement programs can go a long way in reducing the cost of operation for the system. According to “Manufacturing Consumption of Energy – DOE/EIA-0512-1994”, the industrial motors installed in pumps, fans, compressed air and refrigeration devices account for about 36.8% of all motor installations in industrial facilities, but they account for almost 61% of the operational energy consumption of the facility. [1] This fact shows that the

energy usage of the plant in fluid transport would be highly sensitive not only to the quantity of the pumping system drivers, but also to the time this equipment is in use. Following that chain of thought, it can be seen that a small increase in the efficiency of the pumping system can result in significant cost and energy savings over the lifetime of the system, since most fluid transport systems are not changed frequently, once correctly installed.

Fluid transport systems are quite frequently designed to support or be critical parts of other systems, for example, in a refrigeration cycle using chillers, water runs in the secondary cooling loop and plays a vital role in the overall operation. [5] Similarly, in more interconnected systems, critical parameters like temperature, viscosity and flow rates are the major criteria for selection of the key components of the pumping system like the pump, the fluid transfer media and the controlling system in place. The designer must also account for any special material handling requirements of the fluid properties in applications within food, pharmaceutical and nuclear industries.

Another key aspect of a fluid transport system is the behavior of the entire system as a single unit. The pumping system must be looked at from a supply and demand point of view as there are several factors on either side of the system that can have a direct impact on the design, construction and maintenance of the system. Cost-effective sizing of the pumps and the associated equipment, while ensuring that the system performs well even in the worst-case scenario, is a tough task. To add to this complex list of tasks, a system designer must also consider the possibility of any future expansion of the system and take the adequate measures to accommodate those. When looking at any such potential system and analyzing the cost of implementation and subsequent operation, the designer must consider the total operating cost of any component over its expected lifetime and not just the first cost of installation.

1.3.2: Components of a pumping network

The major components of an industrial pumping system include the drivers like pumps or compressors, the fluid transport media like pipes or ducts, the various pipe fittings and valves and the end-use equipment such as heat exchangers, tanks or any other hydraulic equipment.

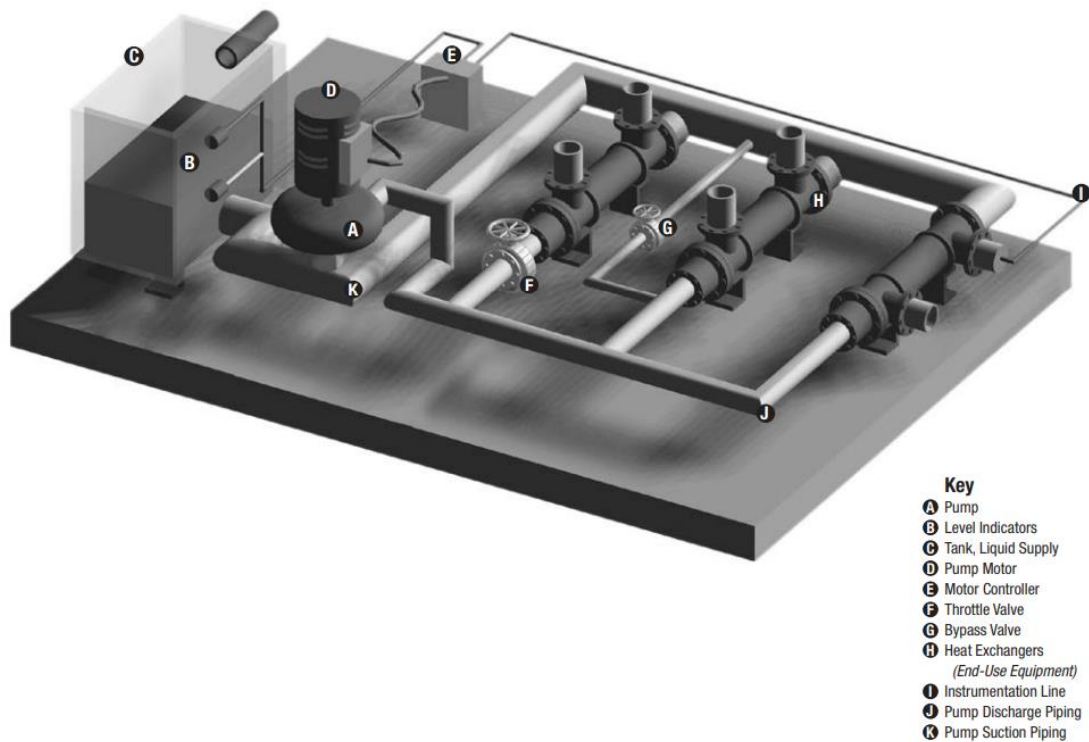


Figure 9: Components of a Typical Pumping System [12]

Pumps are used to induce flow within the system. There are numerous types and sizes of pumps available commercially and Figure 10 shows the classification of pumps. Centrifugal pumps are the most commonly used form of roto-dynamic turbomachines that induce flow in a pumping system by application of centrifugal force on the fluid medium. These are extensively used in manufacturing industries for their ease of maintenance, low first cost and for their general reliability in dealing with commonly handled fluids with viscosities similar to that of water. A centrifugal pump generates flow in a system by imparting kinetic energy to the fluid entering the

pump and then converting this energy into pressure energy by reducing the velocity of the flowing fluid. It accomplishes this process by use of an impeller, which is essentially a rotating disk with blades on its surface, coupled to an electric motor. This impeller rotates at high velocities to fling the fluid outward with a high tangential velocity. After this, the fluid passes through a diffuser ring and the volute casing which together convert this kinetic energy into pressure energy by gradually increasing the flow-path area as flow progresses.

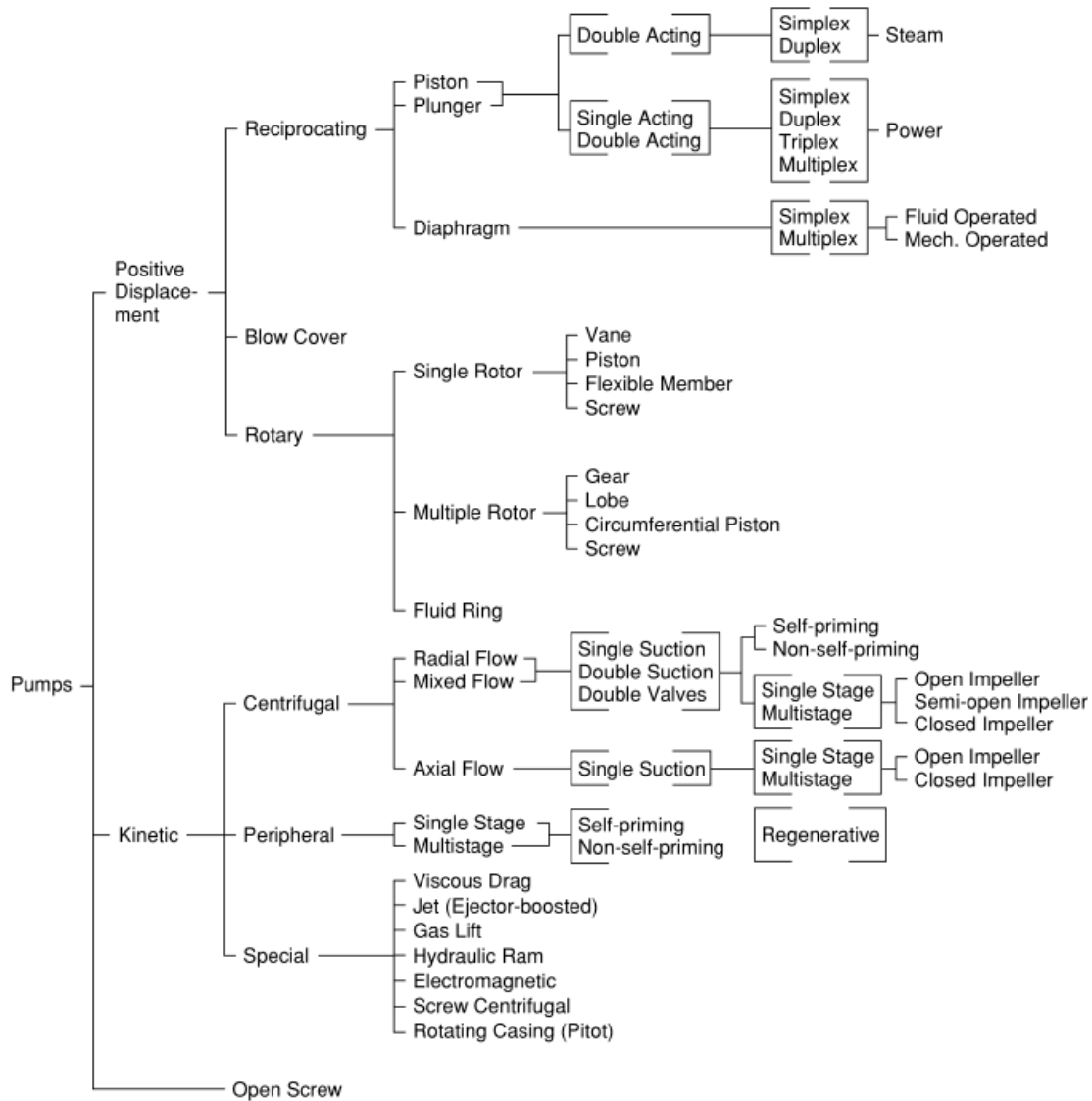


Figure 10: Classification of Pumps [5]

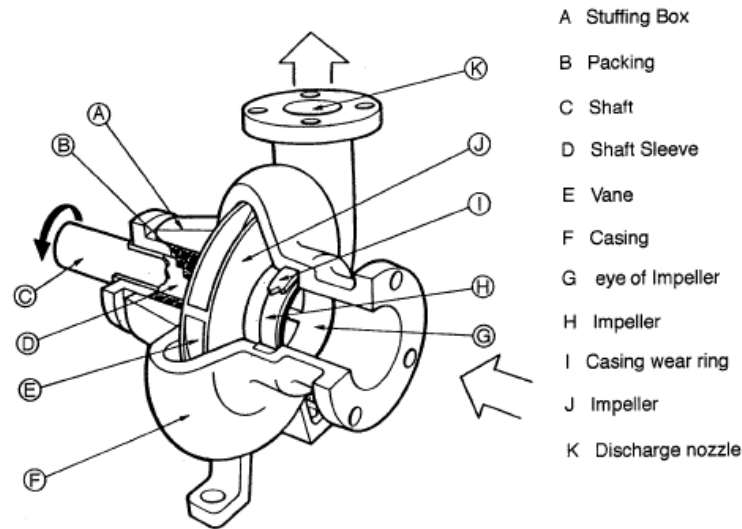


Figure 11: Components of a Centrifugal pump [13]

The transport media is the material carrying medium that allows transport of the fluid from the source to the end use equipment. This consists of pipes for liquids and ducts for air. The sizing and selection of the material of the pipes and ducts is done based on the extent of usage expected, the magnitude of control needed and the spread of the network. The friction offered by the pipes or ducts is thoroughly analyzed to avoid problems due to inadequate pumping power required to overcome frictional resistance.

The goal of designing an effective pumping network is to ensure that the end usage equipment on the network gets the right quantity and quality of fluid. Some examples of such end use equipment include heat exchangers, tanks, water filtration units, drinking water fountains and cooling systems. The end usage equipment would typically have its own individual usage pattern and the nature of the load on the pumping network is accordingly determined. Consider a water storage tank where water is stored at a height over a rigid structure, similar to the tall storage tanks that are often seen in towns across the country. To transport the fluid to such a height counts as a static load, as the only resistance that the pump must work against is the pull of gravity. However,

consider a cooling tower connected to an air-conditioning system for a commercial building. In this case, the quantity of fluid transported in the system may vary with variations in the cooling loads on the building and hence, this is a dynamic load. To accommodate such variable loads in a pumping network, pumps are often employed in various configurations. [14] Two commonly used systems are pumps in series and pumps in parallel. Pumps are said to be in series, when the inlet for a pump is connected to the outlet of the preceding pump. Pumps are said to be in parallel, when multiple pumps share the same inlet lines and possibly, the same outlet lines. A series arrangement is used where a high-pressure head is required at a constant flow rate, whereas pumps in parallel are used to provide a higher fluid flow at a relatively lower pressure head. However, either arrangement can prove to be uneconomical unless the pumps operate near their best efficiency point and are installed considering the losses in the system.

1.3.3: Major and Minor Head losses

In a pumping network, there are several possible elements that can increase the frictional resistance of the flowing fluid. The friction offered to the flow by the fluid carrying medium is always determined by analyzing the network since it directly increases the energy needed by the pump to push the fluid from point A to point B. The pressure energy loss experienced by the fluid when travelling through the pipes, as a result of friction, is termed the major head loss. Major head losses in a flow are determined by the Darcy-Weisbach Equation, which uses the friction factor obtained by the Colebrook equation. [14] The variation of the friction factor with a variation in the roughness of the flow medium has been graphically summarized in the Moody Chart, where this factor can be obtained by simply knowing the Reynolds Number and the relative roughness of the flow medium.

Additionally, in any network, the fluid path is altered by use of fittings, expanders, reducers, plugs and valves. All these devices contribute to the energy loss in the system as there is an associated change in velocity due to either a change in flow direction or a change in the flow path area due to an obstruction, entrance or an exit from the original flow path area. All such energy losses are termed as the minor losses in the system as they are often lower in magnitude than the major losses due to pipe friction. The minor head losses in the system are calculated by estimating the frictional head loss factor 'K' for every such element in the network. Values of 'K' for most commercially available fittings are tabulated and provided in multiple references. [15] The total minor losses in a system are calculated by summing up the individual 'K' values and then applying the Darcy-Weisbach formula for frictional head loss.

1.3.4: Pump Curves

The performance of a pump can be estimated by using various empirical relations that correlate the horsepower, the volumetric flow rate and the outlet pressure head. Since all these relations are interlinked, a pump designer or manufacturer can provide a performance curve as a means of reference for the end user to adequately select the best pump suited for their application. This performance curve can inversely be used to accurately estimate the performance of the pump in a variety of possible scenarios to understand the behavior of the pump as part of the entire system.

Centrifugal pumps are used for either one of two scenarios, when a high volumetric flow rate is needed against a low-pressure head, or when a low volumetric flow rate is needed against a high-pressure head. [14] As stated before, using the interlinked empirical relations, a performance curve of the possible operating conditions can be made on a plot of the volumetric flow rate versus

the pressure head at that flow rate. When selecting a pump, one would wish to achieve the maximum efficiency of the pump, to minimize any energy losses due to inefficient operation. Using the affinity and scaling laws, the pump performance curve can also be used to depict the efficiency of the pump at different flow rates. This allows the user to accurately determine the pump with the maximum efficiency at the point of operation. There is always a maximum efficiency region for a pump, which is the operating region with a specific impeller diameter, flow rate and a rotational speed where the pump performs the best theoretically. This is the Best Efficiency point or the BEP [14].

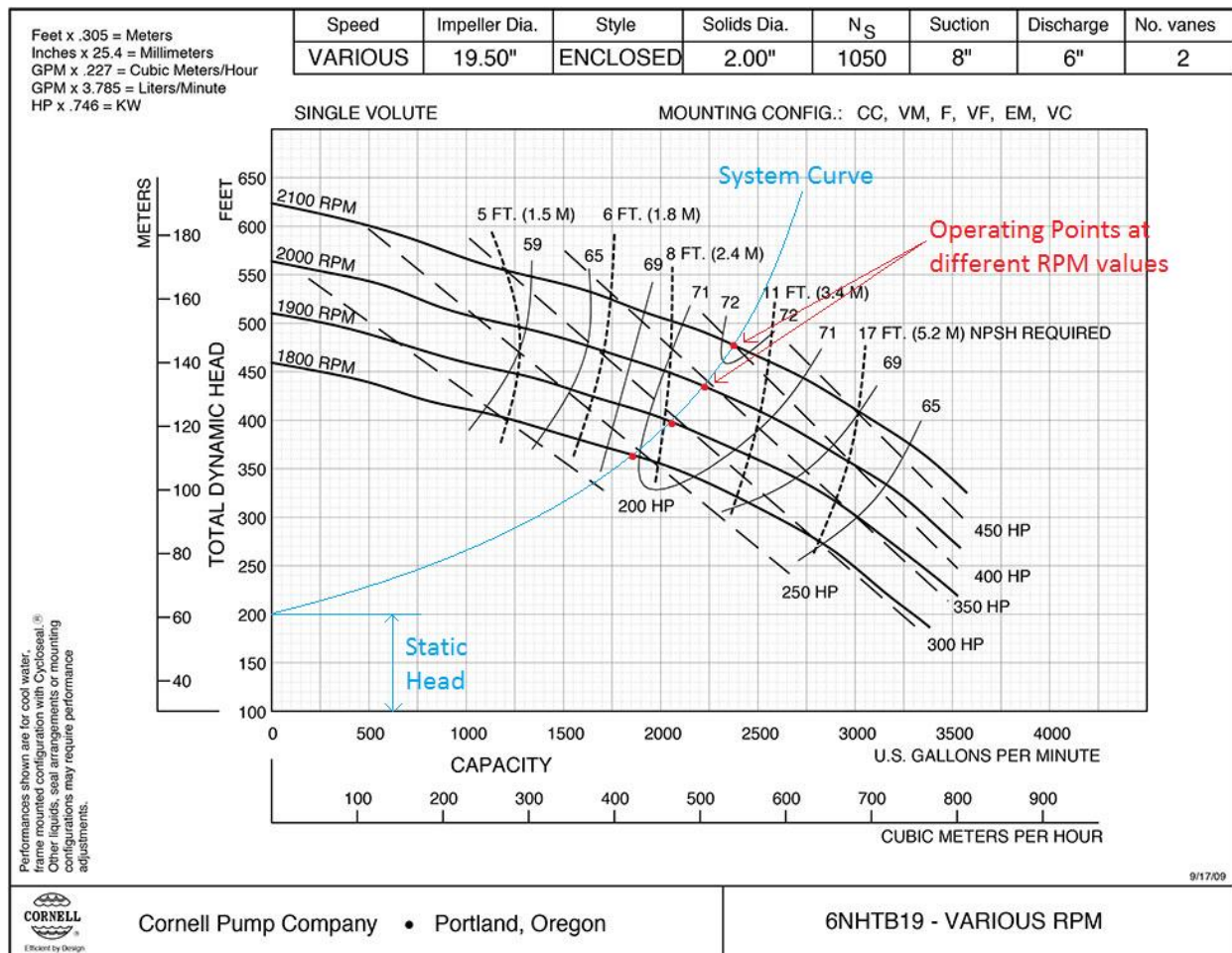


Figure 12: A typical Pump performance curve with a sample System Curve. [16]

When looking at the pumping system from a supply and demand point of view, the location of the operating point for the pump is determined by calculating the major and minor losses. Since these losses are dependent on the square of the flow velocity, they are also dependent on the square of the flow rate and can also be plotted onto the pump performance curve. The plotted curve with the losses is called the system curve and its locus changes with a change in the frictional resistance offered by the various elements in the system. The intersection of the pump curve and the system curve is the operating point for a pump. When designing a system and selecting the pump for the system, it is ensured that the selected pump has its operating point close to the BEP region for that pump. This would ensure minimal loss of energy as the pump will perform at maximum efficiency. The next chapter involves looking at the specific facility and the problem faced by the facility in some of its thermal processing equipment.

CHAPTER 2: OVERVIEW OF COMPANY AND PROBLEM DEFINITION

2.1 Company Background

This processing facility, at its plant in the Southeastern part of the United States, manufactures a variety of custom chemicals that any clientele might demand. The facility consists of one building with a floor area of about 40,000 ft² that includes the manufacturing areas and the finished goods warehouse area. The layout of the facility is shown in Figure 13. In addition to the production areas, the manufacturing building also includes offices, a boiler room, a quality assurance lab and a material receiving area. The quality assurance lab and the administrative offices primarily consist of air-conditioned offices. Office spaces are cooled using dedicated rooftop air-conditioning units. There is a cooling tower right outside the facility behind the processing room wall, which serves the processes in the dry room and the processing room. The facility was established in the early 2000s and has evolved over time to use sophisticated equipment to develop custom chemicals.

The processing room has a number of holding tanks, heat exchangers and product pumping systems. Since the equipment is utilized to make batches of various kinds of chemicals, the equipment is installed to be as interchangeable as possible for the various recipes necessary for the various extraction processes. The facility has six shell and tube heat exchangers, one plate and frame heat exchanger, two specialty heat exchangers, one 15-ton chiller, one 100 hp fire-tube, natural gas fired boiler and one 20 HP screw-type air compressor. The heat exchangers and stills are all located in the processing room. The dry room is used to process temperature and humidity sensitive chemicals. The boiler room houses the air compressor and the fire-tube boiler. A listing of the heat exchangers and their tube surface areas is tabulated below:

Table 1: List of Heat Exchangers at the facility

Sr. No.	Heat Exchanger Type/Designation	Effective Surface Area (sq ft.)
1	Shell & Tube Heat Exchanger A	40
2	Shell & Tube Heat Exchanger B	320
3	Shell & Tube Heat Exchanger C	88
4	Shell & Tube Heat Exchanger D	40
5	Shell & Tube Heat Exchanger E	320
6	Shell & Tube Heat Exchanger F	184
7	Specialty Heat Exchanger G	50
8	Specialty Heat Exchanger H	41

Compressed air is generated in the screw-compressor to operate the diaphragm pumps that control the flow of the solvent and raw material mixture through the entire process. The chiller is located in the space between the boiler room and the processing room. There is a process monitoring setup with multiple displays right outside the processing room that gives real-time readouts of critical process parameters like temperatures, flow volumes and pressures. The plant layout is as shown in the following figure.

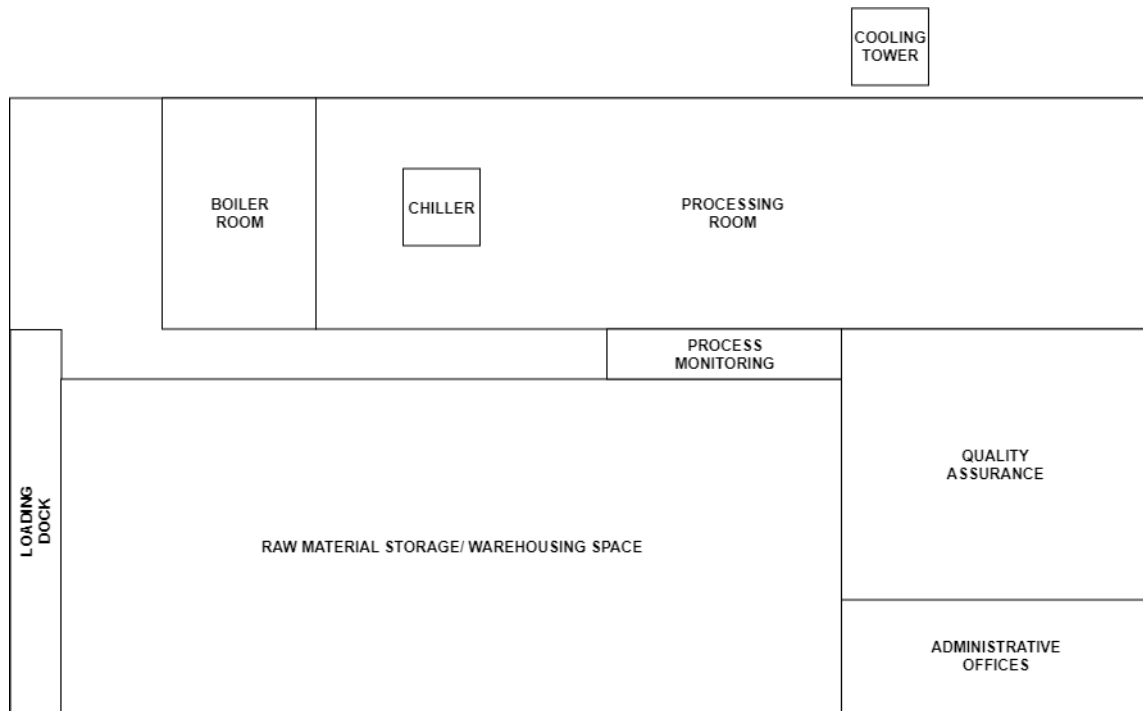


Figure 13: Factory Plant Layout

The plant engineers are very much aware of the importance of energy conservation and are constantly searching for ways to improve productivity. The facility has already upgraded its fluorescent lighting to LED fixtures. The facility is also investigating the best means to install a new chiller. Energy conservation measures have been implemented and additional technologies and concepts are continually being explored.

2.2 Process Description

The facility produces various chemicals by using the following generic process. The raw materials are generally ground into a very fine powder or compacted into a pelletized form, off-site. They are stored in the factory, until processed, at the necessary temperature and humidity conditions.

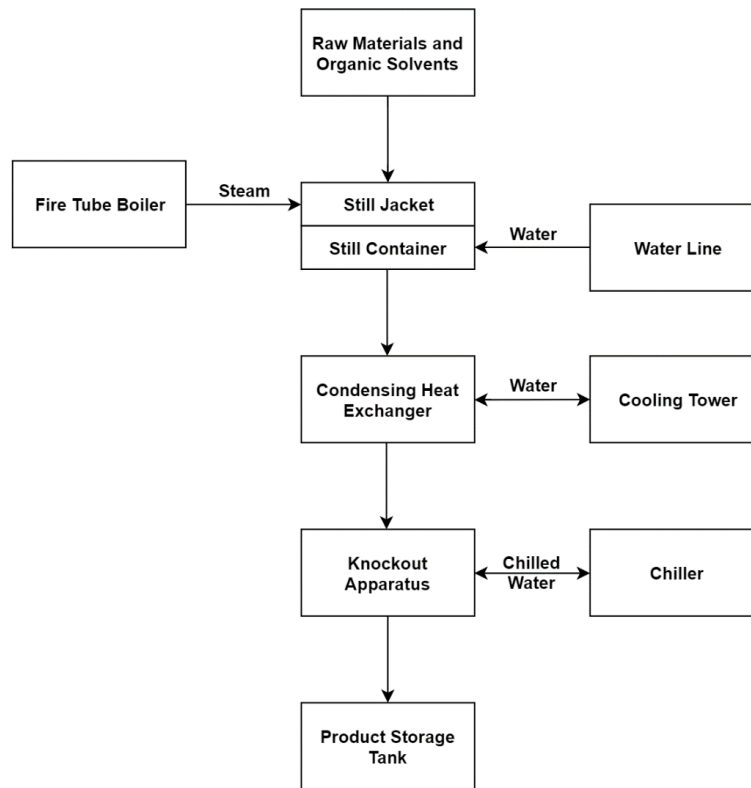


Figure 14: Generic Product Flow

The raw materials are then emptied into jacketed and insulated stainless steel stills and mixed with water and the required amount of organic solvents. The steam jackets on the bottom and around the stills is used to provide the necessary heat needed to boil the raw material and organic solvent mixture diluted with water under a specific vacuum condition. The diluted solvent absorbs the various soluble chemicals from the raw materials. The solvent vapors generated by the boiling process are then passed through a condensing heat exchanger which utilizes cooling tower water as the shell-side fluid and absorbs the heat from the product vapors to condense them. The resulting vapor/fluid mixture is then passed through a condensing heat exchanging apparatus to completely “knock-out” the vapors by further condensation using chilled water from the chiller. The resulting extracted liquid chemicals are then stored in tanks until it is shipped out.

2.3 Problem Overview

As described in the previous section, in the distillation process, the facility currently uses several condensing heat exchangers to condense the chemical vapors incoming from the stills to a liquid state. These condensing heat exchangers utilize a water loop that includes the cooling tower to remove the heat from the incoming vapors and bring about a change of phase. The condensing heat exchangers used at this facility are of the shell and tube type construction with the product vapors running through the tube side and the cooling tower water running through the shell side. The shell and tube materials for heat exchangers dealing with consumables are carefully chosen to allow adequate heat transfer, thermal expansion and preventing corrosion from affecting the quality of the product. To ensure this, most processing equipment, including the tubes inside the heat exchangers, are typically made of stainless steel (SS 316L is the most common grade and is typically referred to as the ‘food grade stainless steel’) as they come directly in contact with the

product. In addition to meeting these requirements, the stainless steel allows for efficient cleaning of smooth surfaces without the risk of biological contamination.

On an average day, the facility produces about 150-200 liters of finished product in its larger heat exchangers every hour. A major inconsistency that the facility is facing is the amount of variation in the volume of the product that is condensed and available at the end of the process line. The variation in the process output is observed across multiple variations of products and across all equipment. This problem occurs throughout the year but is observed to be prevalent in the summer where external conditions in the daytime are particularly hot. At its lowest point, the process output in the summer is about 150 liters per hour. In the winter, the process output is much higher than in the summer and is about 250 liters per hour. This difference in the outputs can only be eliminated by a closer look at the process and the equipment used in the process. Additionally, this causes infiltration of solvent vapors into the diaphragm pump which is undesirable as it is a loss of product, a fire hazard and can cause damage to the diaphragm pumps which are not equipped to handle compressible fluids. Solving these problems are important not only for production planning, but to also prevent overloading or improper use of the equipment which may damage and/or reduce the life of the equipment.

2.4 Initial thoughts

Since there is an hourly variation in the output of the process independent of the type of product, even under constant process parameter set-points, there has to be an equipment-related issue somewhere in the system that causes this problem repeatedly. There may possibly be an issue with the sizing of the equipment, due to which the system equipment is not capable of handling the amount of product and is underperforming. The problem could also stem from incorrect setups

or by an improper fluid transport system. The variation may also be due to the equipment simply being old and having deteriorated over time. However, since most of the equipment at this facility is considered to be purchased in the last 5-10 years, it can be assumed that the equipment is still capable of performing optimally. To further isolate the real cause of the problem, the variables that directly affect the yield quantity of the product must be identified and the equipment associated with those parameters must be looked at in more detail.

The major process parameters that may cause a variation in the process output are the various inputs fed into the system throughout the processing. From the process flow chart, we can see that there are a number of material inputs to the still, which is the first major form of processing equipment in the process flow. The still receives steam from the boiler in the jackets and a mixture of organic solvents and raw materials. Make up water from the main water line is added to this mixture to process this raw material. The steam quality and quantity that the boiler generates is consistent and its working efficiency was verified by checking the boiler stack efficiency which was about 83%, which is an above average value for fire-tube boilers [17]. The make-up water into the still is directly from the city water supply and is assumed to be of above average quality and clean enough for use throughout the year. The organic solvents and raw materials are carefully inspected before usage to maintain a standard quality of the product output as well. The vacuum pumps on the stills are in good condition since the stills perform as intended during normal operation. Thus, we can see that the still must be performing properly and the parameters influencing the still performance are all within normal operating requirements.

The next form of equipment in the process are the various heat exchangers and the cooling tower water loop. The heat exchangers have the cooling tower water running through the shell side and process vapors through the tube side. The loop arrangement is shown in the following figure.

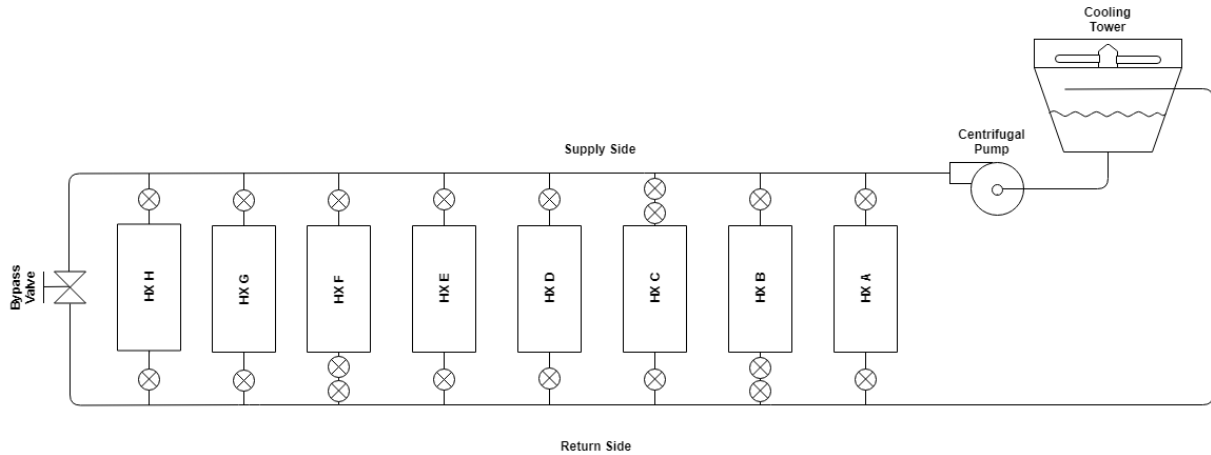


Figure 15: Cooling Tower and Heat Exchangers Loop at facility

This arrangement is called the two pipe system and is very commonly used in the industry for hydronic water loops with a cooling tower or for supplying hot or cool water in a system [18] [19]. These system arrangements are used when multiple loads are present in a system that require simultaneous supply. This system is designed to be used for applications with nearly consistent loads which don't have rapid load changes [18] [19]. The two-pipe system is generally used for large systems and as the name suggests, it consists of two individual pipes, one for supply to the loads and the other one for the return. The arrangement can be implemented in two ways: direct path or the reverse path as shown in the following figure.

The direct return path is the arrangement when the load nearest to the supply source has the smallest supply and return path, whereas the most remote load in the line has the longest supply and return line paths. The reverse return system is the arrangement when the load nearest to the supply source has the shortest supply path and the longest return path whereas the most remote load in the line has the longest supply path, but the shortest return path.

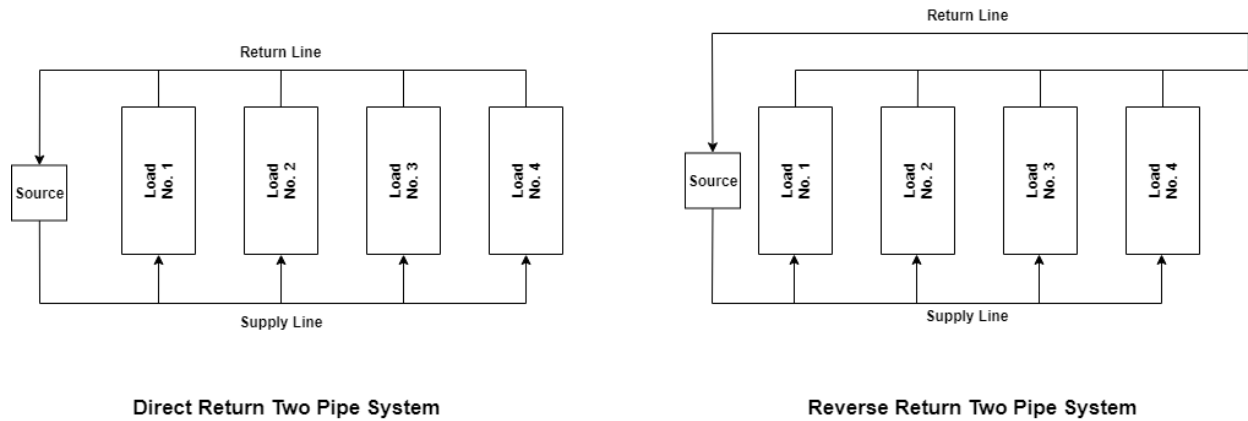


Figure 16: Two Pipe System arrangements

At any flow conditions, there is an inconsistent supply to the various loads in the direct return system where the remote loads are starved. This happens due to the inconsistent pressure differentials seen across the load paths. As a result of the pressure losses in the supply paths, the inlet pressure for the load closest to the pump suction is the highest and the inlet pressure at the most remote load is the lowest. Since water takes the path of least resistance, the closest load sees the maximum flow. This variation in pressure differentials can ultimately cause backflow in the system and in case of cooling applications, unequal cooling due to insufficient flow at each remote load. This problem can be countered by the use of balancing valves or other flow control devices to evenly balance out the flow.

In the reverse return system, the inlet pressures behave in the same way as the former system. However, since the return line is connected from the most remote load, the closest load path now has more friction losses in the return pipe than in the remote load path. This reduces the magnitudes of the pressure differentials in the paths closer to pump suction, improving the distribution of flow to the remote load paths at low flow conditions. In other words, reverse-return

creates approximately equal hydraulic resistance through each flow path without the need for balance valves. [20]

However, the piping for a reverse return system is longer and hence, it typically has a higher first cost over the direct return system. The flow network in place at this facility has a direct return two-pipe system with heat exchangers as the loads on the line. There is a possibility of flow starvation at the remote loads even though there are valves at each heat exchanger inlet and outlet, since these are used only to shut-off heat exchangers when not in use and not for balancing paths. This flow starvation in the heat exchangers at the remote end of the loop, when all exchangers are being used, could theoretically cause a reduction in the heat transfer in the remote heat exchangers, which could be resulting in a lower product yield from those.

Looking more closely at the heat exchangers, there is a possibility of an additional cause of reduction in heat transfer at the surface of the tubes. In the current setup, the facility runs cooling tower water through the shell and the product in the tubes. In most heat exchangers, over time, an accumulation of sediments and residue from fluids flowing through it adheres to the tube surfaces [5] [7] [11]. This is called fouling and it is highly detrimental to the heat transfer taking place within the exchanger. The residues and sediments form an insulating layer on the outer surfaces of the tubes, reducing the heat transfer taking place – and adversely affecting production rates. To this end, the tubes in heat exchangers where there is a high possibility of fouling are expected to be cleaned periodically.

The exchangers at the facility have their tubes cleaned periodically to prevent scale build up and to avoid cross contamination of the products between batches. Since this facility runs untreated cooling tower water directly into the cooling water loop and various heat exchangers, there is a very high likelihood of fouling occurring on the shell side of these heat exchangers. This

seems to be one of the reasons for a reduced product vapor condensation rate and is limiting the output of the process equipment.



Figure 17: Shell side fouling in a petrochemical heat exchanger

Thus, it can be seen that there are several possibilities that may be occurring in this process which lead to the inconsistency in the product output. In order to further understand the possible phenomenon behind this problem, a literature review of fouling and its consequences including flow starvation and pressure drops in heat exchangers is undertaken. Next, pumping arrangements with multiple pumps are examined in order to look at various alternative arrangements. Finally, the working of cooling towers and methods to improve process cooling are examined.

CHAPTER 3: LITERATURE REVIEW

3.1: Heat exchanger Fouling

Stoforos, in his dissertation, [21] looked at the various methods of enhancing the heat transfer across heat exchangers. The author examines the effectiveness of possible fouling reduction measures such as modification of the surfaces of the heat exchangers using computer modelling and simulation. As part of the evaluation process, the author also looks at fouling closely and the reasons behind recurrence of fouling in processing of viscous foods.

Stoforos states that fouling is almost inevitable in viscous food processing and it is a major cause of concern in cooling of viscous foods using conventional cooling techniques. Here, conventional cooling refers to the cooling arrangement using an unmodified heat exchanger that has no method of thermal mixing apart from the inherent turbulent flow mixing within the exchanger. Stoforos also mentions that in thermal processing of viscous foods, there is often a laminar product flow as a result of the high viscosity resulting in low flow velocities. In addition to this, the low thermal conductivity across fluid particle layers in viscous fluids results in a very inconsistent temperature distribution within the product flow that leads to slow and inefficient heat transfer. The lower flow velocities and inconsistent temperature distribution further accelerates deposition of material on the surfaces and reduces the erosion rate of the previously deposited layers which leads to fouling.

At the facility being currently assessed, the product that runs on the tube side of the heat exchangers is considerably less viscous than common food items assessed by Stoforos and the tube side is relatively clean since the tube internal surfaces are scrubbed periodically and in between product batches. However, the exchangers use cooling tower water on the shell side to accomplish condensation of the product vapors and this process may cause fouling on the exterior tube surfaces

since the cooling tower exposes the water in the network to external dirt and dust particles. The heat exchangers are also currently showing signs of flow starvation on the shell side as there is a reduced product output and this suggests that the flow velocity on the shell side might be low. Given these two factors, there is a very high chance that there is indeed fouling in a few heat exchangers at the facility.

Fouling is a complex, time dependent process that can occur at any solid-liquid interface.

The process of fouling in most cases follows the following steps in deposition:

- Fouling components separate in the carrying medium.
- Separated fouling matter is carried to the fluid-solid interface.
- Fouling material attaches, via adhesion, to the walls of the container at the interface.
- Fouling material spalls or partially breaks off from the surface if surface erosion is dominant in the flow stream. Otherwise, it sticks to the surface and bonds with it.
- Deposited material ages and hardens over time if it doesn't break off into the flow.

The rates of product deposition, accumulation and fouling formation depend mainly on the operating conditions such as the fluid and surface temperatures, concentration of insoluble particles and the flow rate within the carrier. The surface properties such as the solid surface material, its surface wettability and the topography also determine the rate and the probability of fouling taking place. Fouling can take place in a number of ways:

- Precipitation or Crystallization fouling: Crystal formation of dissolved salts on the processing surface; occurs in dairy processing and desalination of water.
- Particulate or Sedimentation fouling: Deposition of large particles on the carrying surface due to gravity; occurs in filtration of beverages and processing of amorphous foods.

- Chemical Reaction fouling: Deposition of products of unwanted chemical reactions during heat transfer; occurs in hydrocarbon and crude oil processing.
- Solidification fouling: Deposition of fluid components formed upon solidification by coming into contact with a subcooled surface.
- Corrosion fouling: Accumulation of products of corrosion between flowing fluid and the processing surface; occurs in metal surfaces used in water treatment.
- Biological fouling: Formation of organic films due to attachment of microorganisms and vegetation to the processing surface; occurs frequently in cooling towers and wastewater treatment.

Stoforos states that fouling is most likely to occur in regions of low fluid velocity, due to the absence of eddy currents and inherent shear stresses, which would otherwise cause surface erosion and subsequent removal of the fouling layer in high velocity fluid flows [21]. It is also mentioned that the rate of fouling increases with an increase in the fluid temperature and the surface temperature. This is because for most fluids, the rate of chemical reactions associated with fouling may increase with a rise in temperature, causing an increase in the rate of deposition of the insoluble particles in the flow. However, for certain fluids (such as milk), a higher temperature may be inevitable to eliminate the formation of microorganisms and other biological impurities and special measures must be taken to prevent fouling without compromising on the quality of the product. Corrosion resistance of the fluid carrying surface is another very important parameter as it directly influences the rate of oxide formation which would be deposited on the surface.

Stainless steel is used frequently in food processing equipment since it is a relatively inert structural material and prevents contamination of food items. According to Alliant Metals, Inc, [22] stainless steel is resistant to damage due to denting, nicking and scratching even in extreme

usage conditions. Stainless steel also has very good mechanical properties such as formability, mechanical strength, durability and weldability which makes it a good fluid carrying and holding material. Stainless steel is also chemically neutral to most food items and coloring agents and hence, it does not change the smell, taste and color of the food item. Stainless steel also has a high coefficient of thermal conductivity and is very stable with changes in temperature. Finally, it is also very easy to clean and wash down using chemical agents or detergents. All of these properties aid easy processing of food materials which is why, stainless steel is used for most food and chemical processing equipment, the current facility included. However, stainless steel is not very hydrophobic and hence, it typically has contact angles lower than 90 degrees whenever liquids come in contact with it. A lower contact angle means that a greater quantity of fluid comes into contact with stainless steel surfaces in the form of films or drops. Due to this partial wetting property, there is a high probability of fouling occurring with stainless steel processing equipment, when the flow conditions are conducive.

Apart from surface characteristics and fluid velocity, the rate of fouling is directly related to the shear experienced by the contact surface due to fluid flow. Shear experienced by a film at the contact surface is directly related to the geometry of the heat transfer surface and the velocity of the flowing fluid through that surface [21]. Plate and frame heat exchangers experience heavy shear and turbulent flow even with low fluid velocities, since the fluid flow area is the thin space between two parallel plates. On the other hand, shell and tube heat exchangers with round tubes have a relatively larger fluid flow area within the rounded tubes which necessitates much higher flow velocity to achieve the same amount of shear at the contact surface. This fluid flow geometry is the reason why shell and tube heat exchangers are more prone to heat exchanger fouling than plate and frame heat exchangers. [23]

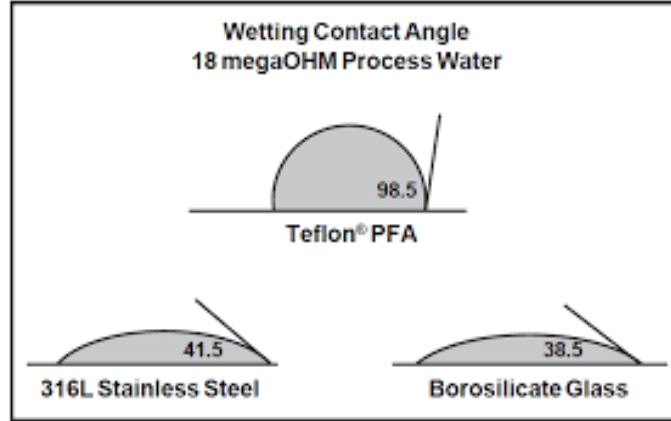


Figure 18: Average contact angles of water with common processing surfaces [23]

There are a number of ways in which fouling can be minimized or even completely eliminated by modifying the surface characteristics of the stainless-steel tubes. [21] Some of these include mimicking the “Lotus effect” which is the natural hydrophobic behavior exhibited by the surface of the leaves of the lotus plant. Fouling reduction in this way can be accomplished by polymer-based or electrochemically deposited coatings on the surface of the exchanger tubes. These surface modification techniques were analyzed by Stoforos and they showed promising results in enhancement of cleaning and heat transfer while processing viscous food materials. However, due to the cost and complexity of the fabrication involved with these processes, these surface modification methods are not widespread in the industry currently.

There are two major detrimental effects caused by fouling in heat exchangers: a decrease in thermal effectiveness and a pressure drop. [5] [11] [24]. The insulating nature of the fouling layer causes a reduction in the overall heat transfer coefficient. The overall heat transfer coefficient for shell and tube heat exchangers is calculated by the given relation [24]:

$$\frac{1}{U \cdot A} = \frac{1}{h_i \cdot A_i} + \frac{R_{fi}}{A_i} + \frac{\ln\left(\frac{D_o}{D_i}\right)}{2 \cdot \pi \cdot k \cdot L} + \frac{1}{h_o \cdot A_o} + \frac{R_{fo}}{A_o}$$

Where, 'U' is the overall heat transfer coefficient,
 'A' denotes the reference surface area,
 'A_i' and 'A_o' denote inner and outer areas respectively,
 'R_{fi}' and 'R_{fo}' are the inner and outer fouling coefficients,
 'D_o' and 'D_i' are the inner and outer diameters,
 'k' is the coefficient of thermal conductivity of the tube material, and
 'L' is the length of each individual tube.

The fouling inside or outside the tubes causes an increase in the fouling resistance coefficients ('R_{fi}' and 'R_{fo}') which are a function of the thickness of the deposited layer (x) and its thermal conductivity (k_f).

$$R_f = \frac{x}{k_f}$$

These relations can be used to quantify the difference in heat transfer that fouling may have caused in the current system. The increased thermal resistance due to the fouling on the shell side should cause an observable reduction in overall heat transfer coefficient. If the values of individual heat transfer coefficients in the heat exchanger can be calculated using the available system parameters, a comparison may be drawn between the current system parameters and product outputs if the possible fouling was eliminated. This can be used to yield a dollar value arising from the increased product generation and sales and can allow calculating a simple payback period that would help justify any maintenance expenditures.

The pattern of change in the value of fouling resistances over time, with increase in deposition at the solid-liquid interface can be one of three possible trends as shown in Figure 19: Linear, falling rate and asymptotic. [5] The linear relation (A) would cause the fouling factor values to increase proportionately with time, the falling rate (B) would have a linear behavior up

to a certain amount of time and a gradual decrease in the slope beyond that. If asymptotic (C), the fouling factor would increase over time but settle to a constant value after a certain time.

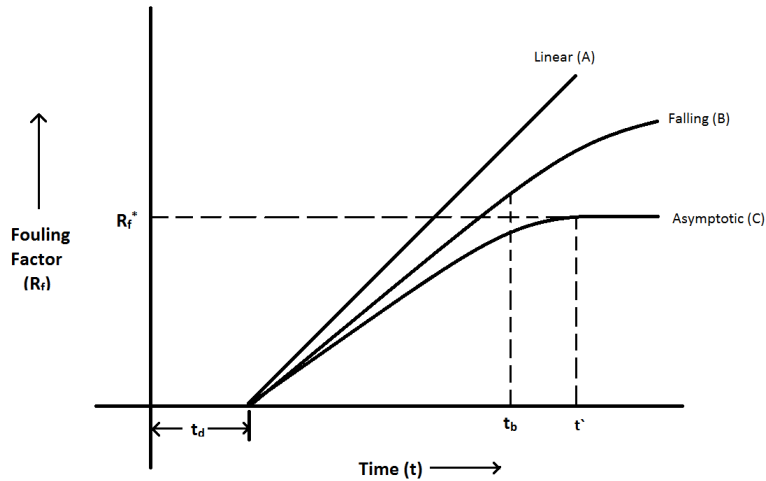


Figure 19: Idealized fouling curves: A) Linear, B) Falling Rate, C) Asymptotic [25]

After a certain amount of induction time t_d , fouling has a noticeable effect due to the difference in the material deposition rate and the removal rate. In a linear curve, the deposition rate remains almost constant and the removal rate is negligible. In a falling rate curve, the deposition rate increases over time but the difference between the deposition rate and the removal rate decreases over time. In an asymptotic curve, the deposition rate gradually increases until a point when the fouling process stabilizes with an equal deposition and removal rate. Asymptotic fouling behavior is the most commonly observed one in the food processing industry.

The residual materials that are deposited can be either low viscosity fluids, high viscosity fluids or cohesive solids depending on the content within the working fluids. Removal of this deposited layer can be achieved by either mechanical removal due to fluid flow action or by some form of cleaning process that breaks the molecular forces of adhesion and cohesion keeping the

material together. Fryer and Asteriadou categorized fouling deposition into three types according to the nature of deposition and the necessary means to remove it. The figure shows a map with ways on how to clean fouling. [25]

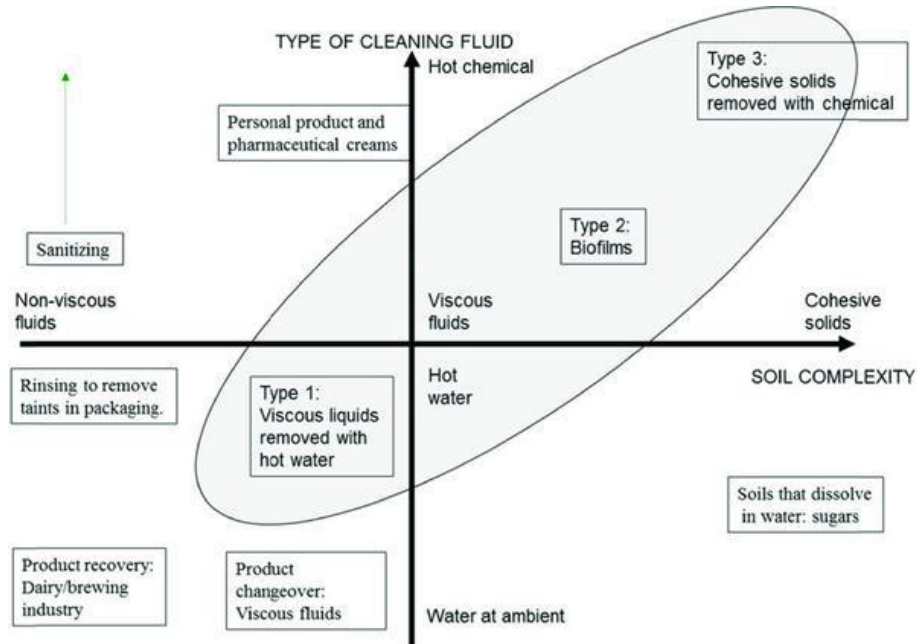


Figure 20: Cleaning Map by Fryer and Asteriadou [25]

Type 1 fouling is the residual fouling left behind after processing viscous fluids that can be easily removed by hot water rinsing, which breaks the weak adhesive and cohesive forces. Type 2 fouling requires cleaning the film formed while also killing the microbiological growth left behind. This is done by using hot water rinsing and some form of chemical cleaning. Type 3 fouling involves cleaning the cohesive solids which are difficult to remove from the contact surface by any means other than chemical cleaning.

It can be seen that heat exchanger fouling is a complicated problem in any heat exchanger application that is difficult to predict and completely eliminate. It is estimated that on a global scale, the cost penalties associated with use of fouled heat exchangers is roughly about 0.25% of

the annual Gross Domestic Product (GDP) for industrially developed countries. [26]. This shows the economic impact that heat exchanger fouling can have on a bigger scale and any means of reducing the impact of this occurrence is important not only on the small scale but also on a global scale. The next sub-section looks closely at the major effects of fouling in heat exchangers.

3.2: Pressure Drop in Heat Exchangers

As discussed in the previous section, the biggest problem that occurs in heat exchangers due to fouling, apart from the change in heat transfer is the reduction in flow rates due to obstruction of flow area. The flow itself is driven by the pressure difference in the flowing medium and this is an important parameter in heat exchangers since the heat transfer is directly dependent on the flow rate. Heat exchangers inherently cause a pressure drop in the tube-side fluid and the shell side fluid due to frictional losses when interacting with the various components [5] [14]. The tube side fluid experiences pressure losses mainly due to friction and changes in flow direction. The shell side fluid experiences a pressure drop due to the friction arising from interaction with the tube bundles and baffles in addition to the changes in flow direction after every baffle. To further understand these pressure variations and the ways in which this can affect the flow within the network, a literature review of pressure drops in heat exchangers was necessary.

In his dissertation [27], Speyer illustrates the complex flow paths followed by the shell-side fluid in a heat exchanger which is shown in Figure 21. He mentions that it is very difficult to get a 100% accurate estimation of the magnitude of either the pressure drop or the heat transfer, simply because there are too many variables involved in the design and fabrication of heat exchangers. Unless obtained via complex iterative methods by someone with considerable prior experience, it is very difficult to account for the flow through the various clearances and leakage

streams using standard published equations. Speyer then proceeds to calculate the pressure drops and heat transfer coefficients for the various individual flow regions within the segmented baffle cuts and across the tube bundle. Since there are considerable variations in the velocity of the fluid within each region, the heat transfer is calculated using a geometric mean of the crossflow and segment cut velocities. However, Speyer aimed to obtain a more accurate result by using a fluid flow value that also considers the velocities and flow areas of the various leakage streams that deviate from the main central stream that flows across the baffle.

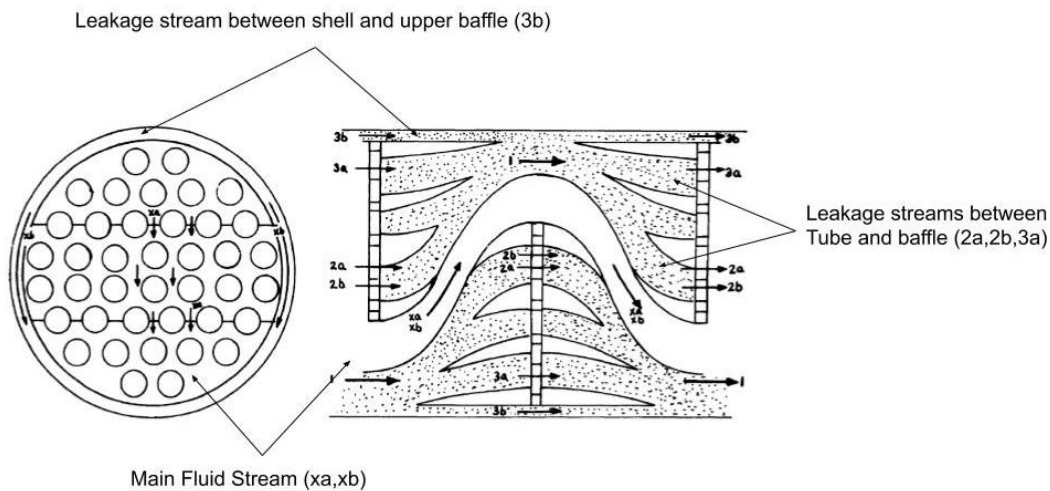


Figure 21: Complex Flow paths taken by the shell side fluid around a segmented baffle [27]

Donohue [8], in his paper on heat transfer and pressure drop in heat exchangers states that in actual industrial applications of heat exchangers, the flow on the shell side does not actually penetrate the entire available flow area within the tube bundle and the flow area is actually less than the entire area between the segmented baffles. This makes sense since, even if the exchanger runs full on the shell side, flow velocities would be constrained by the complex geometry created by the baffles and the tubes. The paper considers the consequent effects of this partial flow penetration on the coefficients of heat transfer and the friction factor for the flow. Since there are

proportional changes observed in the heat transfer coefficient due to minute changes in the fluid flow, Donohue tries to quantify the differences due to different shapes and arrangements of baffles by testing various exchanger geometries under similar operating conditions.

The Sieder-Tate Equation is used by Speyer to calculate the Nusselt number for turbulent flow inside or outside tubes. This correlation has the following form:

$$\frac{h \cdot D}{k} = C \cdot \left(\frac{D \cdot G_C}{\mu} \right)^n \cdot \left(\frac{c_p \cdot \mu}{k} \right)^{0.33} \cdot \left(\frac{\mu}{\mu_s} \right)^{0.14}$$

Where,

- ‘h.D/k’ is the Nusselt Number for the surface,
- ‘h’ is the heat transfer coefficient,
- ‘D’ is the equivalent Diameter of the tube bank,
- ‘G_C’ is the crossflow mass velocity through the tube bundle,
- ‘mu’ is the coefficient of dynamic viscosity,
- ‘k’ is the coefficient of thermal conductivity for the fluid,
- ‘c_p’ is the specific heat capacity of the fluid.

The constant ‘n’ is 0.8 for internal flow and 0.6 for external flow. The constant ‘C’ in this relation changes with the type of heat exchanger unit being examined and is dependent on its construction. The ratio of viscosities is multiplied to account for the variation in the viscosity over the range of temperatures across the flow area under examination.

Donohue tested shells with segmental baffles and disk and doughnut baffles to find values of ‘C’ that correlate the experimentally derived heat transfer coefficients for the shell side. The value for ‘C’ depends on the structural characteristics like the arrangement of tubes and the shell leakage areas and directly influences the heat transfer actually taking place. The author individually varied the baffle spacing, baffle opening size, leakage areas and the tube arrangement within the shell while maintaining the other system parameters in this experimental process.

Increasing the baffle spacing resulted in a lower number of baffles in the shell but yielded a higher heat transfer coefficient since the available flow area to the stream increased, resulting in greater surface contact with the tube bank. Having smaller baffle openings increased the value of 'C' since the flow velocity across the tube banks increased due to a reduction in flow area. The author also mentions that there is a greater variation in the values of 'C' by varying baffle spacing rather than baffle opening size variations. A higher leakage area was obtained by having more diametric clearance between the baffle and the shell internal diameter, and between the tubes and baffle holes. This led to reduced contact between the tube bank and the shell side fluid flow, reducing the value of 'C'.

All of these results were cross verified by using disk and doughnut baffles in place of segmental baffles, and it was found that the results were consistent, regardless of the type of baffle. However, Donohue noted that the heat transfer coefficients obtained when using disk and doughnut type baffles were about 15% higher than when segmental baffles were used. This effect is attributed to the higher loss of flow energy of the shell-side fluid via dissipation as eddy currents within the pockets formed at the baffle openings when using segmental baffles.

Donohue also studied the pressure drop occurring naturally in heat exchangers due to various friction losses in the fluid flow path along the shell. The three main sources of pressure drop were from the flow through the nozzles, flow through the tube bundle and the flow through the baffle opening. Of these, the magnitude of frictional pressure losses through the baffle openings was very high compared to those in flow across the tube bundle. The values of pressure drops showed greater fluctuations and were more inconsistent than the fluctuations observed in the heat transfer coefficients, and this is attributed to the pressure drop being proportional to the square of the flow velocity while heat transfer is proportional to the 0.6 power as per the Sieder-Tate

equation. Since both these quantities are related to the flow velocity, they are interrelated, but because of the difference in their relation to the power of the velocity, pressure head losses are more sensitive to flow velocity variations than heat transfer coefficients.

The inherent pressure drop for the shell and tube heat exchangers in the current network at the facility in question can be obtained by use of the Bell-Delaware method as mentioned by Donohue. This method calculates the pressure drop as the addition of the individual losses in three regions: the entry region, the inter-baffle crossflow space and the inter-baffle ends. This method uses empirical correlations, with three correction factors to account for leakage streams and baffle spacing, to estimate the friction factors. The method is illustrated further in Chapter 4.

3.3: Multi-pump Pumping Systems

When the desired flow requirement and/or pressure head of liquids in a flow network go beyond the capabilities of a single pump, it becomes necessary to use arrangements with multiple pumps. Pumps can be arranged in either series or in parallel and each of those arrangements are suitable for different system characteristics. Most closed loop industrial applications for process and space cooling have an upper pressure head requirement on the supply side and lower pressure head requirement on the return side to prevent backflows and cavitation in the circuit. This is in addition to a minimum flow requirement since the purpose of a pumping network in cooling is to essentially have the cooling medium run through a cooling coil or a heat exchanger where the rate of heat transfer occurring is directly dependent on the flow rate through the device.

Pumps in series are used when there is a consistently high static head requirement that a single pump cannot fulfil, and an increase in flow rate induces a rapid rise in the pressure losses. Pumps in series build up pressure head as a sum of the operating pressure heads of both the pumps

since the discharge of the first pump is connected to the entry of the second pump. However, when using two pumps, the pressure achieved at a given flow will not be twice of the individual pressure head, since the operating point follows the system curve and pump curve intersection. This buildup of pressure head using two impellers can also be achieved via multistage pumps which allow reducing the impeller diameter and eliminating the problems with monitoring and operating multiple motors.

Parallel pumps are used for static-head dominated systems where the head requirement is relatively consistent over a wide range of flows. In such cases, the system curve, which dictates the operating point on the pump curve, is considerably “flatter” which shows that the head losses within the system do not fluctuate much over the operating range of flows. [12] The resultant flow rate for pumps in parallel is the summation of the flow rates from the individual pumps at the given pressure head. However, this still doesn't mean that two similar pumps will result in an operating flow rate twice that of the single pump in practice. This is because the equilibrium point of the pumps is always at the intersection of the system curve and the pump curve. Pumps connected in parallel are practically done so by use of a header or a manifold, which is a large pipe used to collect the discharge from the pumps and provide pressure equalization when mixing fluids from multiple sources.

Parallel pumps are used very frequently in cooling applications to achieve system redundancy and to prevent the associated processes from shutting down out of complete starvation. When pumps are used in parallel, a general rule of thumb is to try and use either similar pumps in parallel or to use pumps with nearly similar flow characteristics. This is recommended by most pump manufacturers in order to ensure that operating efficiencies of the pumps in simultaneous operation still remain within an acceptable range.

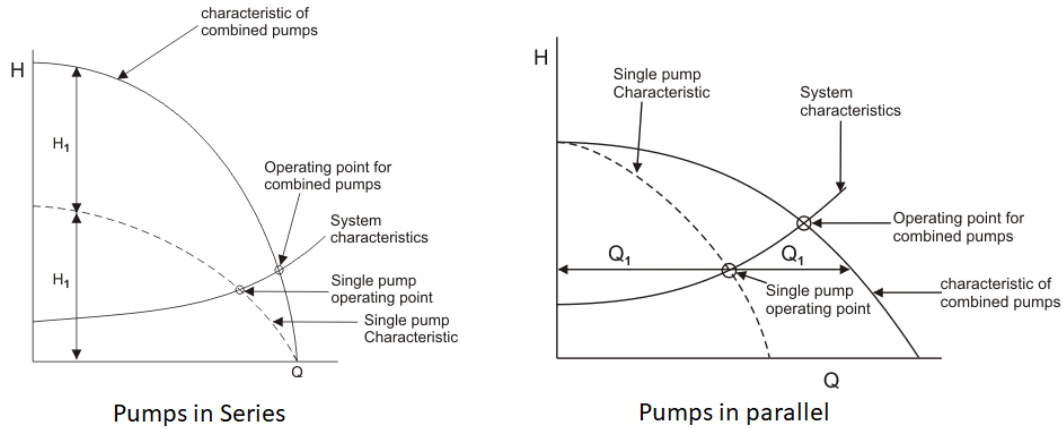


Figure 22: Pump and System Curves for multiple pumps [28]

Wen, Zhang and Wang [29] studied the relationship between maximum efficiency of centrifugal pumps in parallel. Twenty-eight combinations of seven centrifugal pumps with flows ranging from 25 m³/hr to 480 m³/hr and rated heads of 20 meters were tested while operating in parallel and it was observed that when the flow ratios of two unlike pumps operating in parallel is under 1.6, the combined maximum operating efficiency of the system can be as high as 85%. However, as the flow ratios approached 2.0 and above, the operating efficiencies sharply declined to 70% or less. This shows that it is inefficient to use dissimilar pumps with very different rated flow ratios or rated pressure heads in parallel.

At the current facility, the diminished product yield at various times may be due to flow starvation of cooling tower water in the equipment on the network. Since this could have been caused due to the heavy process cooling load on the demand side, there may be a need to increase the flow rate reaching the various condensers. The best way to rectify this problem would be to look at alternative pumping arrangements which can handle the flow and pressure head requirement for the process loads. Since the demand side has plenty of heat exchangers in the circuit, it is likely that the pressure drop across the exchangers also plays a role in the flow distribution and it may be necessary to look at pump arrangements in series and in parallel to find

the best alternative. It may also be cost effective to think of arrangements that can be used to achieve the desired flow parameters via retrofitting on to the current system.

3.4: Cooling towers and Water side Economizers

A number of industrial facilities require year-round means of achieving process cooling, temperature control and/or space cooling within the facility. The standard way to achieve year-round cooling involves use of air-cooled or water-cooled chiller units which can provide low temperature chilled water using the vapor-compression refrigeration cycle. This chilled water can then be used in the cooling coils within process equipment or circulated across the various air-conditioning terminal units for space cooling. As the amount of heat load on the equipment increases, the condenser units within the chillers have to continuously reject heat to the atmosphere to maintain the chilled water entry temperatures to the process or the cooling coils.

Condenser units can be either air-cooled or water-cooled. In water-cooled chillers with cooling towers, the heat transfer on the condenser end occurs due to the temperature difference between the process cooling water and the ambient wet-bulb temperature. In air-based process cooling systems, the heat rejection occurs between the process cooling water and the dry-bulb temperature. Since the ambient wet-bulb temperature in any environmental situation is always lower to or equal to the ambient dry-bulb temperature, a cooling tower based water-cooled chiller system is always more efficient in rejecting heat to the environment than air-cooled systems. The ASHRAE Handbook [30] states that air-cooled heat exchangers can cool water to within 20°F of the ambient dry-bulb temperature while cooling towers can cool water to within 4°F to 5°F of the ambient wet-bulb temperatures. Cooling towers are typically used in the industry as an extension

of the condenser unit of the chiller or along with a heat exchanger in a circuit with the process load.

Open circuit or wet cooling towers cool water by a combination of heat and mass transfer [30]. The heat carried by the chilled water entering the cooling tower is rejected by spraying it over a fill material with narrow passageways that allows direct contact of the water with the incoming airflow. The airflow induces evaporation of a portion of the water by absorbing the enthalpy of vaporization from the remaining water. The water vapor thus generated is carried away into the airflow as drift. Closed circuit or “Dry” cooling towers recirculate water within a secondary external loop which is sprayed over the closed-circuit pipes carrying the refrigerant fluid from the process. A common application of closed circuit cooling towers is for evaporating condensers in ammonia-based refrigerant systems. The cooling towers are illustrated in the figure below.

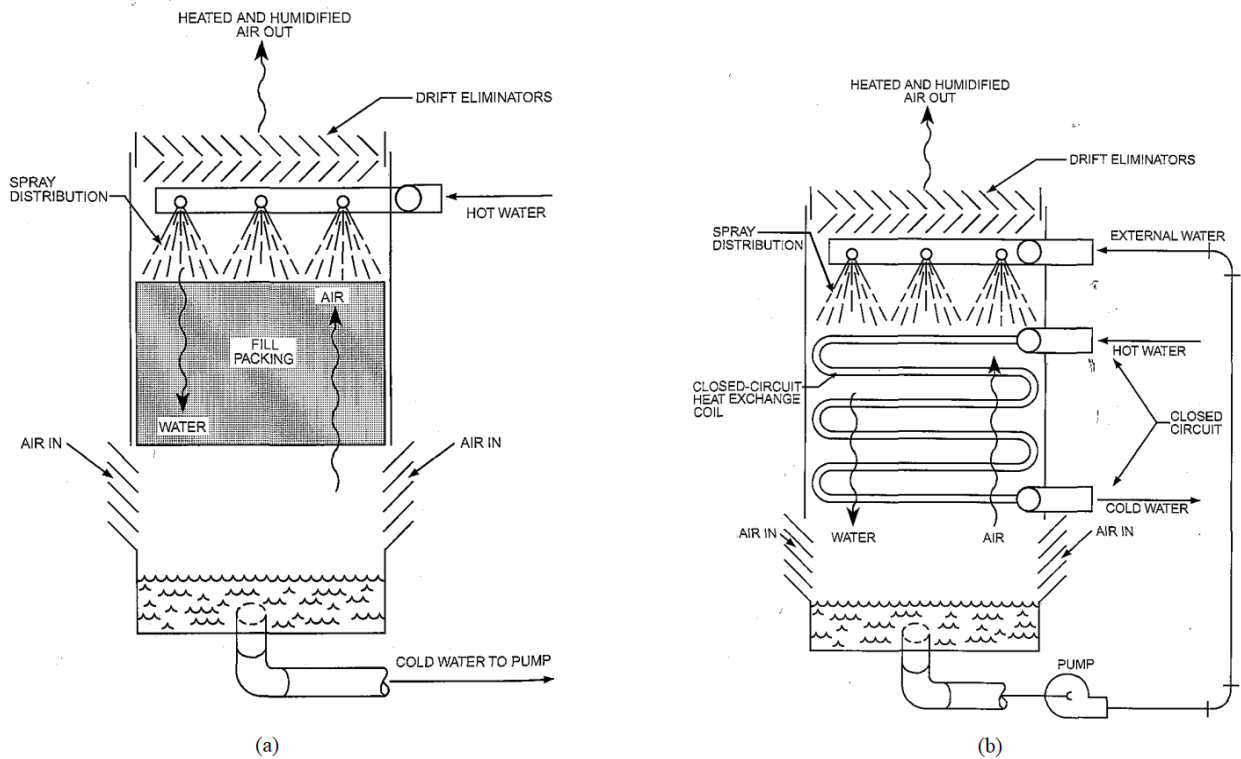


Figure 23: Cooling Towers: (a) Open Circuit/"Wet" Tower (b) Closed circuit/"Dry" tower [30]

Since the cooling tower is a water to air heat exchanger, its performance is dependent on the ambient air temperatures, specifically the ambient wet-bulb temperature. The resulting performance is measured by the approach temperature and range which are performance benchmarks and a way to compare different cooling towers [31]. The cooling tower approach is the positive difference between the ambient wet bulb temperature and the cold-water temperature exiting the cooling tower.

$$\text{Cooling Tower Approach} = T_{\text{Cold water, exit}} - T_{\text{Ambient Wet Bulb}}$$

$$\text{Cooling Tower Range} = T_{\text{Hot water, entry}} - T_{\text{Cold water, exit}}$$

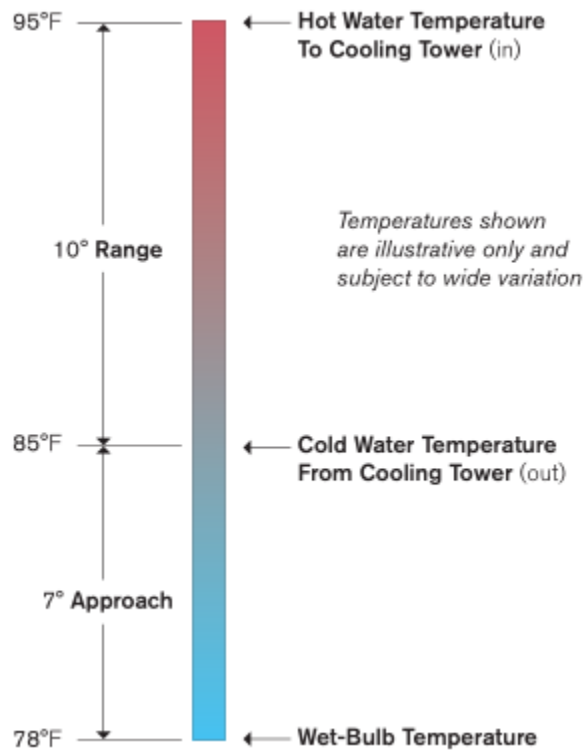


Figure 24: Range and Approach temperature in cooling tower operation [31]

It can be seen that a smaller approach temperature is a sign of good efficiency as this would mean the cooling tower is efficient enough to reduce the cold water exit temperature close to the possible limit, which is the wet-bulb temperature. The approach of any given cooling tower unit is directly proportional to the heat load and inversely proportional to the cooling tower size. The range of a cooling tower is the difference in temperatures of the water at the entry and exit of the cooling tower. It is a measure of the cooling ability of the cooling tower and does not change very much with variation in flow and heat rejection conditions, but can be varied by the cooling tower fan controls. For example, a range of 10°F would mean that the cooling tower is capable of cooling 80°F water to 70°F water, or 50°F water to 40°F water. This is because if the cooling tower exit temperature increases, the temperature of water entering the cooling tower will increase by the same amount since the process heat load, the specific heats and the mass flow rates remain the same [31].

Many geographical regions experience periods of low ambient dry bulb and wet bulb temperatures in the winter months and shoulder months. In such regions, there is a possibility of using the low temperature ambient air as a heat sink. This can help reduce the energy footprint of the cooling system by partially or entirely shutting off the chiller which is the primary consumer of energy. These energy savings can be achieved by employing “free-cooling” which involves bypassing the chiller and running the water in the cooling network directly through a cooling tower. Since the ambient temperature is low enough, chilled water can be obtained without having to run a chiller; the cooling tower allows rejection of process/space heat directly to the air. The energy savings in such a scenario would translate into cost savings in the form of electrical demand and energy savings since the cooling tower fan motor and the pump are the only things operating in the circuit in free-cooling mode. [32]

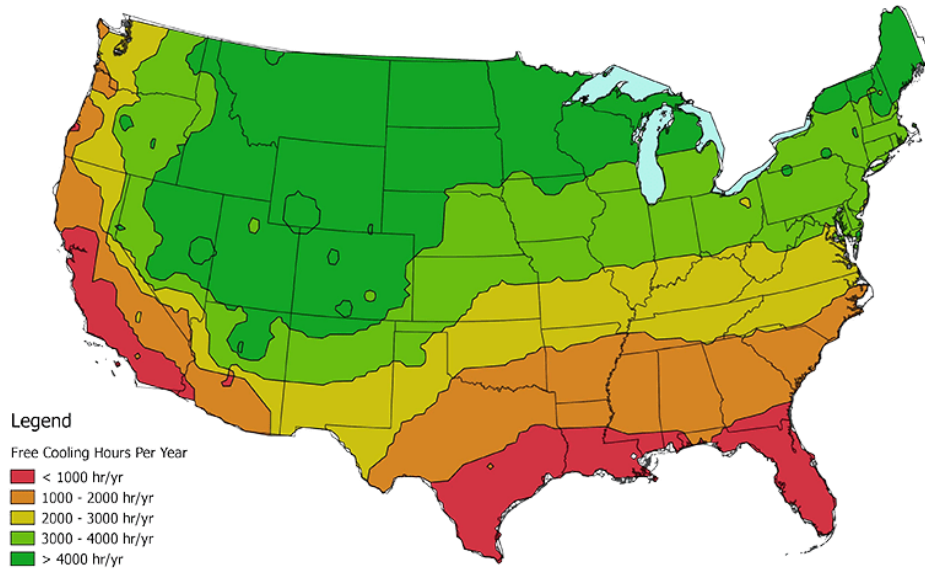


Figure 25: Annual Free-Cooling hours possible with Ambient Wet bulb lower than 50°F [33]

Waterside economizers can be employed in a number of configurations with a chiller as illustrated in Figure 26: via a strainer cycle, via an indirect evaporative precooling coil, via an evaporative cooler with an air-cooled chiller, via a free-cooling chiller or via a plate-and-frame heat exchanger. [34] Most of these arrangements involve using just the cooling tower to obtain chilled water for process or space cooling when the ambient wet bulb temperature is low enough to induce an adequate cooling effect with or without the chiller.

In a strainer cycle, the process cooling loop and cooling tower loops are directly connected, but isolated with valves in normal cooling mode. When the ambient wet bulb temperature is low enough, the cold water from the cooling tower is routed directly into the process cooling loop via automatic shut-off valves in the circuit. The energy and cost savings in this case result from shutting off the chiller. Although, this is a good way of reducing the energy usage, due to the cooling tower water being run directly through the chiller, there is a chance of fouling occurring in the chiller's condenser unit, which can be very expensive to fix!

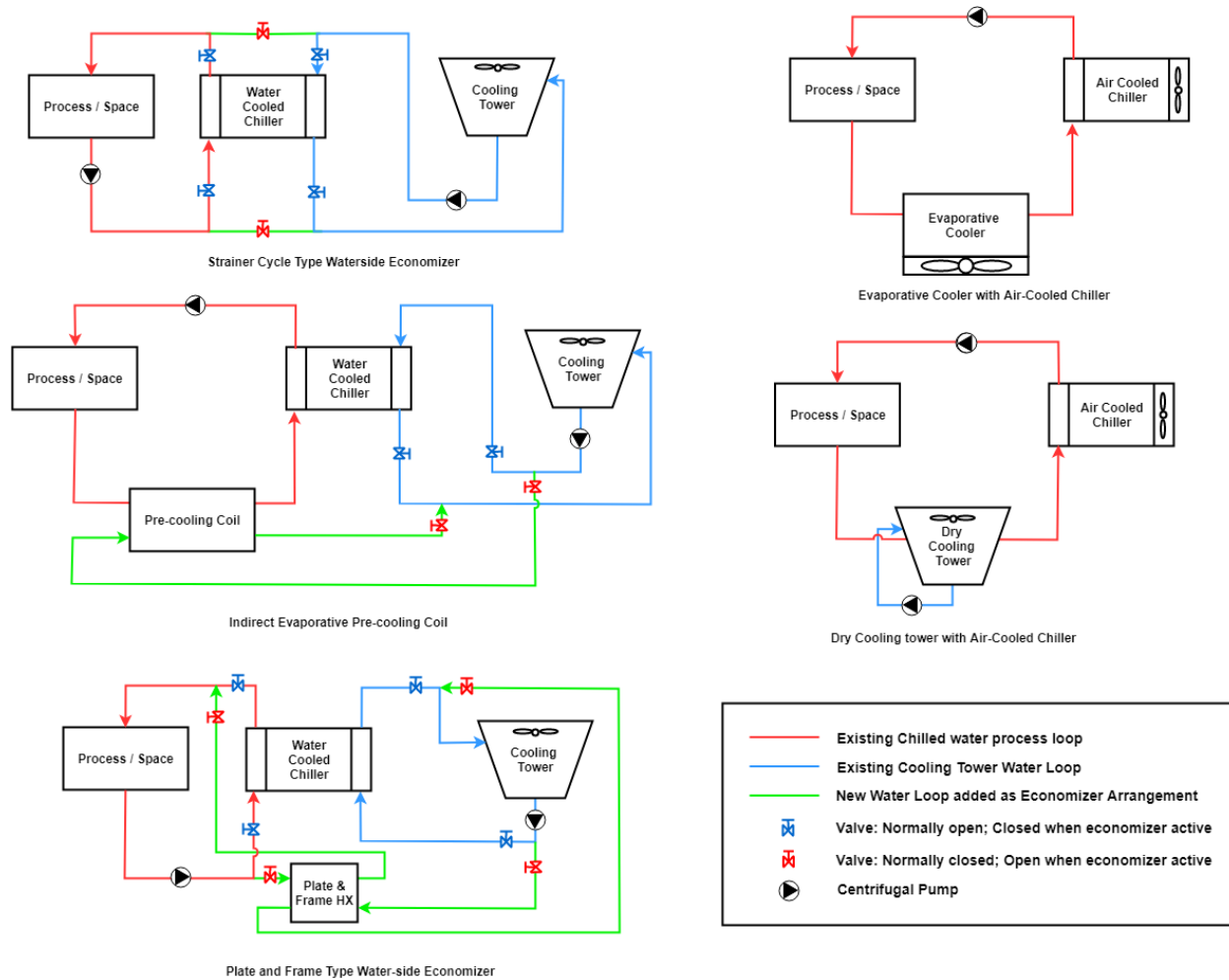


Figure 26: Waterside Economizer Arrangements

An indirect evaporative precooling coil involves use of a cooling coil with cooling tower water to absorb heat from the process water. This additional cooling coil is in series with the chiller evaporator unit, but upstream of it. Thus, it enables a reduction in the cooling load on the chiller, allowing it to run either intermittently or at a lower capacity. This method has the possible problem of fouling and microbial growth occurring in the precooling coil since it runs cooling tower water directly. Additionally, water cooled chillers may not perform as efficiently when partially loaded below their peak efficiency load range at 60%-70%, since the efficiency of the compressor drops when it is operated below 50% of its rated load. [35]

An evaporative cooler can be used in space cooling applications, in series with an air-cooled chiller to reduce the cooling load on the chiller. In this arrangement, the evaporative cooler is the only equipment that runs until the cooling load increases, which is when the air-cooled chiller is turned on. This arrangement allows reduction in electric demand and energy since the air-cooled chiller is not running all the time and evaporative coolers are cheaper to run when the cooling loads are low.

A “Dry” cooling tower can be used in the cooling network when the ambient wet bulb temperature is low enough such that the process entry temperature of the chilled water can be achieved without having to run the air-cooled chiller. This arrangement involves using a dry cooling tower in series with the chiller and allows reduction of energy consumption since the desired chilled water temperature can be attained just by running the cooling tower pump while the air-cooled chiller remains shut off.

The most common way of implementing a waterside economizer is to have separate loops for the cooling tower water network and the chiller evaporator network by installing a plate and frame heat exchanger for clean and efficient heat transfer between them. This arrangement involves using the cooling tower to cool the tower water in its own, separate loop to a temperature as close to the ambient wet bulb temperature as possible and then have it absorb the process or space heat via heat transfer in the plate and frame heat exchanger. The chiller can then be completely shut off or run only intermittently using bypass valves on the evaporator side that are controlled by ambient air enthalpy sensors. This allows for a very efficient way of running the chillers while ensuring little problems due to fouling in the future.

A “free cooling” strategy can also be implemented in modern chillers where the evaporator heat exchanger is installed below the condenser heat exchanger, such as in the Trane CenTraVac

Centrifugal chiller model shown in Figure 27. The phenomenon of refrigerant migration or “thermosiphon” can be used to allow the refrigerant cycle to run without having to use the compressor when the ambient air temperature is lower than the desired chilled water temperature requirement. In this arrangement, when the ambient air temperature falls below the chilled water entry temperature, bypass valves and refrigerant lines connecting the evaporator and the condenser units open up. The evaporator allows exchange of heat from the process chilled water to the liquid refrigerant, causing a phase change and converting it to a vapor. Due to thermosiphon, the refrigerant vapor migrates towards the condenser unit where the temperature is already cooler due to the cold cooling tower water. Heat transfer at the condenser unit causes the refrigerant to change into the liquid phase again and due to gravity, the refrigerant flows back into the lower evaporator where the cycle repeats. Trane states that “free cooling chillers serving systems that can tolerate warmer chilled-water temperatures at part-load conditions can produce over 60% of the rated capacity without compressor operation.” [34] This may be an optimistic value based on laboratory measurements and not practically achievable in industrial environments; about 20% of the rated capacity may be achievable.



Figure 27: Trane CenTraVac Centrifugal Chiller with condenser above evaporator [36]

It can thus be seen that depending on the annual climate of the location in question and the operating condition of the cooling tower, waterside economizers can be used in various arrangements to realize substantial energy savings with well-tuned and well setup cooling systems. Even though waterside economizers add to the upfront installation costs for chillers, they are an energy efficient way to offset the operational expenses arising from the electricity demand in the colder winter months. The facility currently being examined may benefit in the long term from installation of a water-side economizer along with a new dedicated process cooling chiller as such an arrangement would be much easier and cost-effective to incorporate from scratch rather than as a retrofit installation. The feasibility for such an installation can be analyzed by looking at the meteorological data for the location and looking at the amount of time annually when the ambient wet bulb temperature is low enough to justify shutting off the chiller and utilize “Free Cooling”. Chapter 4 takes a closer look at the feasibility and the payback economics of installing a water-cooled chiller along with a water-side side economizer.

CHAPTER 4: ANALYSIS AND PROBLEM SOLVING

As previously stated in Chapter 2, the facility has very specific, identifiable problems with the distillation process, which are observable as a number of symptoms, described further in this section, that seem to point to irregularities in the flow within the various heat exchangers and the piping network associated with it. This chapter looks at pinpointing the core causes of the problems currently observable in the facility via a root cause analysis of the observable symptoms. Following this, a few possible short-term and long-term solutions are identified and analyzed on the basis of equipment sizing, initial implementation costs and the simple payback periods on these investments.

4.1: Root Cause Analysis

Looking at the network from a thermal and hydraulic perspective simultaneously, the problem of low product output can be traced back to the key root causes by looking at the observable symptoms closely. It is worthwhile to think in reverse when analyzing a manufacturing process dependent on a number of parameters and interconnected process equipment, in order to identify critical points of concern that may cause trouble. It could be perceived from the observations done on-site that a reduced product output would only be instigated due to either problems with the primary processing equipment or the energy transfer equipment.

One point of concern in the processing equipment, apparent in the first visit to the facility, was the fact that the cooling tower water is being circulated directly into the heat exchangers. This is not ideal since the cooling tower is open to the atmosphere, exposing it to dust and other contaminants. The cooling tower water can contain traces of external dust matter from the surrounding area which can end up directly into the pipe network and settling in places where there

isn't enough velocity in the immediate stream to dislodge it and push it out again. Although the system might only contain traces of such material, the material may build up in layers within regions with low velocity, resulting in flow blockage and surface accumulation over time. If this happens inside the heat exchangers, there is a possibility of scaling and fouling occurring, which also results in reduced heat transfer. Since the facility is experiencing reduced product output, there is a chance of fouling being the cause behind that. Additionally, no means of monitoring the concentration cycles or the electrical conductivity of the cooling tower water and conducting blowdown were observed within the system. The facility uses make up water entering via a float valve directly into the tower basin which is then circulated through the system. This operating/monitoring method is inefficient and needs to be addressed in the near future to prevent the occurrence of fouling.

A functional and reliable piping network is a basic requirement of any process industry, especially in manufacturing facilities in which the process output is highly dependent on the fluids being handled through the piping network in and around the facility. At the current plant, this is especially true as the magnitude of the process output is directly dependent on the cooling tower water network for the distillation and condensation processes. The heat exchangers at this plant use the cooling tower water on the shell side of the heat exchangers to condense the product, which is running through the tube side. A deeper look at the sizing and pathways within the cooling tower water piping network is necessary in this case as the problem of reduced product generation at various times could be directly linked to flow-related problems within the network that would also partially deteriorate the thermal performance of the cooling tower water loop.

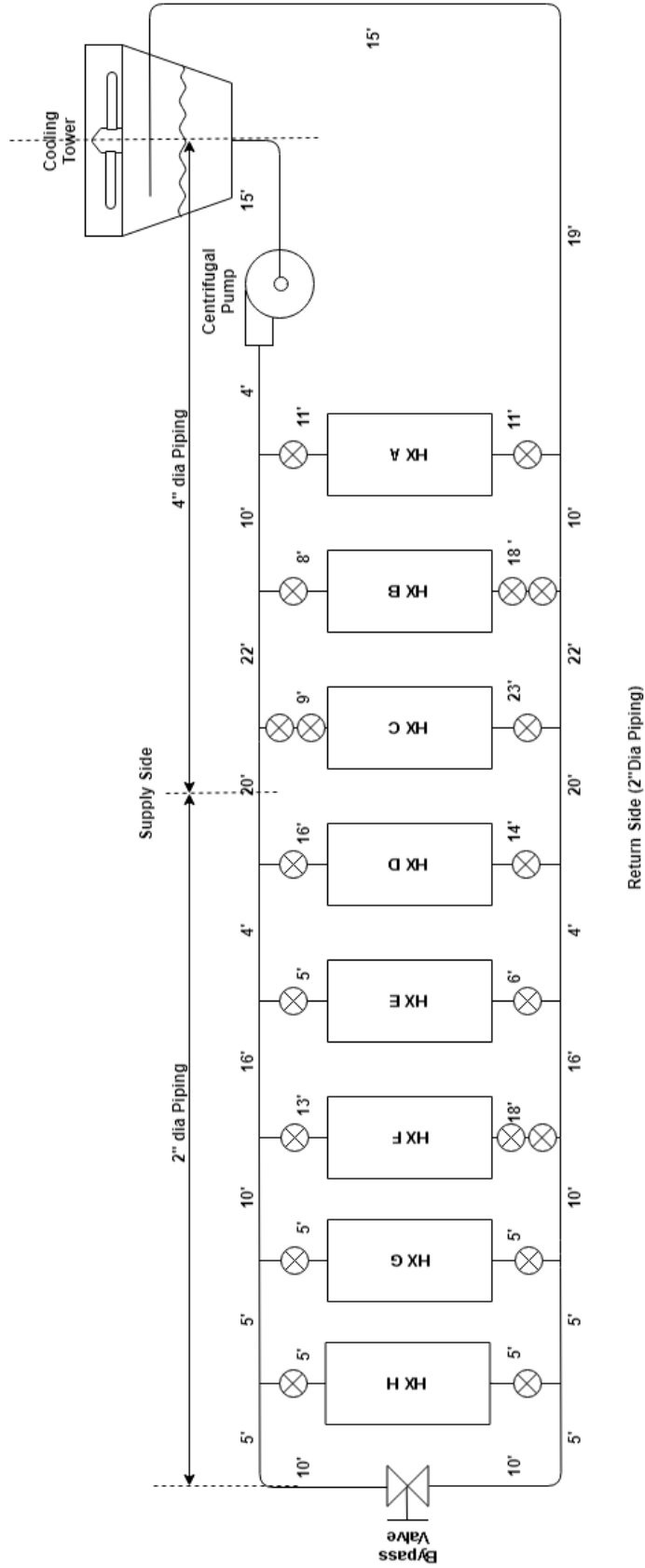


Figure 28: Current Piping network

The pipes in this network run through the facility and are mounted on the walls, about a foot below the ceiling. The supply pipe diameter reduces from four inches from the pump outlet to two inches in the latter part of the network, beyond the first three heat exchangers. The return pipe is two inches in diameter throughout. There are expansion and contraction fittings at the heat exchanger shell inlets which allow connecting the incoming supply pipe with the inlet diameters of the shell entry ports. The cooling water loop uses PVC piping since it is cheap, widely available and easy to work with. The centrifugal pump is located at the base of the cooling tower and these are located right outside the plant wall. The heat exchangers are connected in a two-pipe direct return system with the centrifugal pump and the cooling tower. The network map as shown in Figure 28 was created after visually inspecting and measuring the current system in place.

The biggest point of concern is the deterioration in the operation of the heat exchangers under the current operating conditions. This may be caused by either insufficient heat transfer between the fluids in it or due to problems within the cooling water distribution or both. Since the heat transfer coefficients for the heat exchangers are dependent on the Reynolds Number values of the fluids, it is critical to ensure that the cooling tower water reaches the heat exchangers in the right quantity and quality. The pump and the flow network must be inspected for any blockages or major leakages which may cause insufficient cooling water flow into the heat exchangers.

The facility recently added more heat exchangers to the system, which is when they started observing a lot of variation in the outputs from the system. This points to the possibility of insufficient cooling capacity of the cooling tower network. It may be that the pump is overloaded and is unable to push water at an adequate rate to induce heat transfer in the heat exchangers. This can be cross-checked by analyzing the major and minor head losses in the system and looking at the pump curves and the operating flow requirements. Since the heat exchangers also contribute

to a major portion of the pressure drops across the supply and return pipes, the shell-side pressure drop from all the heat exchangers must also be considered. If the system and pump curves are plotted on a flow versus head graph, the operating point of the pump can be found. If the pump is not operating within reasonable limits from its Best Efficiency Point, it can only mean that the pump is no longer sufficient for the system and alternative arrangements must be examined to prevent recurring financial losses due to inadequate operating conditions.

The facility management also mentioned that they frequently see output variations with changes in ambient temperatures. These changes are definitely linked to the variation in the water temperature which the cooling tower can suitably attain before it goes to the heat exchangers. As seen in Chapter 3, the performance of a cooling tower is not only linked to the ambient wet-bulb temperatures which cannot be controlled, but also to the placement and orientation, which can be controlled. Alternatively, by adopting a cooling scheme that is much more reliable and effective throughout the year, the facility may be able to prevent output variations due to external, uncontrollable circumstances. A chiller can be used to generate the chilled water at the desired process entry temperature throughout the year. The associated costs of installing and operating a chiller can be examined by conducting a heat balance analysis of the maximum capacity of the current equipment and calculating the cooling load on the chiller. With a properly sized chiller in place, ideally, the facility would probably be able to consistently generate more product justifying the installation and operating costs completely over a period of time.

The other possible cause of reduced product generation can be improper heating of the stills via the steam system. The stills are large steam-heated pressure vessels and have jackets on the bottom and the cylindrical walls. Periodically inspecting this equipment for broken or worn-out insulation is very crucial to spot possible leakages and losses from improper steam quantities.

The stills are supplied with about 3000 lb/hr of steam from a 100 bhp fire tube boiler operating at 90 psig and supplying steam at 320°F. The boiler is in good working condition and is serviced regularly. However, there was a small issue with the controls for the gas burner that caused trouble with running the boiler. This problem occurred sometime in the last three months and after the variation in the product output was observed, the issue has been taken care of and the boiler is working normally again. The boiler stack temperatures were also measured via a boiler stack analyzer to be about 20°F more than the steam temperature at low fire. The stack gas composition also showed oxygen and carbon monoxide values within the range of 6-8% and below 100 parts per million respectively for low fire operation. Thus, improper boiler operation does not seem to be a cause of the problem. However, as the boiler is a critical part of the manufacturing process, it is highly recommended that the facility should have a boiler representative come by at least once a year and work with the in-house maintenance personnel to check crucial parameters and conduct a boiler tune-up if necessary.

To summarize, the root causes of the reduction in product are threefold: reduced heat transfer within the heat exchangers due to fouling, incapability of the cooling tower to handle process cooling loads by itself on certain warm days and overloading of the pump due to a very high flow and pressure head demand in the network. To overcome these problems, measures must be examined that would allow a better flow distribution in the cooling tower network and reduce the load on the in-line pump. The thought process behind this analysis is shown in the figure below.

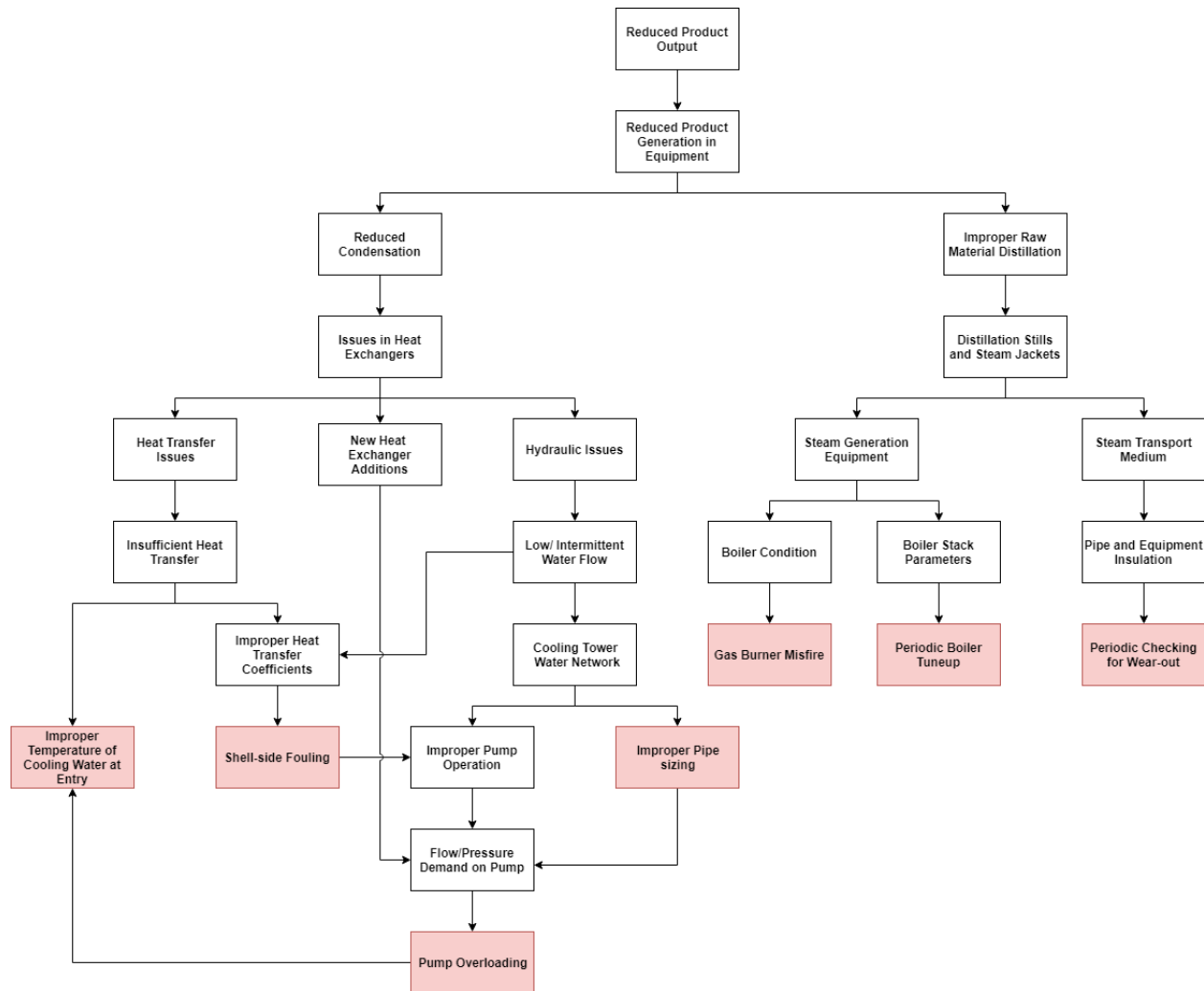


Figure 29: Root Cause Analysis

4.2: Possible Solutions and Economic Analysis

4.2.1: Installing a bigger chiller with a water-side economizer

One of the major results from the observations at the facility was the insufficient cooling effect provided by the cooling tower water loop itself. To remedy this problem, the facility can employ a chiller that generates chilled water via a vapor compression refrigeration cycle. The generated chilled water in the primary loop could run through the various heat exchangers, absorbing heat from the generated product vapors and condense them into the desired liquid state.

Since the cooling effect would be achieved via a refrigeration cycle, it would shift the current dependence of the product generation process on the ambient weather conditions onto the effectiveness of the chiller cycle's refrigerating effect. To test the feasibility of this idea, a look at the heat duty on the various heat exchangers was undertaken which was followed by an estimation of the possible effects on the annual product output and finally, a look at the economics and the payback period of installing and running the chiller throughout the year. As an additional energy efficiency measure, the chiller could also be installed with a water-side economizer that can help offset the annual operating costs by reducing the chiller uptime in the winter. This is also addressed as part of this recommendation.

The distilled product obtained at the end of the process is typically a mixture of ethanol and water, which is most commonly a 50:50 mixture by weight at the start with some suspended particles in it. Reducing the pressure of the liquid mixture in the still allows boiling and vapor formation to occur at a lower temperature than what would be needed at the atmospheric pressure. Since the process of distillation and condensation occurs under a vacuum (25 - 28 inches of mercury), the various thermodynamic properties of the mixture were calculated accordingly. The properties of ethanol were obtained from the online NIST database [37] and the properties of water were obtained from steam tables using an Excel Plugin: X Steam [38]. The process followed for calculation of the various thermodynamic parameters is elaborated in the following paragraphs.

The Antoine Equation is a correlation derived from the Clausius-Clapeyron equation that describes the interrelation between the vapor pressure and temperature for a pure fluid to a good accuracy within a predefined temperature range [39]. The equation is shown below.

$$\log_{10} p = A - \frac{B}{T + C}$$

Where p is the vapor pressure (bar), T is the Temperature (K) and A , B and C are “Antoine coefficients” which are numerical constants. Using this equation, the saturation temperature can be found for the line pressure in the current system on the product side. This can then be used to find the state of the entering fluids, which can be either superheated if the product entry temperature is higher than the saturation temperature, saturated if the product entry and saturation temperatures match or in the liquid state if the entry temperature is below the saturation temperature. The values of constants A , B and C used for this equation and the various temperature ranges in which they are valid, are tabulated below [37]:

Table 2: Antoine Equation ranges and constants

	T1(K)	T2(K)	A	B	C
Range 1	273	351.7	5.37229	1670.409	-40.191
Range 2	292.77	366.63	5.24677	1598.673	-46.424
Range 3	364.8	513.91	4.92531	1432.526	-61.819

At the line pressure of 25 inches of mercury below vacuum or 0.167 bar-gauge, the saturation temperature for ethanol and steam are 101°F (38.63°C) and 133.86°F (56.59°C) respectively. Since the entry temperature of 140°F (60 °C) is higher than the saturation temperatures for both the fluids, the mixture is superheated. Thus, the heat duty on the heat exchangers involves de-superheating the ethanol and steam vapors to the respective saturation temperatures, a phase change of both fluids from vapor to liquid and then sub-cooling the liquid mixture to the exit temperature. It is assumed here that the suspended particles and any other dissolved components are in a low concentration and do not have any major effects on the thermodynamic or physical properties of the mixture. It is also assumed that the various types of liquid chemical that the facility generates are all chemically similar to the extent that their condensation thermodynamic requirements under the designated vacuum conditions are similar.

The NIST Web-book [37] also provides an equation that gives a reasonable estimate of the enthalpy of vaporization of ethanol in relation to the temperature and is obtained from regression analysis of available experimental data. This equation can be used to find the necessary amount of heat that needs to be rejected to enable a phase change of the ethanol vapor within the heat exchanger.

$$h_{fg} \text{ (kJ/mol)} = A \cdot \exp(-\alpha T_r) \cdot (1 - T_r)^\beta$$

The constants in this equation and the applicable temperature range is tabulated below:

Table 3: Enthalpy of Vaporization Calculation for Ethanol [37]

Parameter	Value
Temperature Range (K)	298K – 469K
A (KJ/mol)	50.43
Constant, α	-0.4475
Constant, β	0.4989
Critical Temperature, T_c (K)	513.9
Reduced Temperature, T_r	Desired Temperature T (K) / T_c (K)
Desired Temperature (K)	311.783
Calculated Enthalpy of Vaporization (kJ/mol)	889.96

Using this equation, the latent heat of vaporization at the saturation temperature of 101.54 F (311.783 K) was calculated to be 41.53 KJ/mol or 889.96 KJ/kg using the molecular weight of ethanol (46.07 g/mol).

The Dortmund Data Bank website [40] also has a calculator for the enthalpy of vaporization of ethanol where the PPSD12 Equation shown on the next page is used to calculate this value at the desired temperature.

$$h_{fg} = R \cdot T_c \cdot \left(A \cdot \tau^{\frac{1}{3}} + B \cdot \tau^{\frac{2}{3}} + C \cdot \tau + D \cdot \tau^2 + E \cdot \tau^6 \right)$$

Where, $\tau = 1 - \frac{T}{T_c}$

Table 4: Enthalpy of Vaporization Calculation for Ethanol Using PPSD12 Equation [40]

Parameter	Value
Universal Gas Constant, R, (J/mol-K)	8.3145
Critical Temperature, T _c , (K)	516.2
Constant A	9.1919
Constant B	2.8118
Constant C	8.6931
Constant D	-11.776
Constant E	-31.745
Desired Temperature, T (K)	311.78
Constant τ	0.396
Calculated Enthalpy of Vaporization (KJ/mol)	41.802

Using the PPSD12 Equation resulted in a value of 41.802 KJ/mol or 907.37 KJ/kg using the molecular weight of ethanol (46.07 g/mol). Since both the obtained values are via equations obtained from parametric regression, there is no singular, true value available. Hence, for the purposes of further calculations in the current context, an average value of the enthalpy values obtained was used. The average value for enthalpy of vaporization used is 898.66 KJ/kg.

The next thermodynamic property required for ethanol is the isobaric specific heat capacity in the vapor state and in the condensed state. The NIST webbook [37] has a table of experimentally measured specific heat values at various temperatures, but upon closer inspection, it was seen that there are no values available in any reference for the exact desired temperature and that the value for specific heat varies considerably depending on the temperature. Hence, the specific heat values for the gaseous and liquid states were interpolated from the available data. The specific heat for the gaseous state was interpolated at the average temperature between the entry temperature and the saturation temperature. The specific heat for the liquid phase was interpolated at the average temperature between the exit temperature and the saturation temperature. A summary of the interpolation calculation is tabulated below.

Table 5: Interpolation of Isobaric Specific Heat of Ethanol [37]

Specific Heat of Gaseous State (Entry condition)			
	Available Higher value	Available Lower value	Calculated value at desired temperature
Temperatures (K)	350.01	300	322.47
Specific Heat (KJ/mol.K)	73.15	65.49	68.93
Specific Heat of Liquid State (Exit condition)			
	Available Higher value	Available Lower value	Desired value
Temperatures (K)	313.2	303	308.58
Specific Heat (KJ/mol.K)	118.4	115.1	116.91

Again, using the molecular weight of 46.07 g/mol, the isobaric specific heats for the gaseous state and the liquid states were calculated as 1.496 kJ/kgK and 2.538 kJ/kgK.

Finally, the ethanol liquid density was calculated by the DIPPR105 state equation [41] which is valid between the temperature range of 191 K and 513 K. It is obtained by parametric regression of a number of experimentally obtained data points. The equation is given below:

$$\rho = \frac{A}{B^{1 + \left(1 - \frac{T}{C}\right)^D}}$$

Table 6: Calculation of Ethanol Liquid Density via DIPPR105 State Equation [41]

Parameter	Value
Average Liquid Temperature 'T' (K)	308.58
Constant A	99.3974
Constant B	0.310729
Constant C	513.18
Constant D	0.305143
Calculated Density 'ρ' (kg/m³)	773.4201

The properties of the water vapor entering the condensers was calculated using a digital version of the steam tables called XSteam [38] which is a plugin for MS Excel for evaluating steam properties using "International Association for Properties of Water and Steam Industrial Formulation", 1997 (IAPWS IF-97) data. The unknowns calculated were the latent heat of vaporization and the specific heat capacities of steam and water at the given vacuum conditions.

The superheated steam heat capacity was found to be 1.959 KJ/kgK, the latent heat of vaporization (2,366.924 KJ/kg) was found by subtracting the enthalpy of the saturated liquid (235.31 KJ/kgK) from the saturated vapor enthalpy (2,602.23 KJ/kgK). The isobaric specific heat of water is 4.181 KJ/kgK. The density of liquid water at the line pressure is 985.079 kg/m³.

In summary, the thermodynamic properties of ethanol and water that were calculated are tabulated below.

Table 7: Summary of Calculated Thermodynamic Properties in Vacuum

Properties at 25" Hg vacuum	Specific Heat		Heat of Vaporization	Other Properties			
	C _p (Vapor) (KJ/kgK)	C _p (Liquid) (KJ/kgK)	h _{fg} (KJ/kg)	Boiling pt.(°C)	Density (kg/m ³)	Molecular wt (g/mol)	Mass Fraction
Ethanol	1.532	2.538	889.96	38.63	773.42	46.07	50%
Water	1.946	4.181	2,366.01	56.59	985.08	18.015	50%

The density of the final resulting mixture with 50% of each substance by weight is calculated in the following way:

$$\rho_{mix} = \frac{\text{Total mixture mass}}{\text{Total mixture volume}} = \frac{m_{ethanol} + m_{water}}{v_{ethanol} + v_{water}} = \frac{m_{ethanol} + m_{water}}{\frac{m_{ethanol}}{\rho_{ethanol}} + \frac{m_{water}}{\rho_{water}}}$$

$$\rho_{mix} = \frac{\frac{m+m}{\frac{m}{773.42} + \frac{m}{985.08}}}{\frac{2*m}{\frac{985.08m+773.42m}{985.08*773.42}}} = 866.51 \text{ kg/m}^3$$

Once the product properties were calculated, the heat exchanger dimensions can be used to estimate the mass flow rates of the product that can be obtained via every heat exchanger per hour. The eight heat exchangers at the facility are all functional and in moderate to good operating condition. For the purpose of calculation of heat duty, the heat exchanger sizes were used to calculate the product volume flow rates in each exchanger in relation to the known upper and lower volume flow rates for the heat exchanger 'F'. Since the condensation and cooling effect for every heat exchanger is typically proportional to the surface area of the heat exchanger, simple

proportion was used to calculate the mass flow rates of product flow possible every hour. The mass flow rates per hour for every heat exchanger are obtained by multiplying the density with the volume flow rate per hour.

$$HX \text{ Mass flow}(kg/hr) = \text{Volume flow in HX}(m^3/hr) * \text{Product Density}(kg/m^3)$$

Or by simple proportion with the volume flow rate in the heat exchanger 'F',

$$HX \text{ mass flow}(kg/hr) = \frac{HX \text{ Surface Area}(ft^2)}{HX \text{ "F" Surface Area}(ft^2)} * \text{Volume flow in HX "F" } \left(\frac{l}{hr}\right) * \text{Product Density} \left(\frac{kg}{l}\right)$$

The maximum possible mass and volume flow rates are tabulated below.

Table 8: Estimation of Heat Exchanger Yields

Heat exchanger	Surface Areas (ft ²)	Ratio of Surface Areas to HX 'F'	Est mass flow (kg/hr)		Est Vol flow (l/hr)	
			Upper	Lower	Upper	Lower
A	40	22%	43.33	26.00	50.00	30.00
B	320	174%	363.93	218.36	420.00	252.00
C	88	48%	95.32	57.19	110.00	66.00
D	40	22%	43.33	26.00	50.00	30.00
E	320	174%	363.93	218.36	420.00	252.00
F	184	100%	216.63	129.98	250.00	150.00
G	50	27%	26.00	15.60	30.00	18.00
H	41	22%	26.00	15.60	30.00	18.00
Total			1178.46	707.07	1360.00	816.00

Using these flow values, the amount of heat that needs to be rejected to the chilled water in the condensers is calculated. Since the condition for both substances in the mixture is superheated at the entry temperature and line pressure, the heat duty of the heat exchangers involves sensible heat rejection in de-superheating to reduce the temperature to the saturation temperature, latent heat rejection at saturation temperature to induce phase change and sensible subcooling to the exit temperature. Using a chiller, it is apparent that the plant would be able to make more product annually since it will be able to maintain better temperature control over the chilled water that will have average inlet and outlet temperatures much lower than the cooling

tower water directly being run at the moment. Since the plant currently has a maximum output of about 1,360 liters per hour on days with ambient temperatures in the 50°F to 75°F range, this upper limit on the plant capacity can be assumed to be attained throughout the year with the new process cooling equipment. Thus, the chiller must now be sized for this maximum possible annual product mass flow rate. The process followed for calculation of the total heat duty for all the heat exchangers in the plant is shown below. The product mass flow rate used is the estimated total capacity of the plant which is 1,178 kg per hour.

$$Q_{total} = Q_{desuperheating} + Q_{enthalpy\ of\ vaporization} + Q_{subcooling}$$

$$Q_{total} = [Q_{desuperheating} + Q_{enthalpy\ of\ vaporization} + Q_{subcooling}]_{ethanol}$$

$$+ [Q_{desuperheating} + Q_{enthalpy\ of\ vaporization} + Q_{subcooling}]_{water}$$

$$Q_{total} = [\dot{m} * C_{pvap} * (T_{Entry} - T_{sat}) + \dot{m} * h_{fg} + \dot{m} * C_{pliq} * (T_{sat} - T_{exit})]_{ethanol}$$

$$+ [\dot{m} * C_{pvap} * (T_{Entry} - T_{sat}) + \dot{m} * h_{fg} + \dot{m} * C_{pliq} * (T_{sat} - T_{exit})]_{water}$$

Table 9: Calculation of Total Heat Load on Cooling Tower Water

Parameter	Symbol	Ethanol	Water	Unit
Mass flow rate	\dot{m}	0.164	0.164	kg/s
Specific Heat Capacity at entry state	C_{pvap}	1.532	1.946	KJ/kgK
Entry Temperature	T_{Entry}	60.00	60.00	°C
Saturation Temperature/Boiling Point	T_{sat}	38.63	56.59	°C
Sensible Heat for De-superheating	$Q_{desuperheating}$	5.36	1.09	KJ/s
Enthalpy of Vaporization	h_{fg}	898.66	2366.01	KJ/s
Total Latent Heat Rejected	$Q_{enthalpy\ of\ vaporization}$	147.09	387.26	KJ/s
Exit Temperature	T_{exit}	32.22	32.22	°C
Specific Heat Capacity at exit state	C_{pliq}	2.538	4.181	KJ/kgK
Sensible heat for subcooling	$Q_{subcooling}$	2.66	16.68	KJ/s
Total Heat Rejection per substance	$Q_{ethanol}$	155.11	405.02	KJ/s
Heat Duty on heat exchangers	Q_{water}	159.26		tons
Overdesign Safety Factor	-	30%		-
Final Heat Duty for Chiller	Q_{total}	207.04		tons

Considering the sensible and latent heat for the process, the total heat load on the cooling tower water for the desired product output is about 208 tons of refrigeration. This is the minimum

value of the cooling capacity expected from the chiller that is to be installed. In this range, the possible chiller can be either air cooled or water cooled, but it makes sense to go for a water-cooled chiller since it would be more efficient and consume less energy for the same cooling effect. Additionally, it would be easier for the company to manually increase the cooling capacity of the process cooling network if they choose to expand in the future. The feasibility of installing new equipment can be ascertained by looking at the implementation costs and the annual savings. Calculating these two values will yield a payback period which is the time in which the initial investment will pay for itself. Since the annual savings from the installation would in theory result in a year-round higher production value, this estimated additional production can be calculated. Using the additional product generated, a dollar value on the additional revenue from sales of the product can be predicted which can then be used to arrive at a payback period.

The overall cost of adding a new chiller should also include the consequent increase in the operating expenses of the facility. The chiller will demand more electric energy from the grid annually. Adding a chiller will also increase the annual preventive and breakdown maintenance expenses of the facility. Installing the chiller will involve installing additional piping to connect to the cooling tower and the current piping in the facility along with installation of controls and the necessary electrical connections. There will also be a one-time cost associated with training the personnel on how to operate the equipment and what to do in case of emergencies.

The first step in determining operating expenses is to calculate the demand and energy rates levied by the utility company. This is done by averaging the electricity usage by the facility over a year and the respective charges for each. The values for monthly demand in kW, the monthly energy usage in kWh and the respective charges for these can be found on the electricity bills. Using these bills for the period of April 2017 to April 2018, it was calculated that the facility is

being charged \$7.70 per kW of electrical demand and \$0.0546 per kWh of energy usage on average. A new chiller is an energy-intensive piece of equipment and will definitely dominate the electrical demand of the facility over anything else currently in operation and result in a larger monthly charge for it. The diagram below shows the proposed arrangement with a new chiller.

A commercial chiller closest to the desired capacity is a screw-chiller of 220 tons capacity. A water-cooled chiller requires a minimum water flow rate through the cooling tower loop in order to allow efficient condenser operation. This flow rate is typically 3 gallons per minute for each chiller ton of refrigeration. [30] Thus, the cooling tower must be able to sustain 660 gallons per minute of water flow in its network for a 220 Ton chiller.

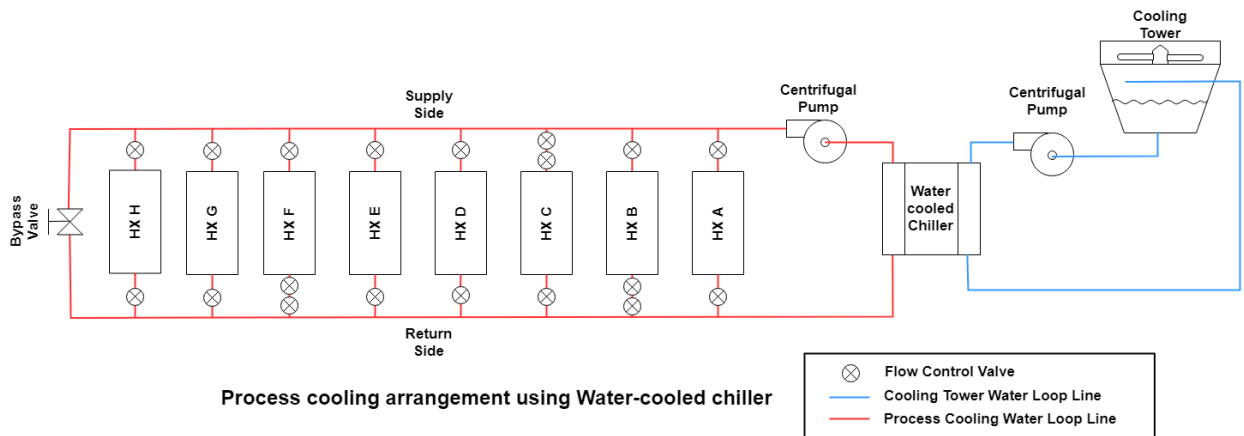


Figure 30: Proposed process cooling arrangement with chiller

Since the current cooling tower and the loop network installed at the facility is designed for 200 tons of refrigeration, it can only sustain 600 gallons per minute of water flowing through it. If this flow value is exceeded, the cooling tower will not be able to cool the process effectively. This means that a new cooling tower will need to be installed at the facility to augment the chiller operation. Since the current cooling tower is still functional, a new smaller cooling tower of 50 tons capacity could just be added on to the system. It is estimated on the basis of the water

requirement, a 25 hp inline centrifugal pump in the process chilled water loop and a 15 hp, 1000 gallons per minute inline centrifugal pump in the cooling tower loop would also need to be purchased and installed.

The costs of installing the chiller and all the associated equipment and annual costs of operating it are calculated below. The cost estimates are obtained from RS Means Mechanical Cost Data, 2015 [42].

Table 10: Implementation Cost Estimation for 220 Ton Chiller Unit

Item	Total Cost
220-ton Chiller Purchase (\$600/ton)	\$132,000
50-ton Cooling Tower Purchase	\$10,400
Cost of 15 hp, 1000 gpm Inline Centrifugal Pump	\$5,125
Cost of 25 hp, 1000 gpm Inline Centrifugal Pump	\$7,450
Cost of Controls and Fittings	\$11,000
Chiller Installation Cost	\$14,500
Cooling Tower Installation Cost	\$2,000
Pumps Installation Cost	\$3,775
Labor Fees for Installation of all Equipment	\$30,000
Total Labor Cost	\$50,000
Training and Overheads	\$1,000
Miscellaneous Costs (<5%)	\$10,000
Total Cost of Implementation	\$256,975

The operating cost of the chiller must include the charges for monthly electrical demand and the charge for electrical energy over the operating hours. The chiller may be shut off during colder days or operated intermittently if a water-side economizer is installed as recommended in the next section. If the chiller is not operated at all through a month, the estimated demand charge for that month may be reduced to the next biggest energy consuming equipment in the facility. But, to get a conservative estimate, it is assumed for the purposes of this calculation that the chillers will always be operated at least once a month and will always dominate the electrical demand for the facility. Since the chiller usage will also require using the pumps in the cooling tower water

loop and the heat exchanger loop at all times, these energy consumers must also be considered. The cooling tower also has a fan motor that is running constantly and adds to these charges. Installing and operating the chiller may also slightly increase the makeup water usage from the city supply, but since that increment is difficult to accurately quantify before actual installation, that value is assumed to be negligible for now. The operating cost calculation is shown below.

Table 11: Operating Cost Estimation for 220 TR Chiller

Item	Specification	Calculated Value
Chiller Capacity	220 Ton	
Operating Hours	4800 hours	
Electricity Demand Rate	\$7.70/kW	
Electricity Energy Rate	\$0.0546/kWh	
Chiller Power Consumption	0.718 kW/ton [43]	157.96 kW
Cooling Tower Power Consumption	0.2 kW/ton [30]	50 kW
Heat Exchanger Loop Pump Power	25 hp	18.65 kW
Cooling Tower Loop Pump Power	15 hp	11.19 kW
Total Demand		237.80 kW
Total Demand Cost	(Demand x 12 months x Rate)	\$ 21,973
Total Energy Cost	(Demand x Op hours x Rate)	\$ 62,323
Annual Maintenance Cost		\$ 2,000
Total Annual Operating Cost		\$ 86,296

The revenue obtained by installing and operating the chiller and the associated equipment is calculated by using the upper production capacity value and considering that value to be generated throughout the year. This value is then multiplied with a correction factor to account for the fact that the product generation process is time dependent and may vary from batch to batch and not all condensers will be running all the time. When this additional quantity is multiplied with the estimated profit per unit volume, a new annual revenue amount can be estimated. This amount can then be used to calculate the payback period on the implementation costs. The estimated additional revenue is in the range of \$2.5 million, which is based on an estimate of 40% profit on the sales price.

Table 12: Calculation of Additional Annual Revenue after Implementation

Item	Specification	Calculated Value
Upper Hourly Production Capacity	1360 litre/hr	
Lower Hourly Production Capacity	816 litre/hr	
Annual Operating hours	4800 hrs/year	
Production Correction Factor	60%	0.6
Current Production Capacity	(50% Upper Capacity + 50% Lower Capacity) * Production Correction Factor	3,133,440 litre/year
New Production Capacity	100% Upper Annual Capacity* Production Correction Factor	3,916,800 litre/year
Additional Production Estimation	(New Capacity)-(Current Capacity)	783,360 litre/year
Sales Revenue	\$ 8/ litre	
Profit from Additional Revenue	40% of Sales	\$ 3.2/litre
Additional Annual Revenue after Implementation		\$ 2,506,752

The payback estimated after implementation of the chiller unit can now be calculated.

$$\text{Payback Period} = \frac{\text{Implementation Cost}}{\text{Annual Additional Revenue} - \text{Annual Operating Costs}} \times 12 \text{ Mos.}$$

$$\text{Or, Payback Period} = \frac{\$ 256,975}{\$2,506,752 - \$86,296} \times 12 = 1.3 \text{ months}$$

Thus, it is seen that the payback period of the chiller is about a month and half. This shows the effectiveness of the chiller in quickly increasing the possible output generated. However, it was assumed in the analysis that the chiller and the associated equipment is running at full load throughout the operating hours. In reality, the chiller may also operate at part-load where it may have a lower efficiency and draw relatively the same amount of electrical energy as it draws at higher loads. Another presiding assumption here is that the company makes the same amount of profit from a given product over time and is able to sell all of the product it generates at a fixed price. This is partially valid since the products being generated by the facility are known to be in very high demand throughout the year as per the owners.

As described in Chapter 3, the operating expenses of a water-cooled chiller can be reduced by utilizing “free-cooling” or water-side economizers if the region receives sufficiently low ambient wet-bulb temperatures for many hours in a year, which is when free-cooling can be employed. In order to test the feasibility of this arrangement at this facility, the number of hours with a low ambient wet-bulb temperature must be found out. To do this, it is essential to understand at what temperatures the cooling tower will function well enough to allow “free-cooling”.

From the various possible arrangements for water-side economizers discussed in Chapter 3, most of them can be eliminated since they are not applicable in the current situation. The strainer cycle would leave open the possibility of fouling within the condenser unit of the chiller. Since an air-cooled chiller is not being considered here, an evaporative cooler or a new dry cooling tower would not be feasible. If the facility chooses to use a centrifugal chiller with the evaporator below the condenser, it may be able to save some energy by using the thermosiphon effect if the manufacturer has provided for it. The best options remaining are to have either a precooling coil or to have a plate and frame heat exchanger operating intermittently between the chiller and the cooling tower. A plate and frame heat exchanger is definitely the better option because of a couple of reasons. It would reduce the occurrence of fouling since, as discussed in Chapter 3, these heat exchangers experience much more turbulent flow within the plates, reducing the possibility of fouling occurring in the system. Additionally, the chiller equipment will also be protected since the chiller loop and the cooling tower loop are both separated.

On the basis of the current condition of the existing cooling tower, its performance benchmarks which are its efficiency and its approach temperature can be taken as 75% and 5°F respectively. The approach temperature of the new plate and frame heat exchanger would ideally be 2°F. The desired process cooling temperature is 50°F. It is expected that the process cooling

loop will raise the temperature of the water by 10°F as per the current performance data. The proposed arrangement is shown below in Figure 29.

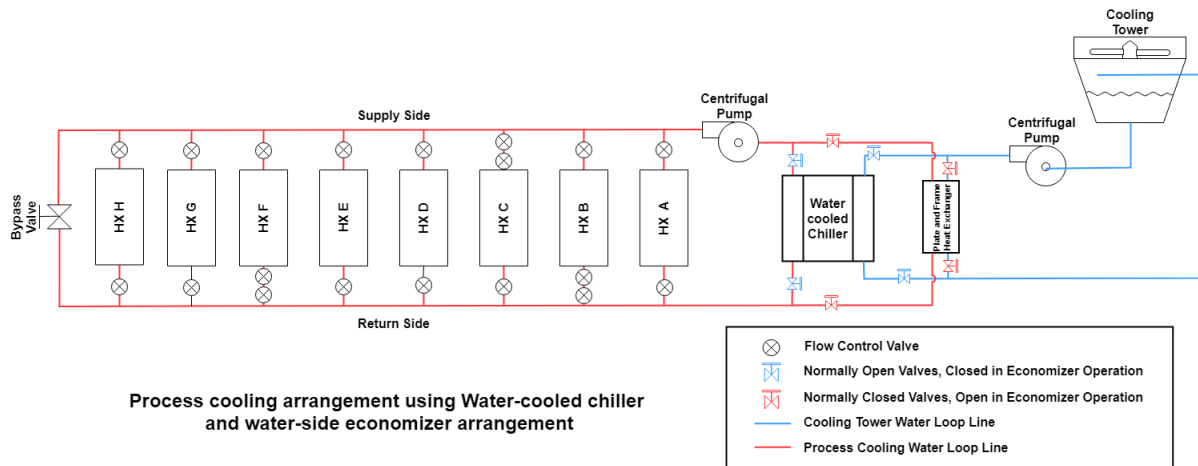


Figure 31: Proposed Water-side Economizer Arrangement

The minimum ambient wet-bulb temperature required for a water-side economizer to operate effectively as seen in the figure above is obtained from the relations below.

$$\text{Min. Amb. WBT} = \text{Desired CHW Temperature} - \text{Plate and Frame HX approach} - \text{Cooling Tower Approach}$$

$$\text{Min. Amb. WBT} = 50^{\circ}\text{F} - 2^{\circ}\text{F} - 5^{\circ}\text{F} = 43^{\circ}\text{F}$$

A lower operating limit is also necessary to prevent freezing anywhere in the system. This limit is set at 35°F. The feasible hours for free-cooling are calculated by looking at the Typical Meteorological Year for the Raleigh-Durham airport which is the closest weather station to NC State and is reasonably similar to the weather at the facility. The TMY data is a set of meteorological values and weather parameters which are calculated by averaging from a database developed over a number of years. It also accounts for the range of weather variations observed over a typical year and are thus, a reliable source of environmental data for HVAC design and building simulations [44]. The TMY data for any weather monitoring station in the United States is accessible via the National Oceanic and Atmospheric Administration (NOAA) website [45].

It was seen from the TMY data that there were 1,196 hours out of the 8,760 hours in a typical year when the water side economizer could be used. This is the time when the ambient wet-bulb temperature is within the desired range of 35°F to 43°F. Out of these hours, for a conservative estimate, it can be assumed that the free-cooling is practically achievable in 1,000 hours. The operating expenses can now be calculated by considering the cost savings when the chiller is completely shut-off during this period. During water-side economizer operation, the cooling tower fan, cooling tower loop pump and the process cooling loop pump, all remain operational even though the chiller is shut-off. It is also assumed here as in the previous calculation that the chiller dominates the electrical demand when operational and is used at least once every month at peak load. This results in electrical energy savings only and no demand savings. The calculated values are shown in the table on the next page.

The next step is to calculate the implementation costs for this recommendation. This can be done by looking at the equipment cost as done in the previous section. Since the cooling tower loop is expected to experience flows in the range of 600-700 gpm, it would be prudent to size the plate and frame heat exchanger to sustain 800 gpm of fluid flow. The remaining implementation costs remain the same as the chiller sizing and operational parameters remain the same. Since the additional product generated is the same with or without the water-side economizer, the additional revenue will also remain the same. Thus, the payback cost can be calculated for this combined arrangement.

Table 13: Water-side Economizer Operational Expenses

Item	Specification	Calculated Value
Energy Demand with Chiller usage	Chiller Demand + Cooling Tower Fan + CT Pump + HX Loop Pump	237.8 kW
Energy Demand with Water-side Economizer usage	Cooling Tower Fan + CT Pump + HX Loop Pump	70.95 kW
Energy Savings	Chiller Operational Demand-Water-side Economizer Demand	166.85 kW
Operational Hours	From TMY Data	1,000 hours
Total Energy Savings	At \$0.0546/kWh	\$9,110/yr
Chiller Annual Operational Costs	From previous calculation	\$86,295/yr
Chiller Annual Operational costs with water-side economizer	Applying Savings from Chiller costs	\$77,185/yr

Table 14: Implementation Costs for Water-side Economizer

Item	Total Cost
220 Ton Chiller Purchase (\$600/TR)	\$132,000
50 Ton Cooling Tower Purchase	\$10,400
Cost of 15 HP, 1000 gpm Inline Centrifugal Pump	\$5,125
Cost of 25 HP, 1000 gpm Inline Centrifugal Pump	\$7,450
Cost of Controls and Fittings	\$11,000
800 gpm Plate and Frame Heat Exchanger purchase	\$63,500
Chiller Installation	\$14,500
Cooling Tower Installation	\$2,000
Pumps Installation	\$3,775
Plate and Frame Heat Exchanger Installation	\$10,000
Labor Fees for Installation of All Equipment	\$70,275
Training and Overheads	\$1,000
Miscellaneous Costs (~5%)	\$15,000
Total Cost of Implementation	\$328,325

Since the additional product generated is the same with or without the water-side economizer, the additional revenue will also remain the same. Thus, the payback period can be calculated for this combined arrangement.

$$\text{Payback Period} = \frac{\text{Implementation Cost}}{\text{Annual Additional Revenue} - \text{Annual Operating Costs}} \times 12 \text{ Mos.}$$

$$\text{Payback Period} = \frac{\$ 328,325}{\$2,506,752 - \$77,185} \times 12 \text{ Mos} = 1.7 \text{ Months}$$

Thus, it is seen that when installing the chiller and the water-side economizer, there is a higher payback period of about 2 months. This is because even though the end result is the same, the implementation costs for a water-side economizer are higher. In spite of this drawback, it is highly recommended to have the water-side economizer installed at this time. The clear benefits are the energy savings attained which add up over time to pay back within the course of 2 months. Additionally, the problem of flow starvation can be overcome by having separate loops for the heat exchanger network and the cooling tower, allowing better distribution between the two. One more benefit would be the reduced instance of fouling and solids deposition from the cooling tower network in the chiller condenser when the water-side economizer is used. Installing the economizer right now, along with a chiller, would be easier and much-more cost effective than retrofitting it at another time in the future.

4.2.2: Reconfigure the pumping arrangement

Since pump overloading seems to be one of the causes for the insufficient heat transfer within the exchanger network, the feasibility of correcting this via a new pump arrangement is examined in this section. There three ways in which the flow rate within the exchangers can be improved: by adding a pump in parallel to the current pump, by replacing the current pump with two new parallel pumps or by replacing the current pump with a single bigger pump to improve operating efficiencies at the current operating point.

To get the operating characteristics of the system to achieve the desired cooling load in either scenario, it is necessary to first figure out the current operating pressure head and flow rate of the system. To do this, the system curve for the current operating condition is needed, which

would require an examination of the piping network for major and minor losses along with the shell side pressure drops for every heat exchanger in the network. The first step in this direction is to calculate the flow velocities in the various parts of the network. This can be achieved by looking at the flow rate at the pump exit and then estimating the velocity in each path of the network via the continuity equation. The current flow rate can be estimated from a simple heat balance between the system and the cooling tower water based on the previous calculation.

Heat rejected in exchangers = Heat absorbed by cooling tower water

$$Q_{load} * Safety\ Factor = \dot{m} * C_p * (T_{CT\ in} - T_{CT\ out})$$

A safety factor is used in pumping systems where a minimum flow rate is critical to operations. Here a safety factor is applicable since a lack of water on the shell side will lead to reduced condensation in the heat exchangers with solvent vapors infiltrating the diaphragm pumps at the end of the line. These pumps will not function correctly and get damaged over time if this happens frequently and hence, it is better to have slightly more water flowing in the system.

Table 15: Heat Balance at Desired Product Output

Description and Symbol	Value
Heat load from previous calculation, Q_{load}	220 ton = 2,640,000 BTU/hr
Factor of safety considered to keep water flow rate slightly higher than exact system demand, <i>Safety Factor</i>	25%
Specific heat of Water, C_p	1 BTU/ lb _m -°F
Temperature of water entering cooling tower from process, $T_{CT\ in}$	60°F
Temperature of water exiting cooling tower into process, $T_{CT\ out}$	50°F
Mass flow rate of Water needed in network, \dot{m}	330,000 lb _m /hr
Volume flow rate of Water, \dot{V}	663 gpm

In order to verify the actual flow demand at the facility, the network and heat exchanger head losses can be computed at this flow rate and then compared to the flow rate at the pressure head seen in the actual network. It is necessary to arrive at this value by an indirect calculation in

this manner since there is no practical way at the facility to directly measure the volumetric flow rate or the network velocities. Most means of flow measurement via commercially available flowmeters require a long piping section upstream of the instrument, which is free of fittings or valves, which is unavailable in this system. Using the obtained value of 663 gpm or $0.04182 \text{ m}^3/\text{s}$, the velocity of the water at the pump exit within the 4-inch diameter pipe was calculated to be 16.93 feet/second or 5.16 m/s. This source velocity can be used within the flow continuity equation to estimate the velocity in each path of the network.

The network was divided into 9 possible paths labeled from letter ‘A’ to letter ‘I’. It must be noted that path ‘I’ is just an extension of path ‘H’ with the bypass valve closed completely at all times, which then blocks flow through that path.

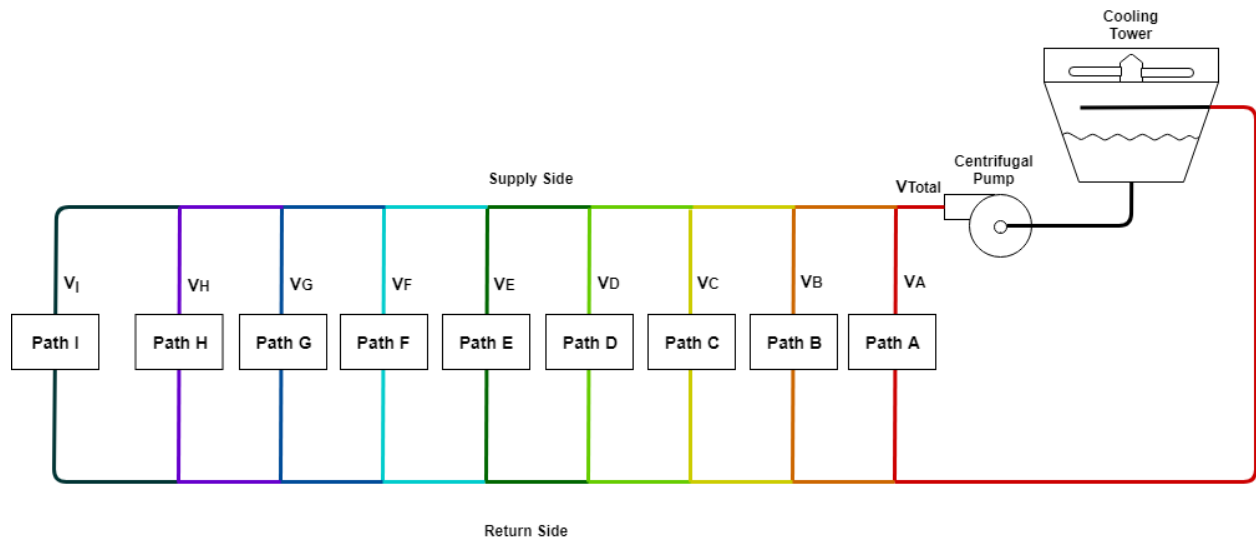


Figure 32: Paths in Heat Exchanger Network

Using the obtained volumetric flow rate in the supply line from the heat balance, the continuity equation that illustrates mass conservation can be used to calculate the in-pipe velocities for paths ‘A’ to ‘I’. Since the flow rate going into the network should add up to the individual path

flow rates, the following equation is applicable, where \dot{V} is the volumetric flow rate in the specified path.

$$\dot{V}_{total} = \dot{V}_A + \dot{V}_B + \dot{V}_C + \dot{V}_D + \dot{V}_E + \dot{V}_F + \dot{V}_G + \dot{V}_H$$

Where, $\dot{V} = \text{Area of pipe} * \text{velocity of fluid} = A.v$

Expanding,

$$(A.v)_{Pump\ exit} = (A.v)_A + (A.v)_B + (A.v)_C + (A.v)_D + (A.v)_E + (A.v)_F + (A.v)_G + (A.v)_H$$

In this equation, the velocities in each individual path are interlinked in order to satisfy mass conservation. However, none of these velocities are known and there is no practical way to measure them at this facility without massive overhauling. Water within a network will always flow towards the path of least resistance. This makes it difficult to accurately estimate the velocities in individual paths in a network of heat exchangers. The one constraint known here is that the main supply and return pipe must act as headers and equalize the upstream and downstream pressures around the exchangers. The unidirectional flow is maintained by this pressure equalization of the head losses through the exchangers. It follows that the difference in pressure across the supply and return pipes must equal the highest pressure drop on the shell-side from all the heat exchangers. The extent of this head loss will also in turn affect the resistance to flow through the exchangers and hence, the velocities. Again, the above obtained equation has too many unknowns and not enough data to proceed. A way of reducing the unknowns in this equation must be identified in order to arrive at individual velocities which can then be used to calculate the head losses in each path.

Since the flow rate will be dictated by the resistance in each path, a function can be defined which estimates the portion of flow going through each path. It can be said that more the volumetric capacity of the heat exchanger, more the flow going towards it. Additionally, the resistance is also

decided by the distance of the heat exchanger in each path from the pump outlet. The further the heat exchanger is, greater is the resistance before the supply port. These proportionalities can be accounted for by use of proportionality or ratio-based numerical coefficients for each path that estimate the division of flow.

Let $C = \text{function} (\text{Heat Exchanger Size in Path, Length of Supply Pipe})$

Substituting all path values of \dot{V} (for $\dot{V}_A, \dot{V}_B, \dot{V}_C \dots \dot{V}_H$) from the previous equation of mass conservation with $C_X \cdot \dot{V}$, where \dot{V} is a temporary fractional value of the total flow rate,

$$\dot{V}_{total} = C_A \cdot \dot{V} + C_B \cdot \dot{V} + C_C \cdot \dot{V} + C_D \cdot \dot{V} + C_E \cdot \dot{V} + C_F \cdot \dot{V} + C_G \cdot \dot{V} + C_H \cdot \dot{V}$$

$$\dot{V}_{total} = \dot{V} \cdot (C_A + C_B + C_C + C_D + C_E + C_F + C_G + C_H)$$

The values for these path coefficients can be obtained by assigning values based on the size and distance characteristics in each path. The value of the path constant is taken as the product of the ratios of the surface areas and path lengths.

$$C_X = \left(\frac{\text{Surface area of HX in Path}}{\text{Surface area of Biggest HX}} * \frac{\text{Supply Pipe Length for HX in path closest to pump}}{\text{Supply Pipe Length for HX in Path}} \right)$$

Table 16: Calculation of Path Flow Constants

Path	Surface area of HX in path (ft ²)	Ratio of HX Surface area to the biggest HX Surface Area	Length of Supply Pipe from Pump Outlet (ft)	Ratio of Path Length of Closest HX to HX in each Path	Value of Constant C for each path
A	40	0.125	30	1.00	0.13
B	320	1.000	37	0.81	0.81
C	88	0.275	60	0.50	0.14
D	40	0.125	87	0.34	0.04
E	320	1.000	80	0.38	0.38
F	184	0.574	104	0.29	0.17
G	50	0.156	106	0.28	0.04
H	41	0.128	111	0.27	0.03

A temporary flow rate through the network is now calculated by substituting the above constants.

$$\dot{V}_{total} = \dot{V} \cdot (C_A + C_B + C_C + C_D + C_E + C_F + C_G + C_H)$$

$$\dot{V}_{total} = \dot{V} \cdot (0.13 + 0.81 + 0.14 + 0.04 + 0.38 + 0.17 + 0.04 + 0.03)$$

$$\dot{V} = \frac{\dot{V}_{total}}{1.74} = \frac{0.04182 \text{ m}^3/\text{s}}{1.74} = 0.02409 \text{ m}^3/\text{s}$$

Now, the flow and the corresponding velocity in each path is obtained by multiplying the constants to the \dot{V} value and dividing those individual path flow rates by the pipe areas as shown in Table 17.

$$\dot{V}_A = C_A \cdot \dot{V}$$

Table 17: Calculation of Network Velocities

Path	Constant in Path	Estimated Flow Rate in Path (m ³ /s)	Supply Pipe Diameter (in)	Supply Pipe Area (m ²)	Velocity in path (m/s)
A	0.13	0.00301	4"	0.00811	0.37
B	0.81	0.01953	4"	0.00811	2.41
C	0.14	0.00331	4"	0.00811	0.41
D	0.04	0.00104	2"	0.00203	0.51
E	0.38	0.00903	2"	0.00203	4.46
F	0.17	0.00400	2"	0.00203	1.97
G	0.04	0.00107	2"	0.00203	0.53
H	0.03	0.00083	2"	0.00203	0.41

These values may be different from the actual velocities seen in the paths, but this is an acceptable estimate with the limited information available. Using these velocities, the major and minor losses as well as the shell side pressure drop can be calculated for each path. The major and minor losses are calculated using the Darcy-Weisbach formula and other relations obtained from the well-known Crane Co. Technical Paper No. 410M [15]. A sample calculation for path 'A' is

shown below and a summary of the friction losses in the remaining paths are shown as part of Appendix A.

$$\text{Major Head Loss in Pipe, } \Delta H_{\text{Pipe}} = \frac{f \cdot L \cdot v^2}{2 \cdot g \cdot D}$$

Where, the value of Friction factor 'f' is obtained from the Moody Chart at the intersection of the Reynolds Number for the pipe and the relative roughness of the pipe.

Relative Roughness = $\frac{\varepsilon}{D}$; where, ε = Absolute Roughness of the pipe surface and D = Pipe Internal diameter. To simplify the calculation of the friction losses, it is assumed that the velocity of the water in the return pipe is the same as when supplied. This is partially justified since there will be a small increase in the velocity at the exit of the heat exchanger due to a reduction in the pipe diameter, but there may be an equal or even higher reduction in velocity due to the numerous changes in the flow path within the heat exchanger. Assuming a constant velocity will thus, yield a conservative estimate by slightly oversizing the pump since flow head losses are directly proportional to the square of the flow velocity.

According to the Moody chart in Figure 34, for a PVC Pipe, the absolute roughness is 0.0025 mm and this value is used with the diameter of the pipes to calculate the Darcy friction factors for head loss at the flow Reynolds Numbers.

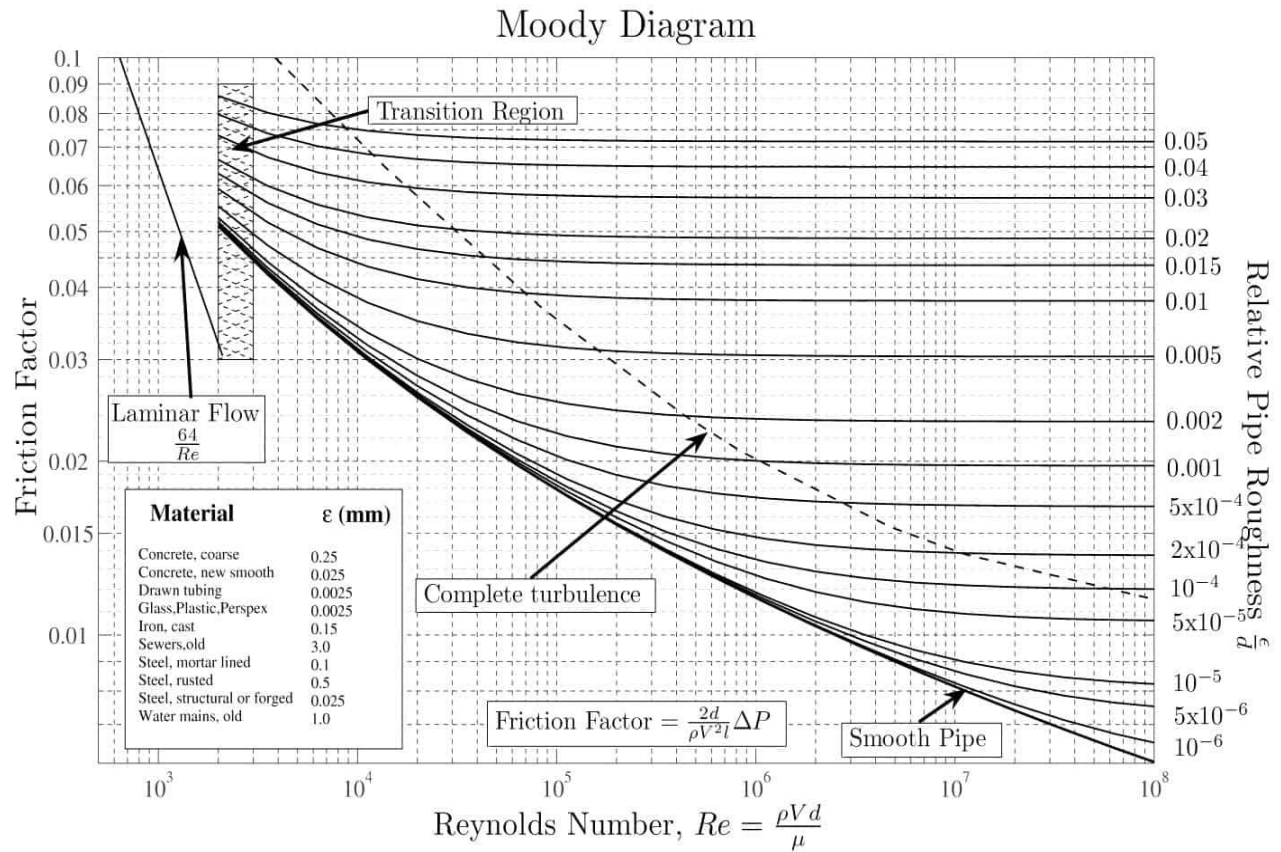


Figure 33: Moody Chart

Minor Head Loss in Valves and, $\Delta H_{\text{minor}} = \frac{K \cdot v^2}{2 \cdot g}$, where, $K = C \cdot f_t$

Here, values of the constant 'K' for various valves and fittings and 'f_t' for various pipe sizes are given in Table 18.

Table 18: Friction Constants for Valves and Fittings [15]

Valve/Fitting	Constant 'K'
Ball Valves	$K = 3 f_t$
Gate Valves	$K = 8 f_t$
90° Elbow	$K = 30 f_t$
Tee Joint	$K = 80 f_t$
Expansions	$K = \frac{1}{2} \left(1 - \frac{D_1^2}{D_2^2} \right)$
Contractions	$K = \frac{1}{2} \left(1 - \frac{D_1^2}{D_2^2} \right)$

For a 4” pipe in complete turbulence, the value of “ f_t ” is 0.017 and for a 2” pipe in complete turbulence, the value of “ f_t ” is 0.014. The value of the dynamic viscosity of water is taken as 0.001307 Pa-s. The Darcy friction factor for the supply and return pipes is obtained from the Moody chart. From the previous calculation, for Path A, the velocity in the 4” diameter pipe is 0.37 m/s. Thus,

$$\text{Reynolds Number in 4” dia Supply pipe} = \frac{\rho \cdot v_A \cdot D_{\text{supply}}}{\mu} = \frac{1000 \cdot 0.37 \cdot (4 \cdot 25.4 / 1000)}{0.001307}$$

$$\text{Reynolds Number in 4” dia Supply pipe} = 28,873$$

$$\text{Relative roughness} = \frac{\varepsilon}{D} = \frac{0.0025}{4 \cdot 25.4 / 1000} = 0.025$$

From the Moody Chart at this relative roughness and Reynolds Number, the Darcy friction factor is observed to be 0.05. Similarly, for the 2” diameter return pipe, the Reynolds Number is 14,437, the relative roughness is 0.049 and the friction factor at this intersection is 0.07. The friction losses are calculated and tabulated below.

Similarly, using the calculated velocities, the head loss in the various paths in the network can be calculated. A detailed listing of the valves and fittings in the various other paths in the network is provided in Appendix A. The following table summarizes the calculated head loss values for the network. The predicted head loss for Path A is thus seen to be 0.1 m of water.

Table 19: Friction Losses in Path A

Major Losses	Pipe Dia (in)	Length (ft)	Velocity (m/s)	Friction Factor	Head Loss (m)	V Sq. Coeff
Supply 4"	4.00	36.00	0.37	0.05	0.01	0.09
Return 2"	2.00	45.00	0.37	0.07	0.02	0.17
Minor Losses						
Ball Valves	D1(in)	ft	K	Velocity(m/s)	Head loss(m)	V Sq. Coeff
Supply 4"	4.00	0.0170	0.05	0.37	0.0004	0.00
Return 2"	2.00	0.0140	0.04	0.37	0.0003	0.00
90 Deg Elbow	D1(in)	ft	K	Velocity(m/s)	Head Loss(m)	V Sq. Coeff
Supply 4"	4.00	0.0170	0.51	0.37	0.0036	0.03
Supply 4"	4.00	0.0170	0.51	0.37	0.0036	0.03
Return 2"	2.00	0.0140	0.42	0.37	0.0030	0.02
Return 2"	2.00	0.0140	0.42	0.37	0.0030	0.02
Return 2"	2.00	0.0140	0.42	0.37	0.0030	0.02
Return 2"	2.00	0.0140	0.42	0.37	0.0030	0.02
Return 2"	2.00	0.0140	0.42	0.37	0.0030	0.02
Tee Joints	D1(in)	ft	K	Velocity(m/s)	Head Loss(m)	V Sq. Coeff
Supply 4"	4.00	0.0170	1.36	0.37	0.0096	0.07
Supply 4"	4.00	0.0170	1.36	0.37	0.0096	0.07
Return 2"	2.00	0.0140	1.12	0.37	0.0079	0.06
Return 2"	2.00	0.0140	1.12	0.37	0.0079	0.06
Expansions	D1(in)	D2(in)	K	Velocity(m/s)	Head Loss(m)	V Sq. Coeff
Cooling Tower Connection Return	2.00	4.00	0.38	0.37	0.0026	0.02
Contractions	D1(in)	D2(in)	K	Velocity(m/s)	Head Loss(m)	V Sq. Coeff
HX Return 4" to 2"	2.00	4.00	0.38	0.37	0.0026	0.02
	Head Loss (ft)	0.32	Total Head Loss(m)	0.1	Total V² Coefficient	0.71

Table 20: Summary of Network Friction Losses

Path	Network Loss (m H₂O)	Network Loss (ft H₂O)
A	0.10	0.32
B	2.54	8.34
C	0.08	0.26
D	0.15	0.48
E	4.21	13.82
F	2.00	6.56
G	0.09	0.29
H	0.05	0.16
I	0.03	0.11
Total Network Losses	9.25	30.36

The static head for any pump is the difference in the suction head and the delivery head which the pump must overcome at all times, irrespective of system resistance. The suction head is the distance between the impeller axis and the supply sump, which in this case is the cooling tower sump, which was measured to be 6 feet from the ground. The delivery head is the distance between the impeller axis and the delivery sump, which for the current cooling tower is the return line which was measured to be 10 feet from the ground. Thus, the static head for the current setup is 4 feet or 1.22 meters.

The final contributing element to the pressure losses in the network is the pressure drop in the shell-side of the shell and tube heat exchangers and the pressure drop in the cooling channels of the non-shell and tube condensers, the double-cone type and spiral type condensers in Path H and Path I. The pressure drop across the supply and return lines will be equal to the maximum head loss in the heat exchangers.

There are 2 major methods of calculating the shell side pressure drops in shell and tube heat exchangers: The Bell-Delaware method and the Kern Method [5] [7]. The Bell Delaware method is selected for the current application because of its proven accuracy and detailed calculation technique for baffled shell and tube heat exchangers, involving correction factors for the various leakage and bypass streams as outlined in chapter 3.

The Bell-Delaware Method involves dividing the heat exchangers as shown in the figure below, into the entry and exit sections, the internal crossflow sections and the window sections and obtaining the total pressure drop as the summation of individual pressure drops. The dimensions of the heat exchanger in path A and the calculation for the corresponding shell side pressure drop is illustrated here and a summary of the calculations for the other heat exchangers is shown below.

$$\text{Total Shell Side Pressure Drop, } \Delta P = \Delta P_c + \Delta P_w + \Delta P_e$$

Where, $\Delta P_c = \text{Pressure Drop in internal crossflow sections}$
 $\Delta P_w = \text{Pressure Drop in baffle window sections}$
 $\Delta P_e = \text{Pressure Drop in entry and exit sections}$

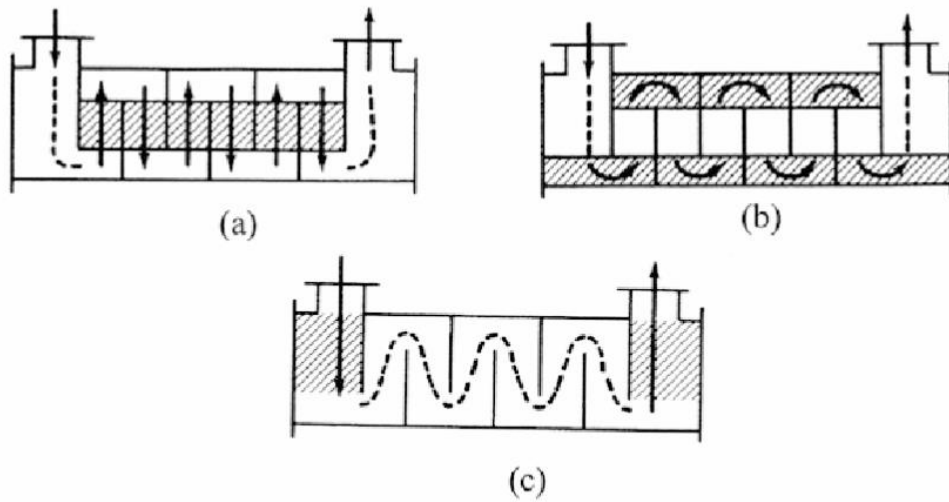


Figure 34: Sections of Shell and Tube Heat exchangers in the Bell-Delaware Method-(a) internal crossflow sections, (b) window sections, (c) entry/exit sections [46]

Table 21: Dimensions of Heat Exchanger A

Item	Dimension
Heat Exchanger Type	Fixed Tubesheet, Single pass in Shell and Tube
Surface Area(ft ²)	40
No. of Tubes	68
Tube Internal diameter(in), D_i	0.277
Tube Internal diameter(in), D_o	0.375
Tube Length(ft), l	6
Shell Internal Diameter, D_s (in)	6
Baffle Spacing(in), B	14.4
Number of Baffles, n_B	5
Baffle Segmental Cut(%), B_c	43%
Tube Arrangement	Triangular, 30°
Pitch between tubes(in)	0.4688
Clearance between tubes(in)	0.0938

The first step is to get the geometrical dimensions of the heat exchanger within the crossflow sections and the window sections in order to get the flow areas. Figure 34 shows the various dimensions required to analyze this.

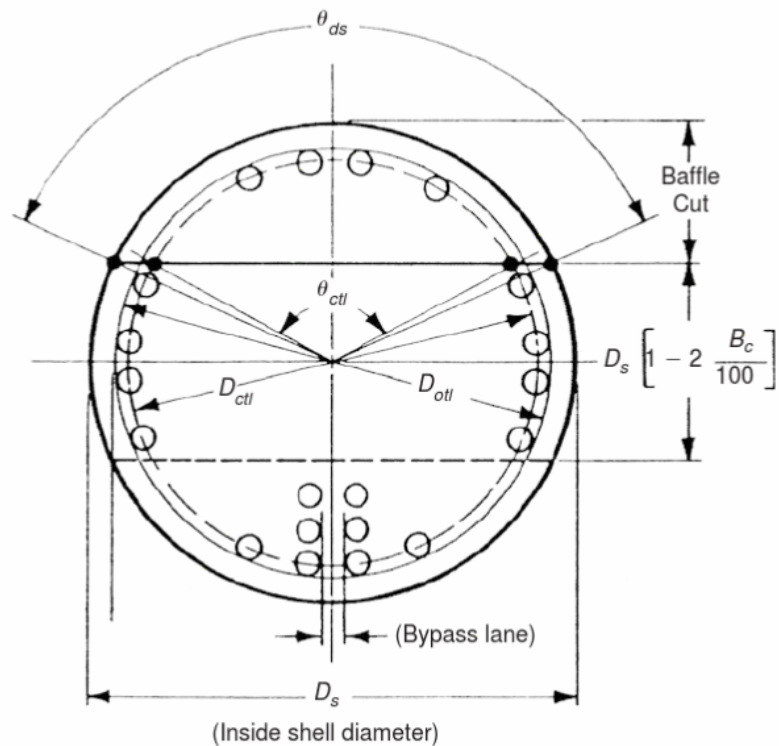


Figure 35: Dimensions within Shell and Tube Heat Exchangers [7]

The Outer tube Limit Diameter and the Central Tube limit diameters can be obtained by finding the value of the diametric shell-to-tube bundle clearance from the following graph.

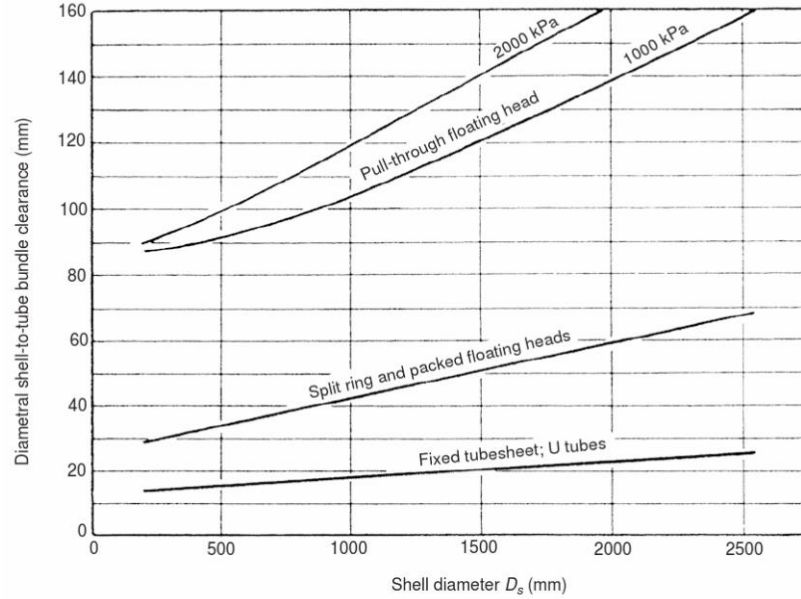


Figure 36: Diametral Shell-to-tube clearance for various heat exchanger configurations [7]

The Outer limit and central tube limit diameters are then calculated as follows.

$$D_{otl} = D_s - \text{Diametral Shell to tube clearance}$$

$$D_{ctl} = D_{otl} - D_o$$

The cross-flow area between each pair of baffles is then calculated as

$$S_m = B \left[(D_s - D_{otl}) + \frac{(D_{otl} - D_o)}{(P_{T_{eff}})} (P_T - D_o) \right]$$

Where, $P_{T_{eff}}$, effective Pitch = P_T for square/triangular layouts

Next, the baffle window angles, θ_{ds} and θ_{ctl} are calculated in radians from the geometry shown in the previous figure. Bc is the segmented baffle cut percentage. This is taken as 43% if not specified in the engineering drawings for the heat exchangers.

$$\theta_{ds} = 2 \cos^{-1}(1 - 2B_C)$$

$$\theta_{ctl} = 2 \cos^{-1} \left[\frac{D_S(1 - 2B_C)}{D_{ctl}} \right]$$

The fraction of tubes in cross-flow, F_C , is then calculated from the following equation:

$$F_C = 1 + \frac{1}{\pi} (\sin \theta_{ctl} - \theta_{ctl})$$

The fraction of tubes in each baffle window, F_W , is then calculated.

$$F_W = 0.5(1 - F_C)$$

Using this, the window-flow area, S_W , can then be calculated.

$$S_W = \frac{1}{8} D_S^2 (\theta_{ds} - \sin \theta_{ds}) - \frac{1}{4} n_t F_W \pi D_O^2$$

The entering mass flux, G , is calculated as the product of the fluid density and the entrance velocity. The Reynolds Number is calculated from the mass flux as shown below. Using the obtained Reynolds Number, the ideal friction factor across the tube bank can be calculated from the correlation below.

$$Re = \frac{G \cdot D_O}{\mu}$$

$$f_{ideal} = b_1 \left(\frac{1.33}{P_T/D_O} \right)^b (Re)^{b_2}$$

Where the numerical constant 'b' is given by the following relation and the numerical constants b_1 , b_2 , b_3 and b_4 are obtained from the following table.

$$b = \frac{b_3}{1 + 0.14(Re)^{b_4}}$$

Table 22: Friction Factor for Heat Exchanger in cross-flow section

Layout Angle	Reynolds Number	b_1	b_2	b_3	b_4
30° (triangle)	$10^5 - 10^4$	0.372	-0.123	7.00	0.5
	$10^4 - 10^3$	0.486	-0.152		
	$10^3 - 10^2$	4.57	-0.476		
	$10^2 - 10$	45.1	-0.973		
	<10	48.0	-1.000		
60° (triangle)	$10^5 - 10^4$	0.303	-0.126	6.59	0.520
	$10^4 - 10^3$	0.333	-0.136		
	$10^3 - 10^2$	3.5	-0.476		
	$10^2 - 10$	26.2	-0.913		
	<10	32	-1.000		
45° (Rotated Square)	$10^5 - 10^4$	0.391	-0.148	6.30	0.378
	$10^4 - 10^3$	0.0815	-0.220		
	$10^3 - 10^2$	6.09	-0.602		
	$10^2 - 10$	32.1	-0.963		
	<10	35.0	-1.000		

The number of tube rows crossed between baffle tips, N_C , is given as follows, where P'_T is the corrected pitch for the type of layout and θ_{tp} is the angle of layout (30° or 60° for triangular layouts).

$$N_C = \frac{D_S(1 - 2B_C)}{P'_T}$$

$$P'_T = P_T \cos \theta_{tp}$$

The effective number of rows crossed in one baffle, N_{CW} is calculated as follows.

$$N_{CW} = \frac{0.8 B_C D_S}{P'_T}$$

It must be noted that neither N_C nor N_{CW} are rounded off even though they are non-integer values. The ideal pressure drop across the tube bank, ΔP_{ideal} and in each baffle window, $\Delta P_{w,ideal}$, can now be calculated as follows.

$$\Delta P_{ideal} = \frac{2 f_{ideal} N_C G^2}{g_c \rho \Phi}$$

$$\Delta P_{w,ideal} = \frac{(2 + 0.6N_{cw}) \dot{m}_o^2}{g_c \rho S_m S_w} \quad (If Re \geq 100)$$

$$\Delta P_{w,ideal} = \frac{26v\dot{m}_O^2}{g_c\sqrt{S_m S_w}} \left[\frac{N_{cw}}{P_T - D_O} + \frac{B_c D_S}{D_w^2} \right] + \frac{\dot{m}_O^2}{g_c \rho S_m S_w} \quad (If Re < 100)$$

Where, the Equivalent Diameter for each Baffle Window is given by:

$$D_w = \frac{4 \cdot S_w}{\pi D_o n_{tubes} * 0.5(1 - F_C) + D_s \cdot \theta_{ds}}$$

The Corrected Pressure drop values for the entire exchanger in the central baffle spaces, P_C , and in the baffle windows, P_w are given by multiplying the ideal values by the number of baffles and by the correction factors for leakage, R_L and bypassed flow, R_B

$$\Delta P_C = (n_B - 1) \cdot \Delta P_{ideal} \cdot R_L \cdot R_B$$

$$\Delta P_w = n_b \cdot \Delta P_{w,ideal} \cdot R_L$$

The correction factors R_L and R_B account for the leakage and bypass streams are based on the condition and design of the heat exchanger. Both have typical values within 0.1 to 1.0, with values in the region of 0.4-0.6 for R_L and 0.4-0.7 for R_B [7]. For all heat exchangers in this calculation, these values are taken as 0.6 and 0.7 respectively.

The pressure drop in the entrance and exit spaces is obtained by the following correlation which uses a correction factor for unequal baffle spacing, R_s . This factor has a range of 0.3 to 1.0, with the value taken as 1.0 if the spacing is uniform. It is taken as 0.9 for all condensers.

$$\Delta P_e = 2 \Delta P_{ideal} \cdot \left(1 + \frac{N_{cw}}{N_c} \right) R_B \cdot R_s$$

Finally, the total pressure drop is given by summing up the pressure drops in each section of the heat exchanger.

$$\text{Total Shell Side Pressure Drop, } \Delta P = \Delta P_C + \Delta P_w + \Delta P_e$$

Using these correlations, the pressure drops of the shell and tube heat exchangers in each path were calculated. A summary of the calculated values for heat exchanger in path A is shown in the following table. Similar tables for all the other heat exchangers are shown in Appendix B.

Table 23: Summary of Pressure drop calculation for Heat Exchanger in Path A

Parameter, symbol and unit	Value
Shell Internal Diameter(m), D_s	0.1524
Tube Outer dia(m), D_o	0.009525
Diametral Shell-tube bundle clearance(m)	0.0130
Outer Tube Limit Dia(m), D_{otl}	0.14
Central Tube Limit Dia(m), D_{ctl}	0.129875
Baffle Spacing(m), B	0.3658
Tube Pitch,(m), P_t	0.0119
Tube Arrangement	Triangle
Effective Tube pitch(m), P_{eff}	0.0119
Cross Flow Area(m ²), S_m	0.0143
Baffle Segmental Cut(%), B_c	43%
Central tube Limit angle(rad), θ_{ctl}	2.8115
Fraction of tubes in Cross-flow,(nond), F_c	0.2082
Baffle Window Angle(rad), θ_{ds}	2.8607
Fraction of tubes in each baffle window,(nond), F_w	0.3959
Window flow Area(m ²), S_w	0.0056
Flow Velocity in Path(m/s), v	0.3714
Mass flow Rate of Shell Side Fluid(kg/s), mdot	3.0113
Entering Mass flux, G, (kg/m ² s),	371.4324
Fluid Viscosity(Pa-s), μ	0.001307
Pitch to Tube dia ratio	1.25
Pitch Parallel to flow(m), P_T'	0.01031
Number of Tube Rows Crossed between baffle tips, N_c	2.07
Effective no. of tube rows crossed per baffle window, N_{cw}	5.08
Reynolds Number, Re	2,706.88
Flow Condition	Turbulent
Kinematic Viscosity(m ² /s), ν	0.0000013
Equivalent Dia of Baffle Window(m ²), D_w	0.0179845
Ideal Friction Factor across tube bank, f_{ideal}	0.1541
Shell-fluid Density (kg/m ³), ρ	1,000.00
Viscosity Correction Factor, ϕ	1.000
Ideal Tube bank pressure drop(Pa), ΔP_{ideal}	87.983
Ideal baffle window Pressure drop(Pa), ΔP_{w_ideal}	287.776
Leakage Correction Factor, R_L	0.60
Bypass Correction Factor, R_B	0.70
Unequal Baffle Spacing Factor, R_s	0.90
Total Pressure Drop(Pa), ΔP	1394.4
Total Pressure Drop (psi)	0.20
Total Pressure Drop (ft of water)	0.41
Shell side pressure drop, P_s, (m H₂O)	0.13

This method of calculation is limited to baffled shell and tube heat exchangers with an ‘E’ Type shell as per TEMA specifications. The pressure drop in the special heat exchangers in paths G and H were taken as the dynamic head ($V^2/2g$) as an estimate based on size and the current path velocity. Further, by using the calculation spreadsheet, it was possible to devise a method of predicting the pressure drop of each heat exchanger as a second order polynomial function of the velocity in that path. The equation coefficients derived for these polynomial functions are shown in Table 22.

A summary of the results for the shell side pressure drops in the heat exchangers in each path is shown in the following table. The graph shows the variation in shell side pressure drop over the expected range of velocity in the network.

Table 24: Summary of Shell-side Pressure drops in each path

Path	Velocity in Path (m/s)	Shell-side pressure drop (m of H ₂ O)	Shell-side pressure drop (ft of H ₂ O)	Coefficients for prediction equation $\Delta P \text{ (m of H}_2\text{O)} = a.v^2 + b.v$	
				a	b
A	0.37	0.13	0.41	0.7803	0.0933
B	2.41	1.55	5.09	0.2314	0.0828
C	0.41	0.07	0.25	0.3791	0.0531
D	0.51	0.10	0.31	0.252	0.0943
E	4.46	4.37	14.35	0.202	0.0848
F	1.97	0.85	2.80	0.1821	0.0733
G	0.53	0.01	0.05	0.051	0.0
H	0.41	0.01	0.03	0.051	0.0

As seen from the above calculations, the heat exchanger in path ‘E’ has the biggest head loss value. Thus, this value will be used for calculation of the system curve.

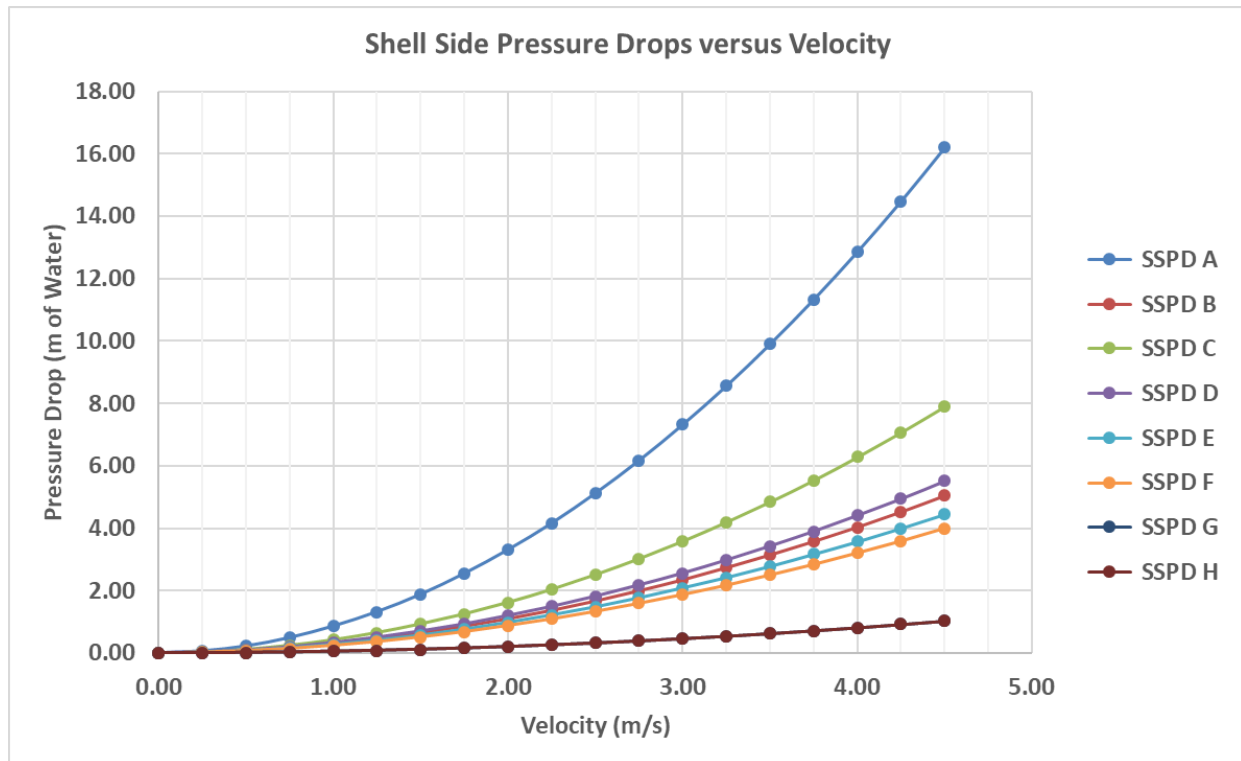


Figure 37: Variation in the Shell side pressure drop with velocity

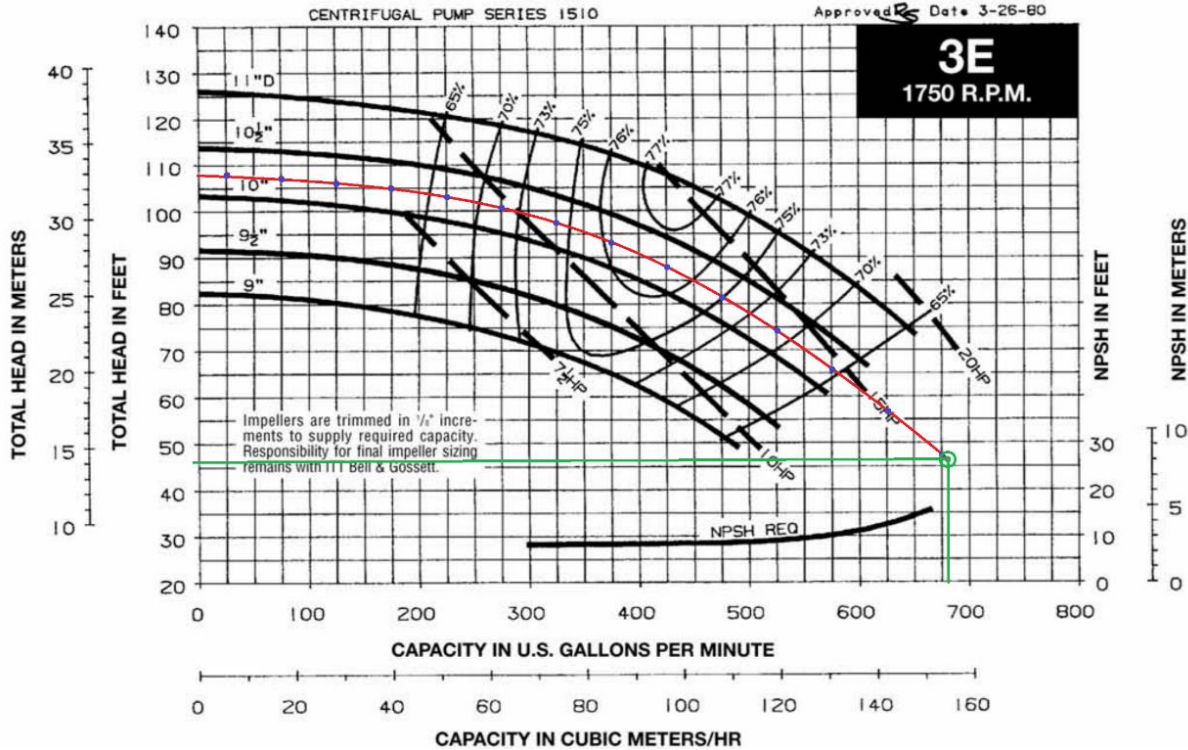
To obtain the system curve, the three sources of head losses in the network, namely the static head, the network head losses and the highest shell-side pressure drop can all be added and analyzed. A summary of the total head loss in the network at the current operating point is shown below in Table 23.

Table 25: Total Head loss at current operating point

Path	Network Pressure Drop (m of H ₂ O)	Network Pressure Drop (ft of H ₂ O)	Shell Side Pressure Drop (m of H ₂ O)	Shell Side Pressure Drop (ft of H ₂ O)
A	0.10	0.3232	0.13	0.41
B	2.54	8.3364	1.55	5.09
C	0.08	0.2643	0.07	0.25
D	0.15	0.4805	0.10	0.31
E	4.21	13.8247	4.37	14.35
F	2.00	6.5604	0.85	2.80
G	0.09	0.2944	0.01	0.05
H	0.05	0.1601	0.01	0.03
I	0.03	0.1119	-	-
Totals	9.25	30.36	4.37	14.35
Calculated Static Head = 1.83 m or 4.00 ft of H₂O				
Total Head Loss at Current Operating Point = 9.25 + 4.37 + 1.83 = 14.84 m or 48.70 ft of H₂O				

Using the frictional network resistance values at various flows, the system curve can be obtained for a plot of head versus flow, which is the conventional method of depicting pump curves.

1750 RPM PUMP CURVES



The pump curve for the Bell and Gossett pump model “E-1510-3E” (shown in Figure 38) currently installed at the facility was recreated in an Excel spreadsheet. Using this spreadsheet with the pressure drop relations, the head loss at any flow rate can be estimated which can then allow curve equations for both the pump curve and the system curve to be generated with a third-order polynomial in order to predict the system performance at other operating flow rates. The intersection of the curves as obtained at the measured pump outlet pressure via this calculation is

at about 665.69 gpm which is slightly higher than the expected operating point at 663 gpm (<1% difference) as per measured pressure at pump outlet.

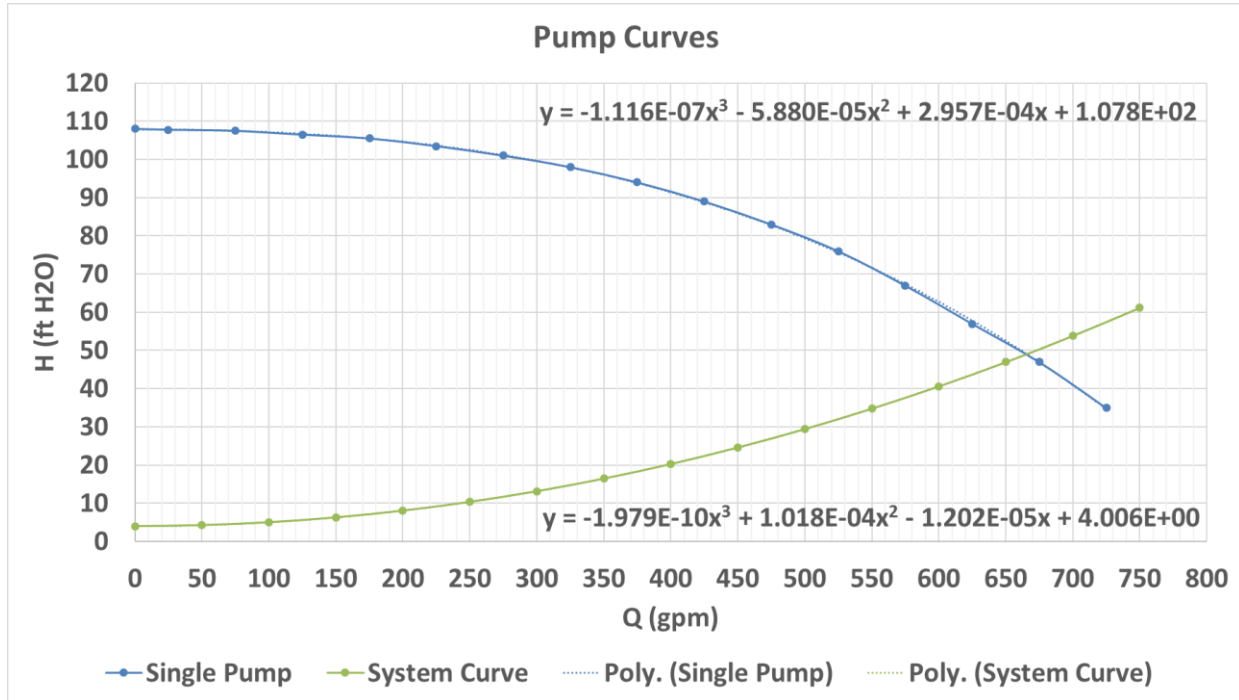


Figure 39: Obtained Pump and System Curve

As seen from the pump curves, the current pump is overloaded and is operating beyond its BEP design point which should technically be near 350 gpm. As per the provided data for the current pump, the pump was sized for 275 gpm and 100 feet of Total Dynamic Head. There is a very high flow requirement in this application along with a minimum head requirement because of the quantity of the heat exchangers on the demand side. Since the intersection of the pump curve and the system curve must be as close to the Best Efficiency Point, it is imperative that the facility switch to either a single larger pump or use multiple pumps in parallel to ensure uninterrupted flow and optimum process performance. Operating an inline centrifugal pump beyond its optimum

design flow point may also damage the pump motor and cause repeated issues which can bring production to a standstill.

In order to verify the obtained flow rate via the heat balance and to size the pump correctly, the pump outlet pressure was examined at the facility via a pressure gauge. The pressure at the pump outlet with all heat exchangers operational was measured to be between 20 and 21 psig which is around 14.5 meters or 48 feet of water. Looking at the obtained system curve and pump curve and extending it for a 10.25-inch impeller diameter, the flow rate at this pressure head is 658 gpm. The frictional head losses as calculated from the calculations above are 21.08 psig or 48.70 ft of water. The higher obtained value from the heat balance can be rounded off to about 680 gpm and 50 feet of head to be used as the system demand to size the pump.

Series e-1510 Performance Curves

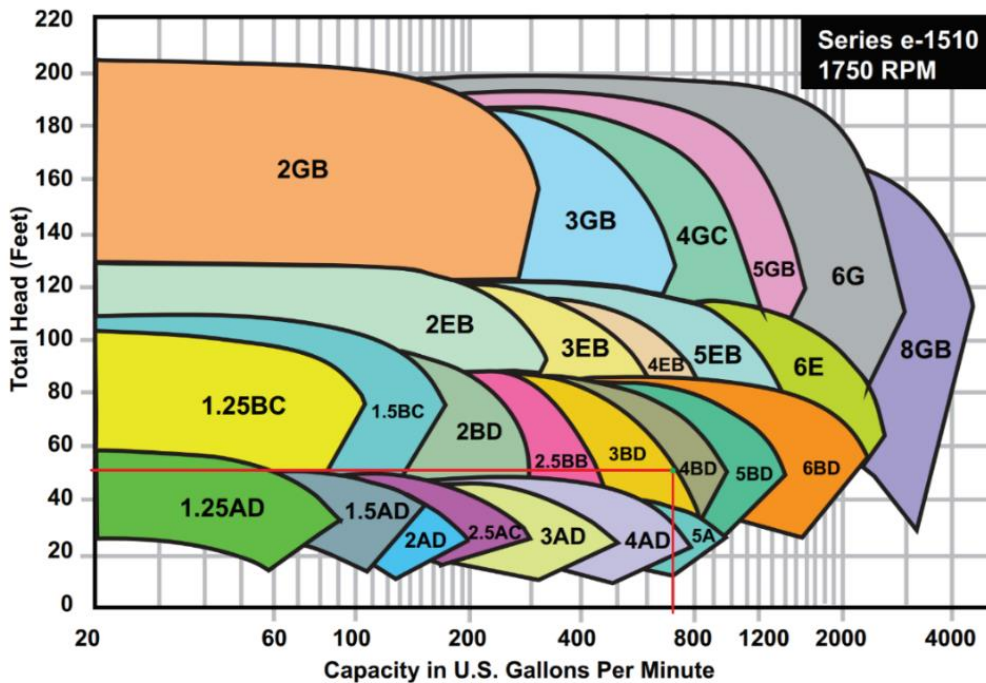


Figure 40: Performance curves for Bell & Gossett in-line pumps from the e-1510 pump manual

If the facility decides to use a single larger pump, the new pump must be selected such that the BEP of the new pump is as close as possible to the current operating flow and head conditions. The new pump may also be slightly oversized in order to allow the possibility of minor expansion of the process and/or to account for any source of pressure losses unaccounted for in the current calculation.

Table 26: Possible new pumps from Manufacturer's catalog

Parameter	Pump e1510-4BD	Pump e1510-3BD	Pump e1510-4GC	Pump e1510-5EB
Operating Flow Rate (gpm)	680	680	680	680
Operating Pressure Head (ft H ₂ O)	50	50	50.1	50
Efficiency at Op. point (%)	84.1%	79.4%	79.6%	82.1%
Power usage at Op. Point (hp)	10.2	10.8	10.8	10.4
Revolutions per minute (RPM)	1574	1630	1087	1509
Impeller Dia Required (inches)	8.5	9.0	12.25	8
NPSH _{req} (ft H ₂ O)	8.97	10.9	12.7	6.45
Suction Diameter (inches)	5	4	5	6
Discharge Diameter (inches)	4	3	4	5
Motor Nameplate Parameters	15hp, 1800 RPM	15hp, 1800 RPM	15 hp, 1200 RPM	20 hp, 1800 RPM
Floor Space Required (ft ²)	5.49	5.23	7.23	7.1
Projected Base Cost of Pump Model	\$10,300	\$9,900	\$14,700	\$14,000

Looking at the online pump manual for Xylem/Bell and Gossett [47], a series of performance curves can be obtained, which can help in selection of the right pump model. As seen in Figure 40, at the desired flow conditions, the pump models “4BD” and “3BD” are suitably within the range of operations. Additionally, the online selection tool on the manufacturer’s website gave more data on these pumps, including one other pump which operates with a 1200

RPM rated motor. We can now look at the initial cost and operating efficiency of these pump models when operating at the desired condition to directly compare them and select a pump. The operating characteristics from the pump curves and other relevant data from the manufacturer's catalog is shown in Figure 25.

It can be seen from the data that pump models "4BD" and "5GB" are more efficient and relatively cheaper than the models "3BD" and "4GC". However, one important factor to account for in pump selection and installation is the Net Positive Suction Head Required (NPSH_R). The NPSH_R is the pressure head that must be available to the pump at its inlet in order for it to operate at the desired condition [48]. This is important in order to avoid cavitation or bubble formation due to spontaneous boiling at the impeller entry, which is the point in the entire system where the pressure is the lowest. To prevent the system pressure from dropping below the vapor pressure head for the water, it is necessary to ensure that the NPSH_{available} is always greater than the NPSH_{Required} at the operating flow rate. The NPSH_{Required} is dependent on the flow through the pump and is provided by the manufacturer as part of the pump curves after testing pumps at multiple flow rates for the suction head, typically, when a 3% decrease in discharge head is observed [49]. The NPSH_{Available} can be calculated for the current setup as follows.

$$NPSH_{Available} = H_{atm} + H_{static\ suct} - H_{cavitation} - H_{f\ suction}$$

Where, H_{Static suct} = Height of sump liquid surface above the pump impeller centerline

H_{atm} = Atmospheric Pressure Head on Liquid in Sump,

H_{Cavitation} = Vapor Pressure of Water at the relevant temperature

H_{f suction} = Friction losses in the suction pipe

The static suction head in the current network is the height of the cooling tower sump from the pump impeller which is 6 feet or 1.83 m. The vapor pressure at the average cooling tower

entry/exit temperature of 15°C is 1,698 Pa or 0.57 feet. The atmospheric pressure head at the facility is 33.9 feet of water.

The suction pipe friction losses are calculated as shown below.

$$H_{f_{suction}} = Major\ losses + Minor\ Losses$$

$$H_{f_{suction}} = \left(K + \frac{fL}{D} \right) \cdot \frac{v^2}{2g}$$

The Suction line is approximately 8 feet in length and there are two elbows, one pipe entrance and one pipe exit on the suction line which will all cause head losses. According to the Crane Technical Paper [15], the ‘K’ values for elbows, pipe entries and pipe exits are 30.0, 0.78 and 1.0 respectively. The friction factor in the pipe at inlet in complete turbulence is 0.049.

$$H_{f_{suction}} = \left((30.0 + 30.0 + 0.78 + 1.0) + \frac{0.049 \cdot 2.44}{0.1016} \right) \cdot \frac{5.16^2}{2 \cdot 9.81} = 0.44 \text{ m or } 1.45 \text{ feet water}$$

$$\text{Thus, } NPSH_{Available} = H_{atm} + H_{static\ suct} - H_{cavitation} - H_{f_{suction}}$$

$$NPSH_{Available} = 33.9 + 6 - 1.42 - 1.45 = 37.04 \text{ ft of H}_2\text{O}$$

Thus, using these values, the $NPSH_{Available}$ can be calculated as 37.04 feet and consequently, any of the listed pumps can be selected without a considerable risk of cavitation in the system. With the given specifications and performance data from the manufacturer’s catalog, installing pump model “4BD” is a very good option. This pump has a discharge diameter directly compatible without fittings to the current discharge piping but will need an expansion fitting on the suction side since its suction flange and inlet size is different from the cooling tower sump flange size. Additionally, upon purchase, this new pump must be installed with minimal fittings on the suction line and as close to the cooling tower as possible to reduce any more friction losses from the piping. A rough analysis of the costs involved are shown in Table 24 and the final pump curve is shown in Figure 41.

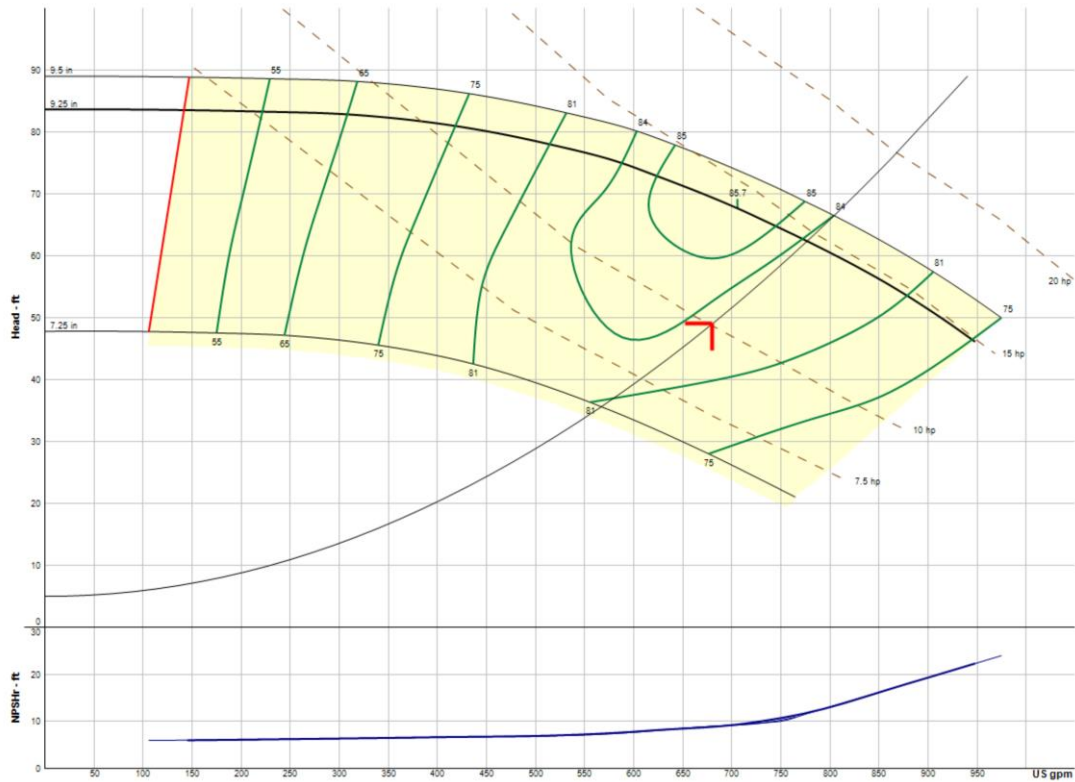


Figure 41: Pump curve after using selected Pump model “e-1510-4BD”

Table 27: New Centrifugal Pump Purchase and Installation Costs

Parameter	Cost
Pump Purchase	\$10,300
Frame	\$2,000
Labor	\$500
Electrical connections	\$500
Mechanical Connections	\$1,000
Overheads	\$1,700
Total	\$16,000

If the facility decides to use pumps in parallel, it is recommended [29] to use either a second unit of the current pump or to replace the current pump entirely with two new pumps capable of a similar capacity. This similarity is necessary to prevent issues with backflow caused due to additional pumping resistance close to the pump outlet. The pump curve obtained in the previous section can be extended for examining pumps in parallel and to get an idea of the operating point if pumps are installed in parallel.

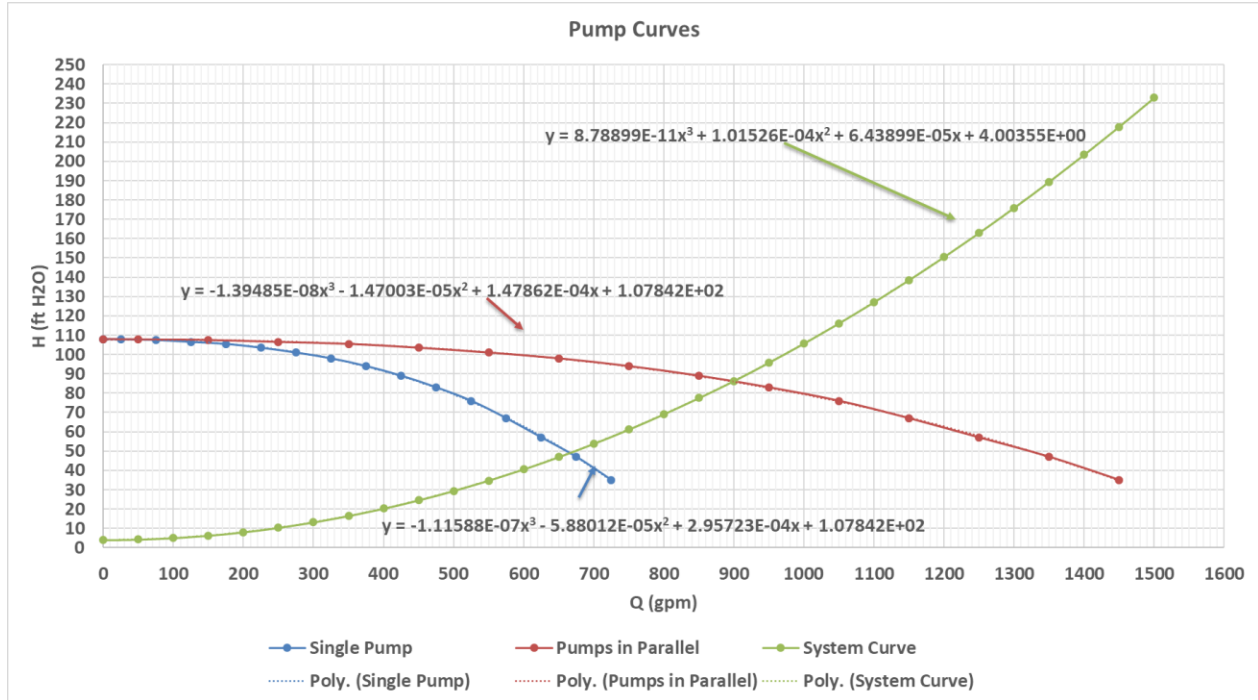


Figure 42: Pump Curve for Pumps in Parallel with 2 units of the current pump

When using two units of the current pump in parallel, we can estimate the pump curve by doubling the flow rates at every operating point. Similarly, the system curve can also be extended to get the operating point at its intersection with the new pump curve. This is shown in Figure 42. From the curves above, the possible operating point for this arrangement can be seen to be at 900 gpm with 84 feet of head. There are a couple of problems with using this arrangement for the system. Such a high flow rate and pressure head at the pump will lead to velocities as high as 7.16 m/s in the 4” diameter pipe and 28.64 m/s in the 2” diameter pipe, which can cause heavy erosional damage to the equipment in use. Also, upon browsing the manufacturer’s website, it was seen that the current pump model (Bell & Gossett Series 1510-Model 3E) has been discontinued by the manufacturer. Hence, a different and slightly less intensive pump model must be selected as a

replacement. From the online pump selection tool on the manufacturer’s website, for 2 parallel pumps, the options are as shown in Table 27.

Table 28: Possible Options for Parallel Pumps

Parameter	Pump e1510-3BD	Pump e1510-4EB	Pump e1510-3GB	Pump e1510-3EB
Operating Flow Rate per pump (gpm)	341	340	340	340
Operating Pressure Head (ft H ₂ O)	49.1	49	49.1	49
Efficiency at Op. point (%)	78.7%	78%	72.5%	73.2%
Power usage per pump at Op. Point (hp)	5.34	5.39	5.79	4.86
Revolutions per minute (RPM)	1672	1146	1094	1527
Impeller Dia Required (inches)	7.875	11	9	11
NPSH _{req} (ft H ₂ O)	6.08	5.36	7.84	4.86
Suction Diameter (inches)	4	5	4	4
Discharge Diameter (inches)	3	4	3	3
Motor Nameplate Parameters	7.5 hp, 1800RPM	7.5 hp, 1200RPM	7.5 hp, 1200 RPM	10 hp, 1800 RPM
Floor Space Required (ft ²)	7.46	11.27	5.29	5.29
Base Cost of Model (2 units)	\$9,800	\$14,600	\$14,600	\$9,600

With this data it can be seen that the pump model “3BD” with the 7.875 inch impeller is a good choice in this arrangement since it has a decent operating efficiency with the operating point is near the BEP and the base cost of the pump is relatively low. An additional benefit observed in the pump curve for this model is that the system curve intersects with the pump curve relatively closer to the Y-axis as compared to the current pump. As a result, if there are minor flow variations in the system, there will be a smaller, almost negligible change observed in the pressure head available. In contrast, the operating point of the current pump as illustrated earlier was very close to the operating flow capacity of the pump curve, causing a relatively larger variation in the

pressure head even with minor changes in the flow. The pump and system curves are illustrated in Figure 42.

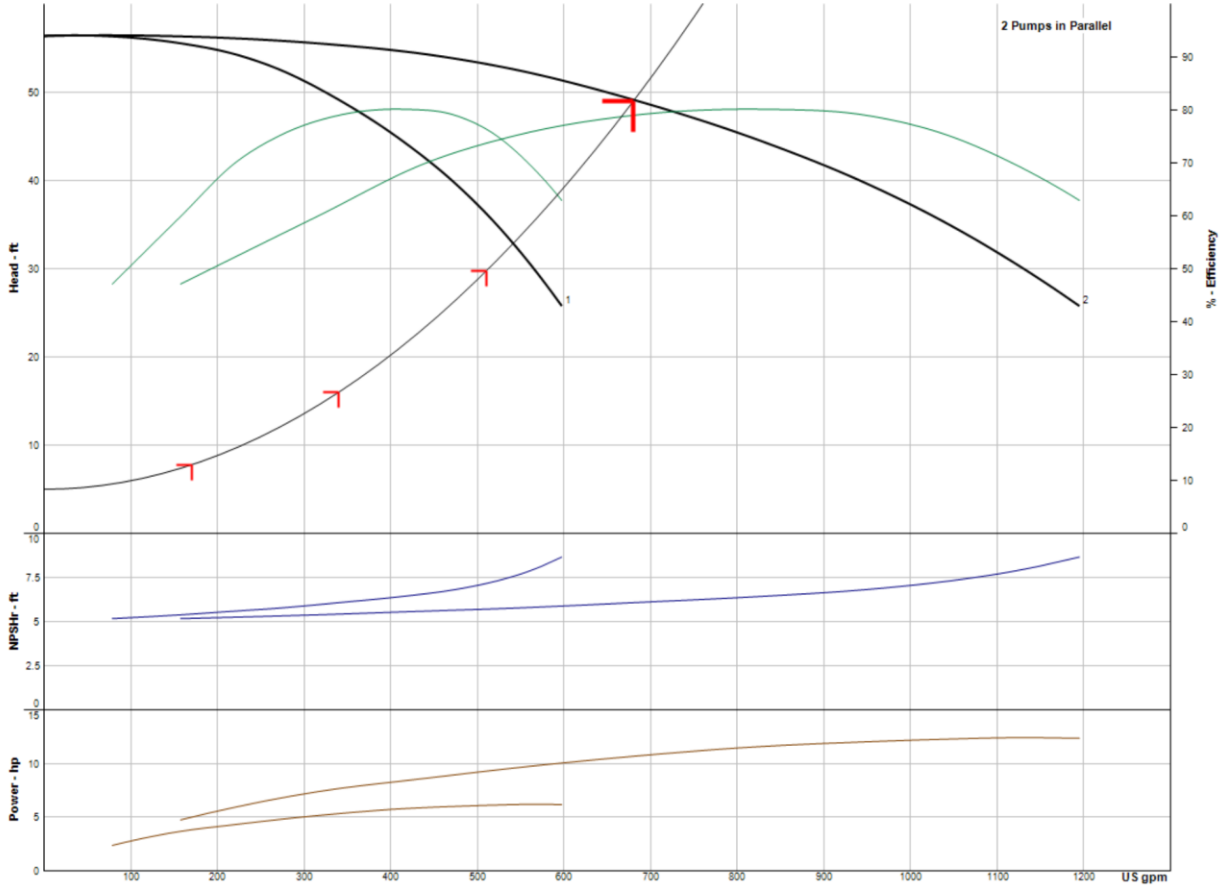


Figure 43: Pump Curves for 2 units of the selected “E1510-3BD” Pumps in Parallel

The cost of installing these pumps is broken down in the following table.

Table 29: Cost of Installing selected pumps in parallel

Parameter	Cost
Pump Purchase	\$9,800
Frames	\$5,000
Labor	\$1,000
Electrical connections	\$1,000
Mechanical Connections	\$1,000
Overheads	\$1,200
Total	\$19,000

The operating costs, energy savings and a simple payback period for the same operating hours and electricity rates as compared to the current pump are shown in Table 29.

Table 30: Calculation of Simple Payback Period from Energy Savings on New Pump Arrangements

Current Energy Rate	\$ 0.0546/kWh	Current Demand Rate	\$ 7.7/kW/month
Annual Operating Hours	4800hrs/yr	Measured Pump Current Demand	16.6 hp / 12.38 kW
Single new Pump		New Parallel Pumps	
New Electric Demand at op. point	10.2 hp / 7.61 kW	New Electric Demand at op. point	10.68 hp / 7.97 kW
Change in Demand	6.4 hp / 4.77 kW	Change in Demand	5.92 hp / 4.42 kW
Current Annual Operating Cost	\$4,388.46/yr	Current Annual Operating Cost	\$4,388.46/yr
New Annual Operating Cost	\$2,697.59/yr	New Annual Operating Cost	\$2,825.21/yr
Total Cost Savings	\$1,691/yr	Total Cost Savings	\$1,563/yr
Implementation Costs	\$16,000	Implementation Costs	\$19,000
Simple Payback Period	10 years	Simple Payback Period	13 years

Even though these payback periods are pretty high, they only consider electric energy and demand savings. Additional costs arising from maintenance and production downtime that can be expected with the current pump operation have not been considered. Thus, these are the two options that the facility can consider when checking the feasibility of replacing the pump of the current system for the heat exchanger network.

4.2.3: Clean the Shell-sides of all Shell and Tube Heat Exchangers

As per the root cause analysis of the problem of reduced product output there is a possibility of fouling on the shell side of the shell and tube heat exchangers. The fouling may be caused due to the use of cooling tower water directly for process cooling. As mentioned in Chapter 3, fouling increases the thermal resistance of the tubes, reducing the heat transfer through the exchanger.

Heat transfer within the heat exchanger is given by the correlations below:

$$Q = U * A * LMTD * F$$

Where, U = Overall Heat Transfer Coefficient

A = Effective Surface Area of the Heat Exchanger

LMTD = Log Mean Temperature Difference

F = LMTD Correction Factor

$$LMTD = \frac{\Delta T_1 - \Delta T_2}{\ln(\Delta T_1 / \Delta T_2)}$$

Where, for a parallel flow heat exchanger,

$$\Delta T_1 = (T_{hot,in} - T_{cold,in}) \text{ and } \Delta T_2 = (T_{hot,out} - T_{cold,out})$$

And, for a counter flow heat exchanger,

$$\Delta T_1 = (T_{hot,in} - T_{cold,out}) \text{ and } \Delta T_2 = (T_{hot,out} - T_{cold,in})$$

To calculate the anticipated savings from elimination of fouling, the amount of heat transfer obtained upon using a cleaner heat exchanger will be calculated and compared to the heat transfer in the exchanger in the current state. The increased amount of condensed product will then be compared to the current value, and the obtained value will then be converted into a dollar value with a payback prediction on the implementation cost of carrying out this recommendation.

As mentioned earlier in Chapter 3, the overall heat transfer coefficient for a shell and tube heat exchanger is governed by the following equation.

$$\frac{1}{U.A} = \frac{1}{h_i.A_i} + \frac{R_{fi}}{A_i} + \frac{\ln(D_o/D_i)}{2.\pi.k.L} + \frac{1}{h_o.A_o} + \frac{R_{fo}}{A_o}$$

This equation can be used to calculate the heat transfer in the current setup by estimating the tube outer fouling factor 'R_{fo}' based on the operating conditions and then recalculating the heat transfer coefficient with a fouling factor value that can be expected after cleaning. The first step is to calculate the inner and outer film coefficients 'h_i' and 'h_o'. The methods used for the calculation of these coefficients via the Nusselt number depends on the Reynolds Number regime of the flow associated with the characteristic length.

To calculate the outer heat transfer coefficient, the crossflow area within the exchanger baffles is calculated to obtain the velocity of flow within this area. Using the mass flow rate of the water into the heat exchanger shell-side, obtained from the previous calculation, the Reynolds number of the flow within the crossflow area is calculated. The Nusselt Number is calculated by the method followed by Holman [50] or by Nitsche [10] depending on the Reynolds Number of the flow.

Nusselt Number (Holman),
$$Nu_o = C * Re_o^n * Pr_o^{1/3}$$
 (Re_o >10,000)

Nusselt Number (Nitsche),
$$Nu_o = 0.196 * Re_o^{0.6} * Pr_o^{1/3}$$
 (Re_o >10, Triangle Pattern)

Where, Nu_o = Nusselt Number on the shell side

Re_o = Reynolds Number within Crossflow area on Shell-side

Pr_o = Prandtl Number of Shell-side fluid

C, n = Numerical Constants, dependent on ratio of Pitch to Tube outer dia

The Cross-flow area for each tube is given by:

$$A_{c/s} = D_{shell\ ID} * Baffle\ Spacing * \left(1 - \frac{Tube\ outer\ Dia}{Pitch}\right)$$

Using the cross-flow area and an estimate of the shell-side liquid flow rate, the maximum velocity was given by:

$$V_{max} = \frac{Shell\ Side\ Volume\ Flow\ Rate}{A_{c/s}} = \frac{Shell\ Side\ mass\ flow\ Rate}{Density * A_{c/s}}$$

The Reynolds Number was then calculated using the following relation:

$$Re = \frac{\rho * V_{max} * D_o}{\mu}$$

The shell side fluid is the cooling tower water and the Prandtl Number for it is calculated from the following correlation.

$$Pr_o = \frac{\mu_o * C_p}{k_o}$$

Where, μ_o = Dynamic viscosity of the shell side fluid

C_p = Isobaric Specific heat capacity of the shell-side fluid

k_o = The coefficient of thermal conductivity of the shell-side fluid

In the Holman method, the coefficients 'C' and 'n' are obtained from a reference [50], considering the ratio of the horizontal and vertical pitch (S_n and S_p respectively) of the tubes to the outer diameter of the tubes, D_o .

Table 31: Values of Constant 'C'

Vertical Pitch Ratio		Horizontal Pitch Ratio, S_n/D_o			
		1.25	1.5	2.0	3.0
S_p/D_p	1.25	0.386	0.305	0.111	0.0703
	1.5	0.407	0.278	0.112	0.0753
	2.0	0.464	0.332	0.254	0.22
	3.0	0.322	0.396	0.415	0.317

Table 32: Values of Constant 'n'

Vertical Pitch Ratio		Horizontal Pitch Ratio, S_n/D_o			
		1.25	1.5	2.0	3.0
S_p/D_p	1.25	0.592	0.608	0.704	0.752
	1.5	0.586	0.62	0.702	0.744
	2.0	0.57	0.602	0.632	0.648
	3.0	0.601	0.584	0.581	0.608

When using the Nusselt number obtained in the Holman method, the ideal heat transfer coefficient h_o for flow across the tube banks is obtained. However, this is an ideal value and hence, a conservative correction factor of 0.6 is multiplied to the obtained value to get a more practical h_o value. This correction factor is not multiplied to the value when the Nitsche method is used instead.

The internal heat transfer coefficient is calculated from the Nusselt Number for the inner surface. This Nusselt number is obtained by the Nitsche Method correlations that are based on the Reynolds Number of the flow inside the tube. These correlations are valid when the Prandtl Number of the fluid is within 0.6 to 500. When turbulent, the correlation used is the same as the Dittus-Boelter Equation.

$$\text{For Laminar flow}(Re < 2,300), Nu_i = \left(\frac{0.186 * Re * Pr * D}{L} \right)^{0.33}$$

$$\text{For Transition flow}(2,300 < Re < 8,000), Nu_i = (0.037 * Re^{0.75} - 6.66) * Pr^{0.42}$$

$$\text{For Turbulent flow}(Re > 8,000), Nu_i = 0.023 * Re^{0.8} * Pr^{0.33}$$

A summary of the calculated internal and external heat transfer coefficient values for the heat exchanger in path C is shown below in Table 31. Similar tables summarizing the calculations for the remaining heat exchangers in the network are shown in Appendix C. The shell side and tube side flow parameters were obtained in the previous calculations and have been converted to metric units to maintain uniformity in this calculation. Since the Shell-side Reynolds Number in this instance was greater than 10 but less than 10,000, the Nitsche method was employed to calculate the external heat transfer film coefficient.

Next, the heat transfer before and after fouling is calculated using the same reference area while considering the fouling factors for both situations. Since there is no practical way to obtain the fouling factors within the exchanger without overhauling and extensive testing, standard fouling factor values are used from available literature and the resulting annual savings are tabulated. Even though the tubes of the heat exchangers are cleaned periodically, in order to get an estimate of the performance for the exchangers in the worst scenario, an internal fouling value for alcohol vapors, obtained from standard heat transfer textbooks [50], [51] are used.

Table 33: Internal and External Heat Transfer Coefficients for Heat Exchanger C

Parameter	Quantity
Tube External Diameter (m)	0.0095
Shell Internal Diameter (m)	0.2032
Baffle Spacing (m)	0.3353
Pitch between tubes (m)	0.0127
Crossflow Area (m ²)	0.0170
Shell side flow rate (m ³ /s)	0.0059
Max velocity in shell (m/s)	0.3492
Reynolds Number in Shell	2545.22
Nusselt Number	45.47
External Heat Transfer Coefficient (W/m²-K)	2824.90
Tube mass flow rate(kg/s)	0.0212
Tube fluid Density(kg/m ³)	866.51
Tube flow rate (m ³ /s)	2.445 x 10 ⁻⁵
Number of Tubes	85
Number of passes	2
Number of Tubes per pass	42.5
Cross-sectional Area per tube (m ²)	3.888 x 10 ⁻⁵
Total Flow Area (m ²)	0.0017
Flow Velocity per tube (m/s)	0.0148
Dynamic Viscosity of Tube fluid (N-s/m ²)	0.011
Specific heat of Mixture (J/kg-K)	4184.67
Reynolds Number in each Tube	8.1994
Prandtl Number of Fluid	145.715
Nusselt Number for internal flow	3.1663
Thermal Conductivity of Fluid (W/m-K)	0.3159
Internal Heat Transfer Coefficient (W/m²-K)	142.163

A summary of the heat transfer calculation before and after cleaning is shown below in Table 32. Since the exchanger in path C is a U-tube Shell and Tube Heat exchanger, A correction factor ‘F’ must be multiplied to the LMTD to correct for the 2 passes on the tube side [24].

$$F = \frac{S \cdot \ln(W)}{\ln\left(\frac{1+W-S+S \cdot W}{1+W+S-S \cdot W}\right)}$$

Where,

$$S = \frac{(R_1^2+1)^{0.5}}{(R_1-1)} \quad ; \quad W = \left[\frac{(1-P_1 \cdot R_1)}{(1-P_1)}\right]^{1/N}$$

$$P_1 = \frac{T_{tube,exit}-T_{tube,entry}}{T_{shell,entry}-T_{tube,entry}} \quad ; \quad R_1 = \frac{T_{shell,entry}-T_{shell,exit}}{T_{tube,exit}-T_{tube,entry}}$$

$N = \text{No. of Shell passes}$

Table 34: Heat transfer in Heat Exchanger C

Parameter	Quantity
Reference Area, A (m ²)	4.27
Internal Fouling factor, R _{fi} , m ² K/W (Before cleaning) [51]	0.00009
External Fouling factor, R _{fo} ,m ² K/W (Before cleaning) [6], [7]	0.00052869
Internal Surface Area, A _i (m ²)	3.150
External Surface Area, A _o (m ²)	4.265
Overall Heat Transfer coefficient, ‘UA’ (Before cleaning)	225.01
External Fouling factor, R _{fo} ,m ² K/W (After cleaning)	0.0
Internal Fouling factor, R _{fi} , m ² K/W (After cleaning)	0.0
Overall Heat Transfer coefficient, ‘UA’ (After cleaning)	231.894
Hot Fluid temp in (°C)	60
Hot fluid Temp out(°C)	32.22
Cold Fluid Temp in(°C)	15.56
Cold Fluid Temp out(°C)	10
LMTD(°C)	30.34
Correction Factor, F	1.0
Heat transfer before cleaning (W)	6794.49
Heat transfer after cleaning (W)	7034.81
Change in Heat Transfer after Cleaning (W)	240.32

The change in heat transfer due to cleaning can now be used to calculate the additional product generated via a heat balance as seen in Section 4.1. The additional product generated annually can then be used to calculate the additional profits that the facility can gain, using the

estimated dollar profit value per liter. It has been assumed here that all the heat exchangers are all fouled equally and that the facility is able to sell all of the additional product generated after cleaning.

$$(Q_{After} - Q_{before}) = \dot{m} * Q_{Heat\ Duty\ per\ kg}$$

$$Q_{Heat\ duty\ per\ kg} = \left[\dot{m} C_{p_{vap}} (T_{Entry} - T_{sat}) + \dot{m} h_{fg} + \dot{m} C_{p_{liq}} (T_{sat} - T_{exit}) \right]_{ethanol}$$

$$+ \left[\dot{m} C_{p_{vap}} (T_{Entry} - T_{sat}) + \dot{m} h_{fg} + \dot{m} C_{p_{liq}} (T_{sat} - T_{exit}) \right]_{water}$$

$$\dot{m} = \frac{(Q_{After} - Q_{before})}{0.5 \left(C_{p_{vap}} (T_{Entry} - T_{sat}) + h_{fg} + C_{p_{liq}} (T_{sat} - T_{exit}) \right)_{ethanol} + 0.5 \left(C_{p_{vap}} (T_{Entry} - T_{sat}) + h_{fg} + C_{p_{liq}} (T_{sat} - T_{exit}) \right)_{water}}$$

Table 35: Calculation of Additional Profit from increased product output from Exchanger C

Parameter	Quantity
Change in Heat transfer after Cleaning (W)	240.32
Specific Heat of Ethanol @ Entry (Superheated Vapor) (KJ/kgK)	1.532
Specific Heat of Ethanol @ Exit (Liquid) (KJ/kgK)	2.538
Specific Heat of water @ Entry (Superheated Vapor) (KJ/kgK)	1.946
Specific Heat of water @ Exit (Liquid) (KJ/kgK)	4.181
Ethanol Vapor $\Delta T (T_{Entry} - T_{sat}), ^\circ C$	21.37
Ethanol Liq $\Delta T (T_{sat} - T_{exit}), ^\circ C$	6.408
Water vap $\Delta T (T_{Entry} - T_{sat}), ^\circ C$	3.41
Water Liq $\Delta T (T_{sat} - T_{exit}), ^\circ C$	24.378
Heat duty per kg of product (KJ/kg)	3,422.19
Additional product generated (kg/s)	0.00007
Additional product generated (kg/hr)	0.25
Annual Operating hours (hrs/yr)	4800
Additional product generated Annually (kg/yr)	1,213.48
Additional product generated Annually (l/yr)	1,400.42
Profit per liter (\$/liter)	\$3.20
Total Additional Profit (\$)	\$4,481.33

The total net profit from the additional product generated in all heat exchangers annually is summarized next. A production correction factor is used as done previously in Section 4.1 to consider the scenarios when some, but not all, heat exchangers may be operational. The annual implementation cost to achieve periodic cleaning is the annual maintenance cost of having the heat

exchangers cleaned by a professional firm familiar with the process. This cleaning can take place on weekends or holidays to prevent production losses due to downtime. Another one-time component of the implementation cost is the cost of installing pipe fittings such as “Tee” Joints at the exchanger inlet and outlet ports to allow periodic cleaning without overhauling the piping network each time. These costs are then used to calculate a simple payback period in months on this investment.

Table 36: Calculation of Payback period on cleaning all shell and tube heat exchangers

Parameter	Quantity
Additional Annual Mass Flow (kg/yr)	8,552.23
Additional Annual Volume Flow(liter/yr)	9,869.74
Production Correction Factor	0.6
Total Additional Annual Revenue	\$18,949.91
Annual Maintenance Costs (\$1,500/HX)	\$9,000.00
Net Annual Savings	\$9,949.91
Implementation Costs (\$2,000/HX + First Cleaning Cost)	\$21,000.00
Simple Payback (months)	25

Since this calculation is highly sensitive to the external surface fouling factor value used in the calculation of the heat transfer increase, the additional product obtained and the consequent simple payback period was calculated for different fouling factor values applicable to the use of untreated cooling tower water as given by multiple sources. The sources, values and the results of those calculations are shown in the following table.

Table 37: Results with external fouling factors from various sources

Source	R_{fo} (m^2K/W)	R_{fo} ($ft^2 \cdot F$ - hr/BTU)	Additional Annual Volume Flow (l/yr)	Additional Revenue	Net Annual Savings	Simple Payback (months)
Kern, Process HT [7]; TEMA [6]	0.00052869	0.003	9,869.74	\$18,950	\$9,950	25
engineeringpage. com [52]	0.00053045	0.00301	9,896.40	\$19,001	\$10,001	25
AHRI Guideline E, 1997 [53]	0.00044058	0.0025	8,532.47	\$16,382	\$7,382	34

As it is seen from the results of this calculation, there is a sizable value of annual savings realizable by simply cleaning the shell and tube heat exchangers at the facility and it is definitely worth examining the various shell and tube heat exchangers for any current fouling. With payback periods of within 2-3 years, it is strongly recommended to have a professional firm come by to thoroughly inspect and flush out the deposits in the entire network.

The fouling in these heat exchangers is probably of Type 1 (Viscous Liquids) and Type 3 (Cohesive Solids). To eliminate these within the stainless steel exchangers, a citric acid based surfactant rinse cycle should work well when employed alternately with a hot water rinse cycle. Additionally, it is recommended to reduce the accumulation of dirt and other deposits in the cooling tower sump by use of a corrosion and fouling inhibitor in the form of a chemical additive to the make-up water. The cooling tower must also be inspected regularly to ensure the sediments at the base of its sump are removed. The facility should also look at retrofitting a replaceable water filter within the exit piping from the cooling tower to the pump. This would allow cleaner water flow into the heat exchanger network.

CHAPTER 5: CONCLUSIONS

5.1: Summary of Recommendations

As described in Chapter 4, the problem of reduced output variation was found via root cause analysis to be caused due to various discernable problems with the process equipment. The three main causes of reduced product output were found to be insufficient cooling capacity for year-round production, an overloaded cooling tower water pump and a high possibility of reduced heat transfer due to shell-side fouling. The process equipment was studied and solutions to fix this problem at the facility were examined within Chapter 4. The findings from this effort to analyze the problem are summarized in this section, followed by a look at the actions this facility has undertaken presently to act upon these findings at the time of writing. A few other ideas that would help improve the system in the short or long term were developed by brainstorming with the facility personnel and are highlighted.

Table 38: Summary of Analyzed Recommendations

Recommendation	Implementation Cost	Annual Operating Cost	Additional Annual Revenue	Net Cost Savings	Payback Period
Install a water-cooled 220-ton Chiller	\$256,975	\$86,296	\$2,506,752	\$2,420,456	1.5 months
Install a 220-ton Chiller and a water-side economizer	\$328,325	\$77,185	\$2,506,752	\$2,429,567	2 months
Install a new, better sized pump to replace the current pump	\$16,000	\$2,698	-	\$1,691	114 months
Install two new similar pumps in parallel to replace the current pump	\$19,000	\$2,825	-	\$1,563	146 months
Clean the shell-side of all the shell and tube heat exchangers	\$21,000	\$9,000	\$18,950	\$9,950	25 months

It was found that the condensing heat exchangers were dependent on the ambient weather conditions to achieve sufficient process cooling. To improve this, the feasibility of installing a chiller to generate chilled water in the right quantity and quality was analyzed. The heat load on the heat exchangers to generate the desired amount of product all year was calculated as a function of the major components in the compound being processed. It was found that a chiller of 220-ton capacity would suffice for the facility. Looking at the economics of installing the chiller, it was seen that there is a sufficiently short payback period for this action which may also justify the installation of a water-side economizer to reduce the operating costs of the chiller by providing free cooling when the ambient wet bulb temperature is low.

To check the current operating characteristics of the cooling tower water pump, the system curve for the network was found. The point of intersection of the system curve with the pump curve gave the current operating pressure head and volumetric flow rate offered by the pump. The system curve was modelled considering the friction losses in the network and the maximum shell-side pressure drop within the heat exchangers. With the system curve and the desired flow characteristics, two new pump arrangements were examined. A single new pump was selected from a manufacturer's catalog to replace the current pump. An installation of two new, similar pumps was also examined for the current operating point. This was followed by an estimate of the energy savings and the economics to be expected for the given installation options.

Finally, the possible increase in the product generated by the condenser network was computed by examining heat transfer relations considering the possible fouling within the condensers. This computation was carried out for multiple possible values of fouling factors for cooling tower water as denoted in available literature as there is no definitive way to measure the fouling factor without overhauling, sampling and rigorous testing, which is impractical in the

current operating condition. Increased sales arising from the additional product generated were estimated and a simple payback period on the initial investment was calculated.

5.2: Current Measures and Future Work

All of the recommendations mentioned in the thesis were based on data from physical observations and measurements made when on-site. The data for the network diagrams and the equipment specifications were collected over a total of three facility visits made at roughly three- or four-month intervals. The facility personnel were very cooperative, helpful and open to suggestions throughout the process of data collection and assessment. As mentioned in the previous section, the facility was in touch with the author of this thesis through the process of data analysis. In this section, the efforts undertaken by the facility to understand the findings and initiate a more in-depth look at the process equipment are described. This is followed by a summary of related items that the facility may examine in the near future in order to further their process capabilities, as and when they elect to expand.

It is evident from the literature review in Chapter 3 that effects of fouling and insufficient flow within heat exchangers would lead to an observable difference in the pressure heads of the heat exchanger inlet and outlet streams. To measure this, the facility undertook gauge pressure readings from the various ports in the cooling tower water network. Unfortunately, the facility did not setup ports for pressure measurement at each heat exchanger inlet and outlet when initially mounting them, which would have been an ideal way to identify the extent of pressure drops. But even though there were only a few pressure taps in the water lines, the pressure gauges on the heat exchangers depicted the pressures on the shell side. The readings obtained with all the condensers running and with specific heat exchangers cut-off are tabulated in Table 37.

Table 39: Pressure gauge readings in network before changes (psig)

Location	All Condensers running	Heat Exchanger B Cut-off	Heat Exchangers B and C Cut off
Pump Outlet	20	26	30
Heat Exchanger A (Supply / Return)	14 / 12	14 / 12	16 / 12
Heat Exchanger B	No Gauge	Cut-Off	Cut-off
Heat Exchanger C	7	6	Cut-off
Heat Exchanger D	8	11	12
Heat Exchanger E	9	11	12
Heat Exchanger F	No Gauge		
Heat Exchanger G	12	14	15
Heat Exchanger H	12	15	17

Although the pressure readings are not obtained at the supply and return ends of the condensers, these readings give a clear indication that the pump is undersized to meet the network flow requirements. There is a small but measurable increase in the shell-side pressures within the heat exchangers when exchanger B was shut and a slightly bigger increase when exchangers B and C both were shut off. This makes sense since the pump faces lesser resistance to push water through when there are fewer paths within the network. It is strongly recommended that the facility find points in the network close to all heat exchanger supply and return ports to install pressure taps in order to ensure the flow within the heat exchangers is optimum.

It was mentioned in Chapter 4 that there is a very high possibility of fouling within the shell and tube heat exchangers in the cooling network. This is because of the cooling tower being open to the atmosphere which can cause entry of dust particles into the sump. It follows that there must be signs of dirt accumulation at certain spots within the network. To act on this possible finding, the facility decided to overhaul and examine the pump casing assembly since it was the closest operational equipment to the cooling tower. It was found that the pump impeller was undamaged and in good working condition, but the casing had a lot of dirt and grime stuck on the inner surface. It is evident that all of the dirt within the cooling tower flows into the water basin and settles there carrying with it all the contaminants from the surrounding area that have been

pulled in. Since the pump draws water directly from the basin, the contaminants at the bottom of the cooling tower accumulated on the inner surface of the pump despite the presence of a filter at the pump inlet. The facility had the impeller and the casing cleaned and could see a small but distinct rise in the pressure head available in the heat exchanger network. The pressure readings before and after cleaning the pump casing are shown below.

Table 40: Pressure Readings before and after overhauling and cleaning pump (psig)

Location	All Condensers running	Heat Exchanger B Cut-off	Heat Exchangers B and C Cut off	All Condensers running, Gauges added, pump cleaned
Pump Outlet	20	26	30	23
Heat Exchanger A (Supply / Return)	14 / 12	14 / 12	16 / 12	12 / 12
Heat Exchanger B (Supply / Return)	No Gauge	Cut-Off	Cut-off	12 / 6
Heat Exchanger C	7	6	Cut-off	8
Heat Exchanger D	8	11	12	10
Heat Exchanger E	9	11	12	11
Heat Exchanger F	No Gauge			
Heat Exchanger G	12	14	15	13
Heat Exchanger H	12	15	17	14

The pressure rise in the shell side of the condensers after cleaning the pump demonstrates that there is a high possibility of fouling in the condensers as well and removal of the fouling will increase the flow rate to all condensers, improving heat transfer. Since fouling now seems to be one of the major causes for the diminished product output, the facility is in the process of identifying the right people to come in and overhaul the heat exchangers in order to examine the fouling that may have taken place. In order to further prevent the contamination in the cooling tower due to corrosion or settling of mineral deposits, a chemical inhibitor feed system has been installed at the cooling tower and is in use whenever the plant is in operation.

As mentioned in Chapter 2, the facility was prompt to fix the burner firing controls issue within the boiler to prevent safety concerns as well as any possibility of production downtime due

to a non-operational boiler. The facility also periodically examines the insulation on the still steam jackets and the piping leading up to it and has taken measures to ensure no hot surface is uninsulated.

The facility has also recently undertaken an initiative to proactively log all the critical parameters in the process equipment with an automatic monitoring system. This system also shows real-time information of the process parameters in easily understandable graphs and charts to assist the operators in making decisions and monitoring the process easily. This effort is commendable as it is difficult to manage something if it is not measured.

A few other ideas to look at in the future are installation of balancing valves, installing a pump with a bigger pipe feeding into the rear end of the network, new sprayers for the cooling tower and modification of the piping network. Installing balancing valves at the supply ports of the heat exchangers after installation of a new bigger pump may allow a better distribution of flow to the heat exchangers in the network. As discussed in Chapter 2, unbalanced flow rates in parallel paths due to the variation in the resistance across paths is an inherent disadvantage of a two-pipe direct return system and tuned balancing valves at the condensers may help fix this.

Installing a pump in parallel to the current pump with a larger pipe, feeding directly into the rear end of the network, may help boost the flow rate towards the rear condensers and improve their condensing ability. If this is done, it is recommended that the new pipe be at least 6" in diameter and have minimal valves and fittings on it, to avoid friction losses.

Changing the nozzle sprayers in the cooling tower may increase heat transfer by increasing the quantity of water coming into contact with the air passing through. The facility is also investigating the piping network and may elect to modify the size of the pipes in the network. It may be a good idea to install larger diameter pipes to carry more water around the network, but

this would again increase the pumping power necessary to maintain the same flow rate in the network. If a network modification of such a large scale is carried out, it is recommended to also install pressure gauge taps on all inlets and outlets to allow periodic pressure measurement and ensure the condensers are operating as expected. Another idea in this area is to reconfigure the placement of heat exchangers in the facility. The larger heat exchangers should be supplied by the pipes closer to the pump outlet and the smaller heat exchangers are supplied after those. This would help ensure the right amount of flow goes through the larger condensers.

In the near future, the facility plans to further analyze the findings of this thesis, in order to make long term changes to the facility. The facility personnel have been in touch with their local pump provider and consulting design engineers to try and figure out other short-term improvements they can make over the summer months to prevent the inevitable drop in production with a rise in ambient temperatures. Since installing a chiller means a large initial investment, the facility wishes to further analyze the economics and thermal behavior behind the use of chilled water for process cooling before investing in a chiller or a water-side economizer.

5.3: Closing Remarks

The interconnectivity of installed process equipment is always subject to issues arising from incompatibility and/or improper operating conditions. It can be seen from this analysis how important the initial selection, setup and maintaining adequate operating conditions of process cooling equipment in a manufacturing plant is. It is imperative to also constantly monitor the process equipment in any manufacturing facility to ensure operations at the maximum efficiency. When the quantity of product generated is directly dependent on heat transfer within process

equipment, there must be checks in place to ensure normal operations by correcting any deviations as soon as possible.

In a lot of engineering applications, there may be multiple factors contributing to an operational issue. As used in this study, root cause analysis is a great way to identify the key sources of such problems by studying the problem in reverse. Once such multiple sources of an issue are identified, a sensitivity analysis can also help understanding the priority and urgency of fixing each cause.

As mentioned earlier, economics drive the majority of decisions in engineering and this thesis was an exercise in demonstrating how to check the feasibility of critical or expensive engineering investments. The annual operational expenses for an equipment must also be considered when selecting such equipment. Simple engineering economics calculations such as payback periods and a cash flow analysis can provide interesting and quick insights that can help the decision-making process. Process equipment such as heat exchangers, pumps and boilers cost a lot of money upfront and ensuring the right selection during installation by trained personnel is paramount to a successful service life. There is always a point of balance between oversizing a process/system and planning to allow for future retrofits and a good engineer must know the difference between the two options.

In summary, this thesis demonstrated how to carry out an engineering analysis on heat exchangers and pumps in an existing system. The analysis of cooling towers, chillers and water side economizers was carried out from an initial selection point of view. Some ideas were generated for future analysis and consequent implementation at this facility. The author would like to thank the management at this facility for the opportunity to work on this problem and learning so much from it.

REFERENCES

- [1] US Energy Information Administration,, "Manufacturing Energy Consumption Survey (MECS) Survey Data," US Energy Information Administration, 1994.
- [2] Thermofin, "Caleos Shell & Tube Heat Exchangers," 2018. [Online]. Available: <http://www.thermofin.net/products/caleos-shell-and-tube-heat-exchangers/>.
- [3] Jennifer Mayo;De Dietrich Process Systems, "Criteria for selecting a Heat Exchanger for your process," De Dietrich Process Systems, 29 January 2015. [Online]. Available: <https://www.ddpsinc.com/blog-0/criteria-for-selecting-a-heat-exchanger-for-your-process>.
- [4] Indian Institute of Technology Delhi, "NPTEL – Chemical Engineering – Chemical Engineering Design - II," [Online]. Available: <https://nptel.ac.in/courses/103103027/pdf/mod1.pdf>.
- [5] R. H. Perry and D. W. Green, Perry's Chemical Engineers' Handbook, McGraw-Hill Book Co, 1985.
- [6] Richard C. Byrne; Tubular Exchanger Manufacturers Association Inc, Standards of The Tubular Exchanger Manufacturers Association, Tubular Exchanger Manufacturers Association Inc, 2007.
- [7] D. Q. Kern, Process Heat Transfer, New York, Toronto, London: McGraw-Hill Book Company, 1950.
- [8] D. A. Donohue, "Heat Transfer and Pressure Drop in Heat exchangers," *Industrial and Engineering Chemistry*, vol. 41, no. 11, 1949.
- [9] J. Saari, "Heat Exchanger Dimensioning," 09 November 2015. [Online]. Available: <https://www.scribd.com/document/289132039/Saari-Heat-Exchanger-Dimensioning#>.
- [10] M. Nitsche and R. Gbadamosi, Heat Exchanger Design Guide, New York: Elsevier, 2016.
- [11] R. S. Subramanian, "Shell and Tube Heat Exchangers," [Online]. Available: <http://online.fliphtml5.com/tjla/rpov/>.
- [12] US Department of Energy; Hydraulic Institute, Improving Pumping system performance (2nd Edition), Oakridge, TN, 2006.
- [13] Nuclear Power website contributors, "Main Parts of a Centrifugal Pump," Nuclear Power, [Online]. Available: <https://www.nuclear-power.net/nuclear-engineering/fluid-dynamics/centrifugal-pumps/parts-of-centrifugal-pump/>.
- [14] F. M. White, Fluid Mechanics (Eighth Edition), New York: McGraw-Hill Education, 2011.
- [15] Crane Co., Flow of Fluids through Valves, Fittings and Pipe : Metric Edition - SI Units, New York City: Crane Co., 1982.

- [16] N. Puck, "Puck Custom Enterprises," September 2013. [Online]. Available: <http://puckenterprises.blogspot.com/2013/09/understanding-pump-performance-curves.html>.
- [17] Micropyretics Heaters International, "Fire Tube Boiler Compared to OAB," [Online]. Available: https://mhi-inc.com/superheated_steam/fire-tube-boiler-vs-one-atmosphere-boiler.html.
- [18] L. Marie (Flow-Pac, "Jackson Systems Blog," 12 October 2011. [Online]. Available: <https://blog.jacksonsystems.com/two-pipe-return-systems-direct-vs-reverse/>.
- [19] Dave; Fraser Engineering, "Fraser Engineering," Fraser Engineering, 19 June 2014. [Online]. Available: <http://www.fraserengineering.com/blog/hydronic-piping-systems/>.
- [20] S. Duda, "Reverse-return Reexamined," *ASHRAE Journal*, vol. 57, no. 8, pp. 40-44, 2015.
- [21] G. N. Stoforos, Enhancement of continuous flow cooling of viscous foods using surface modified heat exchangers., Raleigh, North Carolina, 2017.
- [22] Alliant Metals, INC, "Why is Stainless Steel the Optimum Choice for Food Processing Equipment," [Online]. Available: <https://alliantmetals.com/why-is-stainless-steel-the-optimum-choice-for-food-processing-equipment/>.
- [23] Alfa Laval Thermal Inc, Heat Exchangers for HVAC, Richmond: Hoffman Hoffman Inc..
- [24] F. Incropera and D. Dewitt, Fundamentals of Heat and Mass Transfer, Notre Dame, West Lafayette: John Wiley & Sons, 2002.
- [25] P. Fryer and K. Asteriadou, "A prototype cleaning map: a classification of industrial cleaning processes," *Trends in Food Science and Technology*, vol. 20, pp. 225-262, 2009.
- [26] H. E. F. C. Conference, "Heat Exchanger Fouling and Cleaning XIII - 2019 Synopsis," HTRI, Warsaw, 2019.
- [27] D. M. Speyer, Shell-Side Pressure Drop and Heat Transfer in Baffled Shell-And-Tube Heat Exchangers, New York, 1973.
- [28] NPTEL, "Fluid Machinery," [Online]. Available: https://nptel.ac.in/courses/112104117/chapter_8/8_10.html.
- [29] Y. Wen, X. Zhang and P. Wang, "The Relationship Between the Maximum Efficiency and the Flow of Centrifugal Pumps in Parallel Operation," *Journal of Pressure Vessel Technology*, vol. 132 (3), no. 034501 (Apr 21, 2010), 2010.
- [30] ASHRAE, "2008 ASHRAE Equipment: Chapter 39, Cooling Towers," 2008. [Online]. Available: <https://www.me.ua.edu/me416/s09/pdf/ASHRAE2008Equipment-CoolingTowers.pdf>.

- [31] SPX Cooling Technologies, Inc, "SPX Cooling Technologies: List of Library Publications," 2016. [Online]. Available: <https://spxcooling.com/pdf/TR-017.pdf>.
- [32] Baltimore Aircoil Company, "Minimizing Energy Costs with Free Cooling," [Online]. Available: <http://www.baltimoreaircoil.com/english/resource-library/file/1473>.
- [33] Underground Energy, LLC, "Applied Hydrogeology Geothermal Innovation," 2018. [Online]. Available: <http://underground-energy.com/our-technology/ates/>.
- [34] Susanna Hanson; Jeanne Harshaw, "Trane: Free Cooling Using Water Economizers," 2008. [Online]. Available: <https://www.trane.com/Commercial/Uploads/PDF/11598/News-%20Free%20Cooling%20using%20Water%20Economizers.pdf>.
- [35] R. Kemper, "Part Load Efficiencies," Michaels Energy, [Online]. Available: <https://michaelsenergy.com/briefs/part-load-efficiencies/>.
- [36] Trane, "Centrifugal Chillers | Water-Cooled Chillers," [Online]. Available: <https://www.google.com/url?sa=i&source=images&cd=&ved=2ahUKEwipneruy8jhAhWPv1kKHZYBIQQjxx6BAgBEAI&url=https%3A%2F%2Fwww.trane.com%2Fcommercial%2Fnorth-america%2Fus%2Fen%2Fproducts-systems%2Fequipment%2Fchillers%2Fwater-cooled-chiller%2Fcentrifugal-liquid>.
- [37] National Institute of Standards and Technology, "NIST Chemistry WebBook, SRD 69 : Ethanol," U.S. Department of Commerce, 2018.
- [38] M. Holmgren, "X Steam Tables," 2006. [Online]. Available: <https://www.me.ua.edu/me215/f07.woodbury/ExcelStuff/XSteam-v2a.xlsm>.
- [39] F. Senese and M. Lewis, "What is the Antoine equation?," 07 July 1999. [Online]. Available: <https://antoine.frostburg.edu/chem/senese/101/liquids/faq/antoine-vapor-pressure.shtml>.
- [40] Dortmund Databank GmbH, "Heat of Vaporization Calculation by PPDS12 Equation (Ethanol)," Dortmund Databank GmbH, [Online]. Available: http://ddbonline.ddbst.com/PPDS12HVPCalculation/HVP_PPDS12CalculationCGI.exe.
- [41] Dortmund Databank GmbH, "Liquid Density Calculation by DIPPR105 Equation (Ethanol)," Dortmund Databank GmbH, [Online]. Available: <http://ddbonline.ddbst.de/DIPPR105DensityCalculation/DIPPR105CalculationCGI.exe>.
- [42] RS Means, RSMeans Mechanical Cost Data, Norwell, MA: Construction Publishers & Consultants, 2015.
- [43] FPL, "Water-Cooled Chillers," 2007. [Online]. Available: <https://www.fpl.com/business/pdf/water-cooled-chillers-primer.pdf>.
- [44] B. Gonzalez, "TMY - typical meteorological year- What should it represent and what means P50, P70 and P90," europa.eu, 7 March 2011. [Online]. Available:

- <https://europa.eu/capacity4dev/afretep/blog/tmy-%E2%80%93-typical-meteorological-year-what-should-it-represent-and-what-means-p50-p70-and-p90>.
- [45] National Oceanic and Atmospheric Administration, "Local Climatological Data Station Details," 04 April 2019. [Online]. Available: <https://www.ncdc.noaa.gov/cdo-web/datasets/LCD/stations/WBAN:13722/detail>.
- [46] R. W. Serth, Process Heat Transfer, Principles and Applications, Kingsville, TX: Elsevier, 2007.
- [47] Bell & Gossett, a xylem Brand, "B313F-e-1510," December 2018. [Online]. Available: <http://documentlibrary.xylemappliedwater.com/wp-content/blogs.dir/22/files/2014/01/B-313F-e-1510.pdf>.
- [48] Sulzer Pumps Ltd, Centrifugal Pump Handbook, Third Edition, Winterthur, Switzerland: Elsevier, 2010.
- [49] Xylem Applied Water Systems, "Pump cavitation and how to avoid it, Best Practices in pump system design," August 2015. [Online]. Available: http://buildings.xylem.com/files/2015/09/Cavitation-White-Paper_FINAL-2.pdf.
- [50] J. Holman, Heat Transfer, New York: McGraw Hill, 2010.
- [51] Y. Cengel, Heat Transfer: A Practical Approach, Reno, NV: McGraw-Hill, 2002.
- [52] Engineering Page, "Typical Fouling Factors," [Online]. Available: https://www.engineeringpage.com/technology/thermal/fouling_factors.html.
- [53] Air-Conditioning, Heating and Refrigeration Institute, "AHRI_Guideline_E_1997," 1997. [Online]. Available: http://www.ahrinet.org/App_Content/ahri/files/Guidelines/AHRI_Guideline_E_1997.pdf.
- [54] Corrosion Resistant Products, "Comparison of PFA and Isostatically Moulded PTFE Fittings," [Online]. Available: <http://www.crp.co.uk/technical.aspx?page=269>.

APPENDICES

Appendix A: Summary of Friction Losses Calculation for Paths B-I

Path B

- Supply/Return pipe velocity = 2.41 m/s; Rel. Roughness = 0.025 (Supply), 0.049 (return)
- Reynolds Number in 4" dia Supply pipe = 187,287; Friction Factor = 0.049
- Reynolds Number in 2" dia Supply pipe = 93,643; Friction Factor = 0.072

Table 41: Friction Losses in Path B

Major Losses	Pipe Dia (in)	Length(ft)	Velocity (m/s)	Friction Factor	Head Loss (m)	V Sq. Coeff
Supply 4"	4.00	18.0000	2.67	0.049	0.26	0.045
Return 2"	2.00	28.0000	2.67	0.072	0.60	0.103
Minor Losses						
Ball Valves	D ₁ (in)	f _t	K	Velocity (m/s)	Head loss(m)	V Sq. Coeff
Supply 4"	4.00	0.0170	0.05	2.41	0.02	0.003
Return 2"	2.00	0.0140	0.04	2.41	0.01	0.002
Return 2"	2.00	0.0140	0.04	2.41	0.01	0.002
90 Deg Elbow	D ₁ (in)	f _t	K	Velocity (m/s)	Head loss(m)	V Sq. Coeff
Supply 4"	4.00	0.0170	0.51	2.41	0.15	0.03
Supply 4"	4.00	0.0170	0.51	2.41	0.15	0.03
Return 2"	2.00	0.0140	0.42	2.41	0.12	0.02
Return 2"	2.00	0.0140	0.42	2.41	0.12	0.02
Return 2"	2.00	0.0140	0.42	2.41	0.12	0.02
Return 2"	2.00	0.0140	0.42	2.41	0.12	0.02
Tee Joints	D ₁ (in)	f _t	K	Velocity (m/s)	Head loss(m)	V Sq. Coeff
Supply 4"	4.00	0.0170	1.36	2.41	0.40	0.07
Return 2"	2.00	0.0140	1.12	2.41	0.33	0.06
Expansions	D ₁ (in)	D ₂ (in)	K	Velocity (m/s)	Head loss(m)	V Sq. Coeff
Contractions	D ₁ (in)	D ₂ (in)	K	Velocity (m/s)	Head loss(m)	V Sq. Coeff
HX Return 4" to 2"	2.00	4.00	0.38	2.41	0.11	0.02
	Total Head Loss (ft)	8.34	Total Head Loss(m)	2.54	Total V² Coefficient	0.44

Path C

- Supply/Return pipe velocity = 0.41 m/s; Rel. Roughness = 0.025 (Supply),0.049 (return)
- Reynolds Number in 4" dia Supply pipe = 31,761; Friction Factor = 0.049
- Reynolds Number in 2" dia Supply pipe = 28,517.93; Friction Factor = 0.072

Table 42: Friction Losses in Path C

Major Losses	Pipe Dia (in)	Length (ft)	Velocity (m/s)	Friction Factor	Head Loss (m)	V Sq. Coeff
Supply 4"	4.00	31.00	0.41	0.049	0.013	0.08
Return 2"	2.00	45.00	0.41	0.072	0.028	0.17
Minor Losses						
Ball Valves	D ₁ (in)	f _t	K	Velocity (m/s)	Head loss(m)	V Sq. Coeff
Supply 4"	4.00	0.0170	0.05	0.41	0.0004	0.003
Supply 4"	4.00	0.0170	0.05	0.41	0.0004	0.003
Return 2"	2.00	0.0140	0.04	0.41	0.0004	0.002
90 Deg Elbow	D ₁ (in)	f _t	K	Velocity (m/s)	Head loss(m)	V Sq. Coeff
Supply 4"	4.00	0.0170	0.51	0.41	0.043	0.03
Supply 4"	4.00	0.0170	0.51	0.41	0.043	0.03
Return 2"	2.00	0.0140	0.42	0.41	0.036	0.02
Return 2"	2.00	0.0140	0.42	0.41	0.036	0.02
Tee Joints	D ₁ (in)	f _t	K	Velocity (m/s)	Head loss(m)	V Sq. Coeff
Supply 4"	4.00	0.0170	1.36	0.41	0.012	0.07
Return 2"	2.00	0.0140	1.12	0.41	0.010	0.06
Return 2"	2.00	0.0140	1.12	0.41	0.010	0.06
Contractions	D ₁ (in)	f _t	K	Velocity (m/s)	Head loss(m)	V Sq. Coeff
HX Return 4" to 2"	2.00	4.00	0.38	0.41	0.003	0.02
	Total Head Loss (ft)	0.263	Total Head Loss(m)	0.08	Total V² Coefficient	0.48

Path D

- Supply/Return pipe velocity = 0.51 m/s; Rel. Roughness = 0.025 (Supply),0.049 (return)
- Reynolds Number in 4" dia Supply pipe = 19,911; Friction Factor = 0.051
- Reynolds Number in 2" dia Supply pipe = 19,911; Friction Factor = 0.074
- Reynolds Number in 2" dia Return pipe = 19,911; Friction Factor = 0.074

Table 43: Friction Losses in Path D

Major Losses	Pipe Dia (in)	Length (ft)	Velocity (m/s)	Friction Factor	Head Loss (m)	V Sq. Coeff
Supply 4"	4.00	10.00	0.51	0.051	0.0068	0.03
Supply 2"	2.00	26.00	0.51	0.074	0.0257	0.10
Return 2"	2.00	34.00	0.51	0.074	0.0337	0.13
Minor Losses						
Ball Valves	D ₁ (in)	f _t	K	Velocity (m/s)	Head Loss (m)	V Sq. Coeff
Supply 2"	2.00	0.0140	0.04	0.51	0.0006	0.002
Return 2"	2.00	0.0140	0.04	0.51	0.0006	0.002
90 Deg Elbow	D ₁ (in)	f _t	K	Velocity (m/s)	Head Loss (m)	V Sq. Coeff
Supply 2"	2.00	0.0140	0.42	0.51	0.0056	0.02
Supply 2"	2.00	0.0140	0.42	0.51	0.0056	0.02
Supply 2"	2.00	0.0140	0.42	0.51	0.0056	0.02
Supply 2"	2.00	0.0140	0.42	0.51	0.0056	0.02
Return 2"	2.00	0.0140	0.42	0.51	0.0056	0.02
Return 2"	2.00	0.0140	0.42	0.51	0.0056	0.02
Return 2"	2.00	0.0140	0.42	0.51	0.0056	0.02
Tee Joints	D ₁ (in)	f _t	K	Velocity (m/s)	Head Loss (m)	V Sq. Coeff
Supply 2"	2.00	0.0140	1.12	0.51	0.015	0.06
Return 2"	2.00	0.0140	1.12	0.51	0.015	0.06
Expansions	D ₁ (in)	D ₂ (in)	K	Velocity (m/s)	Head Loss (m)	V Sq. Coeff
HX Entry 2" to 2.5"	2.00	2.5000	0.18	0.51	0.0024	0.01
Contractions	D ₁ (in)	D ₂ (in)	K	Velocity (m/s)	Head Loss (m)	V Sq. Coeff
Supply 4" to 2"	2.00	4.00	0.38	0.51	0.005	0.02
HX Exit 2.5" to 2"	2.00	2.50	0.18	0.51	0.0024	0.01
	Total Head Loss (ft)	0.49	Total Head Loss(m)	0.15	Total V² Coefficient	0.56

Path E

- Supply/Return pipe velocity = 4.46 m/s; Rel. Roughness = 0.049 (Supply),0.049 (return)
- Reynolds Number in 2" dia Supply pipe = 173,225; Friction Factor = 0.072
- Reynolds Number in 2" dia Return pipe = 173,225; Friction Factor = 0.072

Table 44: Friction Losses in Path E

Major Losses	Pipe Dia (in)	Length (ft)	Velocity (m/s)	Friction Factor	Head Loss (m)	V Sq. Coeff
Supply 2"	2.00	9.0	4.46	0.072	0.656	0.03
Return 2"	2.00	10.0	4.46	0.072	0.729	0.04
Minor Losses						
Ball Valves	D ₁ (in)	f _t	K	Velocity (m/s)	Head Loss(m)	V Sq. Coeff
Supply 2"	2.00	0.0140	0.04	4.46	0.0425	0.002
Return 2"	2.00	0.0140	0.04	4.46	0.0425	0.002
90 Deg Elbow	D ₁ (in)	f _t	K	Velocity (m/s)	Head Loss(m)	V Sq. Coeff
Supply 2"	2.00	0.0140	0.42	4.46	0.425	0.021
Return 2"	2.00	0.0140	0.42	4.46	0.425	0.021
Tee Joints	D ₁ (in)	f _t	K	Velocity (m/s)	Head Loss(m)	V Sq. Coeff
Supply 2"	2.00	0.0140	1.12	4.46	1.134	0.057
Expansions	D ₁ (in)	D ₂ (in)	K	Velocity (m/s)	Head Loss(m)	V Sq. Coeff
HX Entry 2" to 4"	2.00	4.0000	0.38	4.46	0.38	0.019
Contractions	D ₁ (in)	D ₂ (in)	K	Velocity (m/s)	Head Loss(m)	V Sq. Coeff
Return 4" to 2"	2.00	4.0000	0.38	4.46	0.38	0.019
	Total Head Loss (ft)	13.82	Total Head Loss(m)	4.21	Total V² Coefficient	0.21

Path F

- Supply/Return pipe velocity = 1.97 m/s; Rel. Roughness = 0.049 (Supply),0.049 (return)
- Reynolds Number in 2" dia Supply pipe = 76,619; Friction Factor = 0.072
- Reynolds Number in 2" dia Return pipe = 76,619; Friction Factor = 0.072

Table 45: Friction Losses in Path F

Major Losses	Pipe Dia (in)	Length (ft)	Velocity(m/s)	Friction Factor	Head Loss (m)	V Sq. Coeff
Supply 2"	2.00	29.00	1.97	0.07	0.4135	0.11
Return 2"	2.00	34.00	1.97	0.07	0.4849	0.12
Minor Losses						
Ball Valves	D ₁ (in)	f _t	K	Velocity (m/s)	Head Loss(m)	V Sq. Coeff
Supply 2"	2.00	0.0140	0.04	1.97	0.0083	0.002
Return 2"	2.00	0.0140	0.04	1.97	0.0083	0.002
Return 2"	2.00	0.0140	0.04	1.97	0.0083	0.002
90 Deg Elbow	D ₁ (in)	f _t	K	Velocity (m/s)	Head Loss(m)	V Sq. Coeff
Supply 2"	2.00	0.0140	0.42	1.97	0.0832	0.02
Supply 2"	2.00	0.0140	0.42	1.97	0.0832	0.02
Supply 2"	2.00	0.0140	0.42	1.97	0.0832	0.02
Supply 2"	2.00	0.0140	0.42	1.97	0.0832	0.02
Return 2"	2.00	0.0140	0.42	1.97	0.0832	0.02
Return 2"	2.00	0.0140	0.42	1.97	0.0832	0.02
Tee Joints	D ₁ (in)	f _t	K	Velocity (m/s)	Head Loss(m)	V Sq. Coeff
Supply 2"	2.00	0.0140	1.12	1.97	0.2218	0.06
Return 2"	2.00	0.0140	1.12	1.97	0.2218	0.06
Expansions	D ₁ (in)	D ₂ (in)	K	Velocity (m/s)	Head Loss(m)	V Sq. Coeff
Supply 2" to 3.5"	2.00	3.50	0.34	1.97	0.067	0.02
Contractions	D ₁ (in)	D ₂ (in)	K	Velocity (m/s)	Head Loss(m)	V Sq. Coeff
Return 3.5" to 2"	2.00	3.50	0.34	1.97	0.067	0.02
	Total Head Loss (ft)	6.56	Total Head Loss(m)	2.00	Total V² Coefficient	0.51

Path G

- Supply/Return pipe velocity = 0.53 m/s; Rel. Roughness = 0.049 (Supply),0.049 (return)
- Reynolds Number in 2" dia Supply pipe = 19,059.31; Friction Factor = 0.074
- Reynolds Number in 2" dia Return pipe = 19,059.31; Friction Factor = 0.074

Table 46: Friction Losses in Path G

Major Losses	Pipe Dia (in)	Length (ft)	Velocity (m/s)	Friction Factor	Head Loss (m)	V Sq. Coeff
Supply 2"	2.00	15.00	0.53	0.074	0.016	0.06
Return 2"	2.00	15.00	0.53	0.074	0.016	0.06
Minor Losses						
Ball Valves	D ₁ (in)	f _t	K	Velocity (m/s)	Head Loss(m)	V Sq. Coeff
Supply 2"	2.00	0.0140	0.04	0.53	0.0006	0.002
Return 2"	2.00	0.0140	0.04	0.53	0.0006	0.002
90 Deg Elbow	D ₁ (in)	f _t	K	Velocity (m/s)	Head Loss(m)	V Sq. Coeff
Supply 2"	2.00	0.0140	0.42	0.53	0.006	0.02
Return 2"	2.00	0.0140	0.42	0.53	0.006	0.02
Tee Joints	D ₁ (in)	f _t	K	Velocity (m/s)	Head Loss(m)	V Sq. Coeff
Supply 2"	4.00	0.0170	1.36	0.53	0.019	0.07
Return 2"	2.00	0.0140	1.12	0.53	0.016	0.06
Expansions	D ₁ (in)	D ₂ (in)	K	Velocity (m/s)	Head Loss(m)	V Sq. Coeff
HX Supply 2" to 4"	2.00	4.00	0.38	0.53	0.0053	0.02
Contractions	D ₁ (in)	D ₂ (in)	K	Velocity (m/s)	Head Loss(m)	V Sq. Coeff
Return 4" to 2"	2.00	4.00	0.38	0.53	0.0053	0.02
	Total Head Loss (ft)	0.295	Total Head Loss(m)	0.09	Total V² Coefficient	0.32

Path H

- Supply/Return pipe velocity = 0.41 m/s; Rel. Roughness = 0.049 (Supply),0.049 (return)
- Reynolds Number in 2" dia Supply pipe = 15,996; Friction Factor = 0.075
- Reynolds Number in 2" dia Return pipe = 15,996; Friction Factor = 0.075

Table 47: Friction Losses in Path H

Major Losses	Pipe Dia (in)	Length (ft)	Velocity (m/s)	Friction Factor	Head Loss (m)	V Sq. Coeff
Supply 2"	2.00	10.00	0.41	0.075	0.0065	0.04
Return 2"	2.00	10.00	0.41	0.075	0.0065	0.04
Minor Losses						
Ball Valves	D ₁ (in)	f _t	K	Velocity (m/s)	Head Loss(m)	V Sq. Coeff
Supply 2"	2.00	0.0140	0.04	0.41	0.0004	0.002
Return 2"	2.00	0.0140	0.04	0.41	0.0004	0.002
90 Deg Elbow	D ₁ (in)	f _t	K	Velocity (m/s)	Head Loss(m)	V Sq. Coeff
Supply 2"	2.00	0.0140	0.42	0.41	0.0036	0.02
Return 2"	2.00	0.0140	0.42	0.41	0.0036	0.02
Tee Joints	D ₁ (in)	f _t	K	Velocity (m/s)	Head Loss(m)	V Sq. Coeff
Supply 2"	4.00	0.0170	1.36	0.41	0.012	0.07
Return 2"	2.00	0.0140	1.12	0.41	0.01	0.06
Expansions	D ₁ (in)	D ₂ (in)	K	Velocity (m/s)	Head Loss(m)	V Sq. Coeff
HX Supply 2" to 2.5"	2.00	4.00	0.38	0.41	0.0032	0.02
Contractions	D ₁ (in)	D ₂ (in)	K	Velocity (m/s)	Head Loss(m)	V Sq. Coeff
Return 2.5" to 2"	2.00	4.00	0.38	0.41	0.0032	0.02
	Total Head Loss (ft)	0.164	Total Head Loss(m)	0.05	Total V² Coefficient	0.29

Path I

- Supply/Return pipe velocity = 0.41 m/s; Rel. Roughness = 0.049 (Supply),0.049 (return)
- Reynolds Number in 2" dia Supply pipe = 15,996; Friction Factor = 0.075
- Reynolds Number in 2" dia Return pipe = 15,996; Friction Factor = 0.075

Table 48: Friction Losses in Path I

Major Losses	Pipe Dia (in)	Length (ft)	Velocity(m/s)	Friction Factor	Head Loss (m)	V Sq. Coeff
Supply 2"	2.00	15.000 0	0.41	0.075	0.01	0.06
Return 2"	2.00	15.000 0	0.41	0.075	0.01	0.06
Minor Losses						
90 Deg Elbow	D ₁ (in)	f _t	K	Velocity(m/s)	Head Loss(m)	V Sq. Coeff
Supply 2"	2.00	0.0140	0.42	0.41	0.0036	0.02
Return 2"	2.00	0.0140	0.42	0.41	0.0036	0.02
Expansions	D ₁ (in)	D ₂ (in)	K	Velocity(m/s)	Head Loss(m)	V Sq. Coeff
HX Return 1" to 2"	1.00	2.0000	0.38	0.41	0.0032	0.02
Contractions	D ₁ (in)	D ₂ (in)	K	Velocity(m/s)	Head Loss(m)	V Sq. Coeff
Supply 2" to 1"	2.00	4.0000	0.38	0.41	0.0032	0.02
Gate Valves	D ₁ (in)	f _t	K	Velocity(m/s)	Head Loss(m)	V Sq. Coeff
Bypass 2"	0.05	0.0140	0.11	0.41	0.001	0.01
	Total Head Loss (ft)	0.098	Total Head Loss(m)	0.03	Total V² Coefficient	0.20

Appendix B: Summary of Heat Exchanger Dimensions and Shell Side

Pressure Drops for Paths B-F

Table 49: Summary of Heat Exchanger Dimensions

Item	HX B	HX C	HX D	HX E	HX F
Heat Exchanger Type	Fixed Tubesheet, Single pass in Shell and Tube	U-tube, Single pass in Shell, Double pass in Tube	Fixed Tubesheet, Single pass in Shell and Tube	Fixed Tubesheet, Single pass in Shell and Tube	Fixed Tubesheet, Single pass in Shell and Tube
Surface Area(ft ²)	320	88	40	320	184
No. of Tubes	136	85	68	136	78
Tube Internal diameter (in), D_i	0.652	0.277	0.277	0.652	0.652
Tube Outer Diameter (in), D_o	0.75	0.375	0.375	0.75	0.75
Tube Length(ft), l	11	5.5	6	11	12
Shell Internal Diameter, D_s (in)	13	8	6	13	10.75
Baffle Spacing(in), B	33	33	14.4	33	28.8
Number of Baffles, n_B	4	5	5	4	5
Baffle Segmental Cut(%), B_c	43%	43%	43%	43%	43%
Tube Arrangement	Triangular, 30°	Triangular, 30°	Triangular, 30°	Triangular, 30°	Triangular, 30°
Pitch between tubes(in)	0.9375	0.5	0.4688	0.9375	0.9375
Clearance between tubes(in)	0.1875	0.125	0.0938	0.1875	0.1875

Table 50: Summary of Pressure drop calculation for Heat Exchanger in Path B

Parameter, symbol and unit	Value
Shell Internal Diameter(m), D_s	0.3302
Tube Outer dia(m), D_o	0.01905
Diametral Shell-tube bundle clearance(m)	0.0150
Outer Tube Limit Dia(m), D_{otl}	0.32
Central Tube Limit Dia(m), D_{ctl}	0.296150
Baffle Spacing(m), B	0.8382
Tube Pitch,(m), P_t	0.0238
Tube Arrangement	Triangle
Effective Tube pitch(m), P_{eff}	0.0238
Cross Flow Area(m ²), S_m	0.0622
Baffle Segmental Cut(%), B_c	43%
Central tube Limit angle(rad), θ_{ctl}	2.8281
Fraction of tubes in Cross-flow,(nond), F_c	0.1979
Baffle Window Angle(rad), θ_{ds}	2.8607
Fraction of tubes in each baffle window,(nond), F_w	0.4010
Window flow Area(m ²), S_w	0.0197
Flow Velocity in Path(m/s), v	2.4093
Mass flow Rate of Shell Side Fluid(kg/s), mdot	19.5329
Entering Mass flux, G, (kg/m ² s),	2409.2911
Fluid Viscosity(Pa-s), μ	0.001307
Pitch to Tube dia ratio	1.25
Pitch Parallel to flow(m), P_T'	0.02062
Number of Tube Rows Crossed between baffle tips, N_c	2.24
Effective no. of tube rows crossed per baffle window, N_{cw}	5.51
Reynolds Number, Re	35,116.29
Flow Condition	Turbulent
Kinematic Viscosity(m ² /s), ν	0.0000013
Equivalent Dia of Baffle Window(m ²), D_w	0.0186893
Ideal Friction Factor across tube bank, f_{ideal}	0.1043
Shell-fluid Density (kg/m ³), ρ	1,000.00
Viscosity Correction Factor, ϕ	1.000
Ideal Tube bank pressure drop(Pa), ΔP_{ideal}	2714.328
Ideal baffle window Pressure drop(Pa), ΔP_{w_ideal}	827.122
Leakage Correction Factor, R_L	0.60
Bypass Correction Factor, R_B	0.70
Unequal Baffle Spacing Factor, R_s	0.90
Total Pressure Drop(Pa), ΔP	17228.76
Total Pressure Drop (psi)	2.50
Total Pressure Drop (ft of water)	5.09
Shell side pressure drop, Ps, (m H₂O)	1.55

Table 51: Summary of Pressure drop calculation for Heat Exchanger in Path C

Parameter, symbol and unit	Value
Shell Internal Diameter(m), D_s	0.2032
Tube Outer dia(m), D_o	0.009525
Diametral Shell-tube bundle clearance(m)	0.0140
Outer Tube Limit Dia(m), D_{otl}	0.19
Central Tube Limit Dia(m), D_{ctl}	0.179675
Baffle Spacing(m), B	0.3353
Tube Pitch,(m), P_t	0.0127
Tube Arrangement	Triangle
Effective Tube pitch(m), P_{eff}	0.0127
Cross Flow Area(m ²), S_m	0.0198
Baffle Segmental Cut(%), B_c	43%
Central tube Limit angle(rad), θ_{ctl}	2.8236
Fraction of tubes in Cross-flow,(nond), F_c	0.2007
Baffle Window Angle(rad), θ_{ds}	2.8607
Fraction of tubes in each baffle window,(nond), F_w	0.3996
Window flow Area(m ²), S_w	0.0109
Flow Velocity in Path(m/s), v	0.4086
Mass flow Rate of Shell Side Fluid(kg/s), mdot	3.3125
Entering Mass flux, G, (kg/m ² s),	408.5756
Fluid Viscosity(Pa-s), μ	0.001307
Pitch to Tube dia ratio	1.33
Pitch Parallel to flow(m), P_T'	0.01100
Number of Tube Rows Crossed between baffle tips, N_c	2.59
Effective no. of tube rows crossed per baffle window, N_{cw}	6.36
Reynolds Number, Re	2,977.57
Flow Condition	Turbulent
Kinematic Viscosity(m ² /s), ν	0.0000013
Equivalent Dia of Baffle Window(m ²), D_w	0.0273219
Ideal Friction Factor across tube bank, f_{ideal}	0.1438
Shell-fluid Density (kg/m ³), ρ	1,000.00
Viscosity Correction Factor, ϕ	1.000
Ideal Tube bank pressure drop(Pa), ΔP_{ideal}	124.180
Ideal baffle window Pressure drop(Pa), ΔP_{w_ideal}	147.935
Leakage Correction Factor, R_L	0.60
Bypass Correction Factor, R_B	0.70
Unequal Baffle Spacing Factor, R_s	0.30
Total Pressure Drop(Pa), ΔP	832.74
Total Pressure Drop (psi)	0.12
Total Pressure Drop (ft of water)	0.25
Shell side pressure drop, Ps, (m H₂O)	0.07

Table 52: Summary of Pressure drop calculation for Heat Exchanger in Path D

Parameter, symbol and unit	Value
Shell Internal Diameter(m), D_s	0.1524
Tube Outer dia(m), D_o	0.009525
Diametral Shell-tube bundle clearance(m)	0.0130
Outer Tube Limit Dia(m), D_{otl}	0.14
Central Tube Limit Dia(m), D_{ctl}	0.129875
Baffle Spacing(m), B	0.3658
Tube Pitch,(m), P_t	0.0119
Tube Arrangement	Triangle
Effective Tube pitch(m), P_{eff}	0.0119
Cross Flow Area(m ²), S_m	0.0143
Baffle Segmental Cut(%), B_c	43%
Central tube Limit angle(rad), θ_{ctl}	2.8115
Fraction of tubes in Cross-flow,(nond), F_c	0.2082
Baffle Window Angle(rad), θ_{ds}	2.8607
Fraction of tubes in each baffle window,(nond), F_w	0.3959
Window flow Area(m ²), S_w	0.0056
Flow Velocity in Path(m/s), v	0.5123
Mass flow Rate of Shell Side Fluid(kg/s), mdot	1.0383
Entering Mass flux, G, (kg/m ² s),	512.2763
Fluid Viscosity(Pa-s), μ	0.001307
Pitch to Tube dia ratio	1.25
Pitch Parallel to flow(m), P_T'	0.01031
Number of Tube Rows Crossed between baffle tips, N_c	2.07
Effective no. of tube rows crossed per baffle window, N_{cw}	5.08
Reynolds Number, Re	3,733.31
Flow Condition	Turbulent
Kinematic Viscosity(m ² /s), ν	0.0000013
Equivalent Dia of Baffle Window(m ²), D_w	0.0179845
Ideal Friction Factor across tube bank, f_{ideal}	0.1457
Shell-fluid Density (kg/m ³), ρ	1,000.00
Viscosity Correction Factor, ϕ	1.000
Ideal Tube bank pressure drop(Pa), ΔP_{ideal}	158.236
Ideal baffle window Pressure drop(Pa), ΔP_{w_ideal}	34.212
Leakage Correction Factor, R_L	0.60
Bypass Correction Factor, R_B	0.70
Unequal Baffle Spacing Factor, R_s	0.90
Total Pressure Drop(Pa), ΔP	1057.75
Total Pressure Drop (psi)	0.15
Total Pressure Drop (ft of water)	0.31
Shell side pressure drop, Ps, (m H₂O)	0.10

Table 53: Summary of Pressure drop calculation for Heat Exchanger in Path E

Parameter, symbol and unit	Value
Shell Internal Diameter(m), D_s	0.3302
Tube Outer dia(m), D_o	0.01905
Diametral Shell-tube bundle clearance(m)	0.0150
Outer Tube Limit Dia(m), D_{otl}	0.32
Central Tube Limit Dia(m), D_{ctl}	0.296150
Baffle Spacing(m), B	0.8382
Tube Pitch,(m), P_t	0.0238
Tube Arrangement	Triangle
Effective Tube pitch(m), P_{eff}	0.0238
Cross Flow Area(m ²), S_m	0.0622
Baffle Segmental Cut(%), B_c	43%
Central tube Limit angle(rad), θ_{ctl}	2.8281
Fraction of tubes in Cross-flow,(nond), F_c	0.1979
Baffle Window Angle(rad), θ_{ds}	2.8607
Fraction of tubes in each baffle window,(nond), F_w	0.4010
Window flow Area(m ²), S_w	0.0197
Flow Velocity in Path(m/s), v	4.4568
Mass flow Rate of Shell Side Fluid(kg/s), mdot	9.0332
Entering Mass flux, G, (kg/m ² s),	4456.8037
Fluid Viscosity(Pa-s), μ	0.001307
Pitch to Tube dia ratio	1.25
Pitch Parallel to flow(m), P_T'	0.02062
Number of Tube Rows Crossed between baffle tips, N_c	2.24
Effective no. of tube rows crossed per baffle window, N_{cw}	5.51
Reynolds Number, Re	64,959.53
Flow Condition	Turbulent
Kinematic Viscosity(m ² /s), ν	0.0000013
Equivalent Dia of Baffle Window(m ²), D_w	0.0186893
Ideal Friction Factor across tube bank, f_{ideal}	0.0963
Shell-fluid Density (kg/m ³), ρ	1,000.00
Viscosity Correction Factor, ϕ	1.000
Ideal Tube bank pressure drop(Pa), ΔP_{ideal}	8575.763
Ideal baffle window Pressure drop(Pa), ΔP_{w_ideal}	176.896
Leakage Correction Factor, R_L	0.60
Bypass Correction Factor, R_B	0.70
Unequal Baffle Spacing Factor, R_s	0.90
Total Pressure Drop(Pa), ΔP	48586.04
Total Pressure Drop (psi)	7.05
Total Pressure Drop (ft of water)	14.35
Shell side pressure drop, Ps, (m H₂O)	4.37

Table 54: Summary of Pressure drop calculation for Heat Exchanger in Path F

Parameter, symbol and unit	Value
Shell Internal Diameter(m), D_s	0.2731
Tube Outer dia(m), D_o	0.01905
Diametral Shell-tube bundle clearance(m)	0.0150
Outer Tube Limit Dia(m), D_{otl}	0.26
Central Tube Limit Dia(m), D_{ctl}	0.239000
Baffle Spacing(m), B	0.7315
Tube Pitch,(m), P_t	0.0238
Tube Arrangement	Triangle
Effective Tube pitch(m), P_{eff}	0.0238
Cross Flow Area(m ²), S_m	0.0459
Baffle Segmental Cut(%), B_c	43%
Central tube Limit angle(rad), θ_{ctl}	2.8203
Fraction of tubes in Cross-flow,(nond), F_c	0.2028
Baffle Window Angle(rad), θ_{ds}	2.8607
Fraction of tubes in each baffle window,(nond), F_w	0.3986
Window flow Area(m ²), S_w	0.0152
Flow Velocity in Path(m/s), v	1.9713
Mass flow Rate of Shell Side Fluid(kg/s), mdot	3.9954
Entering Mass flux, G, (kg/m ² s),	1971.2786
Fluid Viscosity(Pa-s), μ	0.001307
Pitch to Tube dia ratio	1.25
Pitch Parallel to flow(m), P_T'	0.02062
Number of Tube Rows Crossed between baffle tips, N_c	1.85
Effective no. of tube rows crossed per baffle window, N_{cw}	4.55
Reynolds Number, Re	28,732.10
Flow Condition	Turbulent
Kinematic Viscosity(m ² /s), ν	0.0000013
Equivalent Dia of Baffle Window(m ²), D_w	0.0230360
Ideal Friction Factor across tube bank, f_{ideal}	0.1071
Shell-fluid Density (kg/m ³), ρ	1,000.00
Viscosity Correction Factor, ϕ	1.000
Ideal Tube bank pressure drop(Pa), ΔP_{ideal}	1542.944
Ideal baffle window Pressure drop(Pa), ΔP_{w_ideal}	54.048
Leakage Correction Factor, R_L	0.60
Bypass Correction Factor, R_B	0.70
Unequal Baffle Spacing Factor, R_s	0.90
Total Pressure Drop(Pa), ΔP	9475.35
Total Pressure Drop (psi)	1.37
Total Pressure Drop (ft of water)	2.80
Shell side pressure drop, Ps, (m H₂O)	0.85

Appendix C: Summary of Heat Exchanger Shell side and tube side heat transfer coefficient calculations and additional revenue calculations

Table 55: Summary of External and Internal Heat transfer coefficients

Parameter	Path A	Path B	Path D	Path E	Path F
Tube External Diameter (m)	0.007	0.0191	0.0095	0.0191	0.0191
Shell Internal Diameter (m)	0.1524	0.3302	0.1524	0.3302	0.2731
Baffle Spacing (m)	0.3658	0.8382	0.3658	0.8382	0.7315
Pitch between tubes (m)	0.0119	0.0238	0.0119	0.0238	0.0238
Crossflow Area (m ²)	0.0111	0.0554	0.0111	0.0554	0.0399
Shell side flow rate (m ³ /s)	0.0027	0.0216	0.0008	0.0064	0.0037
Max velocity in shell (m/s)	0.2425	0.3908	0.0713	0.1149	0.0914
Reynolds Number in Shell	1767.52	5695.60	519.76	1674.87	1332.89
Nusselt Number	36.53	73.72	17.53	35.37	30.84
External Heat Transfer Coefficient (W/m²-K)	2269.79	2290.13	1089.06	1098.82	958.11
Tube mass flow rate(kg/s)	0.0096	0.0809	0.0096	0.08087	0.06042
Tube fluid Density(kg/m ³)	866.51	866.51	866.51	866.51	866.51
Tube flow rate (m ³ /s)	1.11126E-05	9.33326E-05	1.11126E-05	9.33326E-05	6.97225E-05
Number of Tubes	68	136	68	136	78
Number of passes	1	1	1	1	1
Number of Tubes per pass	68	136	68	136	78
Cross-sectional Area per tube (m ²)	3.8879E-05	21.5E-5	3.8879E-05	21.5E-5	21.5E-5
Total Flow Area (m ²)	0.00264	0.02929	0.00264	0.02929	0.01680
Flow Velocity per tube (m/s)	0.0042	0.0032	0.0042	0.00319	0.00415
Dynamic Viscosity of Tube fluid (N-s/m ²)	0.011	0.011	0.011	0.011	0.011
Specific heat of Mixture (J/kg-K)	4184.67	4184.67	4184.67	4184.67	4184.67
Reynolds Number in each Tube	2.3296	4.1563	2.3296	4.1563	5.4136
Prandtl Number of Fluid	145.72	145.72	145.72	145.72	145.72
Nusselt Number for internal flow	2.0311	2.6700	2.0311	2.6700	2.8309
Thermal Conductivity of Fluid (W/m-K)	0.3159	0.3159	0.3159	0.3159	0.3159
Internal Heat Transfer Coefficient (W/m²-K)	91.1950	50.9314	91.1950	50.9314	54.0001

Table 56: Calculation of change in heat transfer after cleaning

Parameter	Path A	Path B	Path D	Path E	Path F
Reference Area, A (m ²)	3.72	27.30	3.72	27.30	17.08
Internal Fouling factor, R _{fi} , m ² K/W (Before cleaning) [51]	0.00009	0.00009	0.00009	0.00009	0.00009
External Fouling factor, R _{fo} , m ² K/W (Before cleaning) [6], [7]	0.00053	0.00053	0.00053	0.00053	0.00053
Internal Surface Area, A _i (m ²)	2.749	23.730	2.749	23.730	14.847
External Surface Area, A _o (m ²)	3.722	27.296	3.722	27.296	17.078
Overall Heat Transfer coefficient, 'UA' (Before cleaning)	163.63	752.98	160.26	743.27	565.46
External Fouling factor, R _{fo} , m ² K/W (After cleaning)	0.000	0.000	0.000	0.000	0.000
Internal Fouling factor, R _{fi} , m ² K/W (After cleaning)	0.000	0.000	0.000	0.000	0.000
Overall Heat Transfer coefficient, 'UA' (After cleaning)	168.442	766.343	164.878	756.291	577.552
Hot Fluid temp in (°C)	60	60	60	60	60
Hot fluid Temp out(°C)	32.22	32.22	32.22	32.22	32.22
Cold Fluid Temp in(°C)	15.56	15.56	15.56	15.56	15.56
Cold Fluid Temp out(°C)	10	10	10	10	10
LMTD(°C)	30.34	30.34	30.34	30.34	30.34
Correction Factor, F	1	1	1	1	1
Heat transfer before cleaning (W)	4963.79	22842.59	4861.71	22548.12	17154.06
Heat transfer after cleaning (W)	5109.92	23248.03	5001.80	22943.09	17520.82
Increase in Heat Transfer after Cleaning (W)	146.13	405.45	140.09	394.97	366.76

Table 57: Calculation of Additional Annual Revenue from generated product

Parameter	Path A	Path B	Path D	Path E	Path F
Change in Heat transfer after Cleaning (W)	146.13	405.45	140.09	394.97	366.76
Specific Heat of Ethanol @ Entry (Superheated Vapor) (KJ/kgK)	1.532	1.532	1.532	1.532	1.532
Specific Heat of Ethanol @ Exit (Liquid) (KJ/kgK)	2.538	2.538	2.538	2.538	2.538
Specific Heat of water @ Entry (Superheated Vapor) (KJ/kgK)	1.946	1.946	1.946	1.946	1.946
Specific Heat of water @ Exit (Liquid) (KJ/kgK)	4.181	4.181	4.181	4.181	4.181
Ethanol Vapor ΔT ($T_{Entry} - T_{sat}$), °C	21.37	21.37	21.37	21.37	21.37
Ethanol Liq ΔT ($T_{sat} - T_{exit}$), °C	6.408	6.408	6.408	6.408	6.408
Water vap ΔT ($T_{Entry} - T_{sat}$), °C	3.41	3.41	3.41	3.41	3.41
Water Liq ΔT ($T_{sat} - T_{exit}$), °C	24.378	24.378	24.378	24.378	24.378
Heat duty per kg of product (KJ/kg)	3,422.19	3,422.19	3,422.19	3,422.19	3,422.19
Additional product generated (kg/s)	0.00004	0.00012	0.00004	0.00012	0.00011
Additional product generated (kg/hr)	0.15	0.43	0.15	0.42	0.39
Annual Operating hours (hrs/yr)	4800	4800	4800	4800	4800
Additional product generated Annually (kg/yr)	737.85	2047.25	707.39	1994.36	1851.90
Additional product generated Annually (l/yr)	851.52	2362.64	816.37	2301.60	2137.19
Profit per liter (\$/liter)	\$3.20	\$3.20	\$3.20	\$3.20	\$3.20
Total Additional Profit (\$)	\$2,724.88	\$7,560.46	\$2,612.37	\$7,365.11	\$6,839.02